The Dissertation Committee for Aaron Alexander Jones Certifies that this is the approved version of the following dissertation:

Mineralogical Controls on Microbial Community Structure and Biogeochemical Processes in Subsurface Environments

Committee:

Philip C. Bennett, Supervisor

Daniel O. Breecker

Christopher R. Omelon

Christopher J. Bell

Christine V. Hawkes

Mineralogical Controls on Microbial Community Structure and Biogeochemical Processes in Subsurface Environments

by

Aaron Alexander Jones, B.S.Geo.Sci; M.S.Geo.Sci

Dissertation

Presented to the Faculty of the Graduate School of

The University of Texas at Austin

in Partial Fulfillment

of the Requirements

for the Degree of

Doctor of Philosophy

The University of Texas at Austin

December 2015

Dedication

To my family, friends and especially my wife.

Acknowledgements

I would like to thank the friends who supported me through these years. There were many periods of extreme self-doubt and I relied heavily on you to keep me positive and get me back on track. I know this is a cliché, but there really aren't words to express the level of my gratitude to you all, but here I go… I would not have been able to do this without the love, support, patience, and encouragement of my wife, Holly. Thank you Holly for bringing joy to my life. Thank you Jay Santillan for being the best friend I've ever had. I am forever indebted to Chris Omelon for his insight, support, and friendship.

I thank my advisors, committee members, and research group members for their support, guidance, and insights over these many years. Specifically, I owe Phil Bennett a huge debt of gratitude for his mentorship. Phil's guidance is primarily responsible for the scientist I have become. Thank you, Phil, for the countless times you helped me see the forest for the trees. I would like to thank Annette Engel for laying the groundwork for this research. I would like to thank the GEO 381G (Geomicrobiology) students of the past 5 years for "enthusiastically" assisting me with field research. You made crawling into a stinky, hot, toxic hole in the ground to spend hours collecting slime much more bearable.

I acknowledge that my research was funded from the contributions of The Geological Society of America, The National Science Foundation, and the Jackson School of Geosciences.

Mineralogical Controls on Microbial Community Structure and Biogeochemical Processes in Subsurface Environments

Aaron Alexander Jones, Ph.D.

The University of Texas at Austin, 2015

Supervisor: Philip C. Bennett

Abstract

Nearly every ecological habitat in the microbiological world is predominately occupied by complex assemblages of multicellular, multifunctional communities attached to surfaces as biofilms. The motivating factors for this stationary community lifestyle appear to be as diverse as the organisms that occupy these habitats. However, there are also many commonalities primarily relating to nutritional requirements and environmental tolerances. Broadly, this dissertation focuses primarily on linking these motivating factors to specific microorganisms within diverse biofilm communities attached to mineral surfaces. To do this I used continuous-flow laboratory biofilm reactors (inoculated with a diverse subsurface biofilm community) to assess the roles of surface type, media pH, and carbon and phosphate availability on biofilm accumulation, community structure, function, and phylogenetic variability. I demonstrate that in nutrient-limited systems, taxonomy and growth of biofilm communities is highly dependent on surface chemistry to support their nutritional requirements and environmental tolerances. Moreover I present rigorous statistical evidence that, for a variety of environments, microbial communities attached to similar natural surfaces types

(carbonates vs. silicates vs. aluminosilicates) are more phylogenetically similar. I find that surface type controls up to 90% of the variance in phylogenetic diversity of a system regardless of environmental pressures. This is strong evidence that mineral selection is genetically ingrained.

We provide validated methodology for the use of continuous flow-bioreactors to expose the fundamentally dynamic nature of microbial structure within biofilms. I demonstrate that these shifts in community structure can occur rapidly, impacting geochemistry and carbonate mineral solubility. Specifically, carbonate dissolution is highly accelerated under autotrophic conditions dominated by sulfur-oxidizers. Immediately after adding acetate the community shifts to heterotrophic sulfur-reducers resulting in carbonate precipitation. Additionally, these functional shifts can be inferred by monitoring geochemical indicators ($\delta^{13}C_{CO2}$, $[CO_2]$, Ca^{2+}, and pH). I provide evidence that the responsiveness of carbonate system reactions to the metabolic products of sulfuric acid cave ecosystems are ideal model ecosystems for studying the effects of microbial community structure on stable carbon isotope fractionation.

I submit that biogeochemical interactions with mineral surfaces have influenced development, evolution, and diversification of microbial life. Throughout geologic time, microorganisms have enhanced survival by colonizing mineral surfaces and developing complex biofilm communities genetically primed for specific mineral habitats.

Table of Contents

List of Tables xi

List of Figures xvii

Chapter 1: Introduction 1

1.1 Motivation and Problem Statement 1

1.2 Novel Questions 6

1.3 Dissertation Organization 7

Chapter 2: Mineral microniches control the diversity of subsurface microbial populations 11

2.1 Abstract 11

2.2 Introduction 12

2.3 Materials and Methods 15

2.3.1 Mineral Substrata Preparation 16

2.3.2 Microbial Inoculant 19

2.3.3 Biomass Accumulation 20

2.3.4 Community Analysis 21

2.4 Results 25

2.4.1 Biofilm Accumulation 25

2.4.2 Microbial Diversity 31

2.5 Discussion 38

2.6 Conclusions 49

Chapter 3: Revealing hidden diversity: investigating the impact of minerals on biofilm community structure and diversity 52

3.1 Abstract 52

3.2 Introduction 53

3.3 Materials and Methods 55

3.3.1 Flow through Biofilm Reactor (CDC) 55

3.3.2 Mineral Substrata Preparation 57

3.3.3 Biomass measurement and extraction 60
3.3.4 Biodiversity Metrics and Statistical Analysis 62
3.4 Results 66
3.4.1 Effect of reactor conditions on bacterial diversity 66
3.4.2 Effect of mineralogy on bacterial diversity 73
3.4.3 Taxonomic composition and condition sensitive taxa 78
3.4.4 Biofilm Abundance 88
3.5 Discussion 92
3.5.1 Sulfur-Metabolizers 93
3.5.2 Acidophiles 96
3.5.3 Gram-positives and other potential biophysical/mineral relationships 98
3.5.4 Biofilm Accumulation and Mineralogy 101
3.5.5 Planktonic vs. Attached Communities 104
3.6 Conclusions 107

Chapter 4: Biogeochemical dynamics of sulfuric-acid speleogenesis: A proof of concept environment for inferring microbial community structure and function using $\delta^{13}C_{CO2}$ 109
4.1 Abstract 109
4.2 Introduction 110
4.3 Materials and Methods 113
4.3.1 Solid Surface Preparation and Characterization 113
4.3.2 Liquid Media Preparation for Chamber Experiments 115
4.3.3 Microbial Inoculants 115
4.3.4 Experimental Variations 116
4.3.5 PCR Amplification and 454 Sequencing of 16S rRNA 117
4.4 Results 120
4.4.1 Abiotic Experiments 120
4.4.2 *Thiothrix unzii* Experiments 125
4.4.3 LKC Mixed Culture Experiments 126
4.4.4 Changes in Mixed Culture Community 132

4.4.5 SEM Observations of Surface Features 136
4.4.6 Results of Sulfur Chemistry 139
4.5 Discussion 139
4.5.1 Limestone Dissolution by *Thiothrix unzii* 139
4.5.2 Limestone Dissolution by LKC Mixed Communities 144
4.6 Conclusions 152
Chapter 5: Synthesis and Concluding Remarks 154
5.1 Synthesis of Doctoral Research 154
References 158

List of Tables

Table 2.1: General composition, common subsurface environments, potential benefits to microorganisms, and special properties specific to the rocks/minerals used in the biofilm reactor experiments. Superscripts refer to papers with additional information (1-Bennett and Others 2001, 2-Steinhauer and Others 2010, 3-Edwards and Others 2005).....18

Table 2.2: Dry mass of biofilm values and standard deviations. The standard deviation for the pure culture experiment are the result of triplicate experiments with the dry biomass values in the table as the mean of the three. The standard deviations of the mixed culture are for all three mixed culture experiments shown in the table.....27

Table 2.3: Alpha microbial community diversity from 16S rRNA based classification of microorganisms attached to solid surfaces after 3-weeks within the reactor. Measures of alpha diversity: Simpson's dominance index (D), which favors OTUs with more sequences, and Shannon Weiner index (H'), which favors OTUs with fewer sequences (rare OTUs), Number of OTUs (species richness (S)), and Species Evenness (E). 33

Table 2.4: Proportional abundance (%) of representative class (Bold) and representative genera from 16S rRNA gene sequence taxonomic classification for microorganisms in the LKC inoculant and those removed from each surface after 3-weeks within the biofilm reactor. Potential sulfur-oxidizing genera and total proportion of sulfur-oxidizing genera are shaded. 36

Table 3.1: Media recipes for each of the four reactor conditions. (-) represents none added. 58

Table 3.2: Surface types, general compositions, and biogeochemical significance of the rocks/minerals used in these biofilm reactor experiments. This table is modified from Jones & Bennett 2014. Superscripts refer to papers with additional information.[1]Bennett et al, 2001 [2]Steinhauer et al, 2010 [3]Edwards et al, 2005.....59

Table 3.3: Effects of reactor conditions and surface type on bacterial β-diversity. [a]Effects of surface type and [b]reactor conditions as assessed by multivariate permutational analysis of variance (PERMANOVA). Surface factors are buffering capacity (high vs. low based on whether surface is a carbonate or non-carbonate), mineral type (carbonate, silicate, aluminosilicate, planktonic), and mineral phosphate (high vs. low). Reactor correlation factors are carbon amendment (yes vs. no), phosphate amendment (yes vs. no), media pHin (high vs. low), and media pHout (high vs. Low). Values represent the pseudo-F ratio (F), the permutation-based level of significance (*P*), and the 'adonis' (R^2). Values at $P<0.05$ are shown in bold. Negative variance components (Neg) can result from underestimations of small or zero variances. [c]Pairwise comparisons between reactors. Values represent the univariate t-statistic (t) and the between reactor UniFrac (phylogenetic) similarity ($Ø_{sim}$). The permutation-based level of significance was adjusted for multiple comparisons using the Benjamini-Hochberg procedure (P_{adjust}). Values at $P_{adjust}<0.05$ are shown in bold.....69

Table 3.4: Bacterial α-diversity and effects of mineralogy and reactor conditions on α-diversity. [a]Measures of species richness (S) and Shannon Diversity (H') for each surface and each reactor. Values are based on rarefied data sets in order to allow comparisons across reactors. 70

Table 3.4 caption continued: [b]Impact of surface factors and reactor conditions assessed by PERMANOVA. Surface factors are buffering capacity (high vs. low based on whether surface is a carbonate or non-carbonate), mineral type (carbonate, silicate, aluminosilicate, planktonic), and mineral phosphate (high vs. low). Reactor correlation factors are carbon amendment (yes vs. no), phosphate amendment (yes vs. no), media pHin (high vs. low), and media pHout (high vs. Low). Values are the pseudo-F ratio (F) and the level of significance (*P*). Values at $P < 0.05$ indicate a significant differences in a factor and are shown in bold. [c]Pairwise comparisons of overall alpha diversity between reactors using PERMANOVA as described above. 71

Table 3.5: Bacterial α-diversity on each surface and for each whole reactor. High-quality sequences are the total sequences that were used in diversity analyses. Table also includes measures of species richness (S), Shannon Diversity (H'), Evenness (E), Simpson's diversity index (1-D), and Good's Coverage (%) for each surface and each reactor. Values are based on rarefied data sets for sequences from surfaces within each reactor and then for whole reactors in order to allow comparisons across reactors. 72

Table 3.6: CP-Limited reactor samples as proportional abundance (%) of taxa of representative class (bold) and genera from 16S rRNA gene sequences in the LKC inoculant, for each surface, and the planktonic sample after 3-weeks within the CP-Limited reactor. Potential sulfur-oxidizing genera (SOB), sulfur reducing genera (SRB), acidophilic genera, and gram-positive genera are highlighted (Adapted from Jones and Bennett 2014). 84

Table 3.7: CP-Amended reactor samples as proportional abundance (%) of taxa of representative class (bold) and genera from 16S rRNA gene sequences for each surface and the planktonic sample after 3-weeks within the CP-Amended reactor. Potential sulfur-oxidizing genera (SOB), sulfur reducing genera (SRB), acidophilic genera, and gram-positive genera are highlighted. 85

Table 3.8: C-Amended reactor samples as proportional abundance (%) of taxa of representative class (bold) and genera from 16S rRNA gene sequences for each surface and the planktonic sample after 3-weeks within the C-Amended reactor. Potential sulfur-oxidizing genera (SOB), sulfur reducing genera (SRB), acidophilic genera, and gram-positive genera are highlighted. 86

Table 3.9: P-Amended reactor samples as proportional abundance (%) of taxa of representative class (bold) and genera from 16S rRNA gene sequences for each surface and the planktonic sample after 3-weeks within the P-Amended reactor. Potential sulfur-oxidizing genera (SOB), sulfur reducing genera (SRB), acidophilic genera, and gram-positive genera are highlighted. 87

Table 3.10: Dry mass of biofilm values and standard deviations. The standard deviations for all experiments are the result of triplicate experiments with the dry biomass values as the mean of the three. [a]Sum of the mean values of dry biomass for each reactor. [b]Standard deviation in for dry biomasses on surfaces within each reactor. [c]Dry biomass of biofilm values for CP-Limited reactor from Jones and Bennett 2014.....91

Table 3.11: Summary of impact of reactor and surface variables on microbial community structure in each reactor. Alpha diversity metrics are (S) species richness and (H') Shannon diversity. Beta diversity is UniFrac (phylogenetic) diversity. In the table (×) signifies no significant impact, (✔) significant impact, (COR) correlation type, (+) positive correlation, (–) negative correlation, (CPL) CP-Limited reactor, (CA) C-Amended reactor, (PA) P-Amended reactor, (CPA) CP-Amended reactor. ...106

Table 4.1: Table showing the mean, high, and low $\delta^{13}C_{CO2}$ (‰) within the *Thiothrix unzii* reactor for intervals when the reactor was amended with acetate, thiosulfate, both, or neither. Table also shows the likely dominant metabolism during each of these intervals. Note: this reactor had ambient CO_2 in the air into the reactor with a $\delta^{13}C_{CO2}$ = -12 to -14.5‰. 122

Table 4.2: Table showing the mean, high, and biotic/abiotic limestone dissolution rates ($mol \bullet cm^2 \bullet s^{-1}$) within the *Thiothrix unzii* reactor for intervals when the reactor was amended with acetate, thiosulfate, both, or neither.124

Table 4.3: Table showing the mean, high, and low $\delta^{13}C_{CO2}$ (‰) within the *LKC Mixed Culture* reactor for intervals when the reactor was amended with acetate, thiosulfate, both, or neither. Table also shows the likely dominant metabolism during each of these intervals.....129

Table 4.4: Table showing the mean, high, and biotic/abiotic limestone dissolution rates ($mol \bullet cm^2 \bullet s^{-1}$) within the *LKC Mixed Culture* reactor for intervals when the reactor was amended with acetate, thiosulfate, both, or neither. 131

Table 4.5: Inoculant and reactor samples as proportional abundance (%) of taxa of representative class (bold) and genera from 16S rRNA gene sequences. Putative sulfur-oxidizing genera (SOB), sulfur reducing genera (SRB), and gram-positive genera are highlighted.....135

Table 4.6: Summary of mean Δ [Sulfur] (mM) of various sulfur species during specific periods and overall summary of findings from this study. When $S_2O_3^{2-}$ in is 0.89mM, Acetate in is 2mM, SO_4^{2-} in from $MgSO_4$ is 0.94mM.....151

List of Figures

Figure 2.1: Dry weight (mg/cm^2) of biomass accumulation on rock and mineral surfaces for both *Thiothrix unzii* and a mixed culture obtained from Lower Kane Cave. Error bars denote standard deviation, n=3 (see Table 2.2). 26

Figure 2.2: SEM images of microbial colonization on surfaces after 3-weeks exposure to *Thiothrix unzii* (a,c, & e, g, & i) and the mixed LKC community (b,d, f, h, & j). (a) & (b) are quartz. (c) is albite and d is microcline. (e) & (f) are images of the biofilm accumulation on the basalt surface. (g) and (h) are Madison Limestone. (i) and (j) are calcite. Note that Madison Dolostone is excluded because it is nearly identical to Madison Limestone. Horizontal white lines are scale bars.....29

Figure 2.3: SEM images of Abiotic vs. Microbial (LKC mixed culture) carbonate corrosion after 3 weeks within a CDC reactor at pH=6.6: (a) abiotic calcite, (b) microbial calcite, (c) abiotic Madison Limestone, (d) microbial Madison Limestone, (e) abiotic Madison Dolostone, (f) microbial Madison Dolostone. All scale bars are 10 μm.....30

Figure 2.4: Dendrogram of bacterial β-diversity displaying the overlap in bacterial communities colonizing various solid surfaces. The key (bottom left) contains class level taxonomy associated with each mineral surface (see Table 2.4 for proportional abundances). The scale bar represents 0.05 (5%) dissimilarity in sequences isolated from each mineral/rock surface (proportion of sequences belonging to unshared OTUs). Dissimilarity increases with branch length in the outward direction. Each of the carbonate branches are ≤2% in length. Branch lengths were calculated using the abundance based Sorenson similarity index wherein OTUs were assigned at ≥ 97% similarity in sequences. 37

Figure 3.1a: Growth curves for biofilm accumulated on limestone surfaces in pure culture (*Thiothrix unzii*) and *LKC mixed culture* reactors under CP-Limited, C-Amended, and P-Amended media conditions. Error bars represent duplicate experiments. 64

Figure 3.1b: Rarefaction curves of 16S rRNA sequences. OTUs were defined at 97% similarity cutoff. The figure depicts the comparison between samples from all four reactors. 65

Figure 3.2: Principal coordinate analysis (PCoA) plot based on the relative abundances and phylogenetic diversity of 16S rRNA gene sequences using a UniFrac weighted distance matrix, colored according to reactor conditions and labeled according to solid substrate type; blue, CP-Limited; green, P-Amended; orange, CP-Amended; red, C-Amended. Percentage of the diversity distribution explained by each axis is indicated in the figure. The colored ellipses encircle variations in reactor conditions. 68

Figure 3.3: Unweighted pair group method with arithmetic mean (UPGMA) trees constructed using weighted UniFrac (phylogenetic) distance matrix constructed from 16S rRNA sequences clustered at 97% similarity for each of the four reactors (CP-Limited, P-Amended, C-Amended, CP-Amended). The trees display the phylogenetic overlap in bacterial communities colonizing various solid surfaces within each reactor. The key (center) contains the class level taxonomy associated with each mineral surface (see S-TableTaxonomy for proportional abundances). The scale bars for the CP-Limited and C-Amended reactors represents 0.05 (5%) dissimilarity in 16S rRNA sequences isolated from each surface and the scale bars for the P-Amended and CP-Amended reactors 0.02 (2%) dissimilarity. Note that although the taxonomy of the CP-Limited reactor is the same as Jones and Bennett 2014, the UPGMA tree here is based on UniFrac distances, while the tree in Jones and Bennett 2014 (Fig. 4) used the OTU based Sorenson similarity index. 75

Figure 3.4: Venn diagram of the shared bacterial genera found in the four reactors (CP-Limited, P-Amended, C-Amended, CP-Amended). Overlaps between the reactors are indicated by overlaps in the diagram. 83

Figure 3.5: Dry weight (mg/cm2) of biomass accumulation on surfaces for each reactor. Error bars denote standard deviation, n=3. See Table 3.10 for numerical values. 90

Figure 4.1: Flow-through bioreactor diagram with multi-port lid for pure and mixed culture limestone dissolution experiments. F denotes sources of carbon flux in moles. Subscripts are: F-microbial fixation, R-microbial respiration, LS-Limestone, AI-Air In, AO-Air Out, MI-Media In, MO-Media Out. Liquid media flow was set to 1.4ml/min. Air flow was 25ml/min. CO_2 Scrubber was not used during *T. unzii* experiments. Gas and liquid are filtered through 0.2μm filters before entering the reactor. 119

Figure 4.2: Log of CO_2 gas concentration (atm) in the headspace and $\delta^{13}C_{CO2}$ (‰) within the *Thiothrix unzii* pure culture reactor. Also shown are the flux from air in CO_2 gas concentration (atm) and the air in $\delta^{13}C_{CO2}$ (‰) since the air in for this reactor was not CO_2 scrubbed. Periods when acetate (Yellow), thiosulfate (Blue), or both acetate and thiosulfate (Green) are shaded accordingly. Note that this figure shows a representative period taken from the much longer experiment. 121

Figure 4.3: Log of calcium concentration (mM) and pH within the *Thiothrix unzii* pure culture reactor. Periods when acetate (Yellow), thiosulfate (Blue), or both acetate and thiosulfate (Green) are shaded accordingly. Note that this figure shows a representative period taken from the much longer experiment.....123

Figure 4.4: Log of CO_2 gas concentration (atm) in the headspace and $\delta^{13}C_{CO2}$ (‰) within the *LKC Mixed Culture* reactor. Also shown are the $\delta^{13}C_{Acetate}$ (‰) and $\delta^{13}C_{CaCO3}$ (‰) from limestone. The CO_2 was scrubbed from the air into this reactor. Periods when acetate (Yellow), thiosulfate (Blue), or both acetate and thiosulfate (Green) are shaded accordingly. Note that this figure shows a representative period taken from the much longer experiment.....128

Figure 4.5: Log of calcium concentration (mM) and pH within the *LKC Mixed Culture* reactor. Periods when acetate (Yellow), thiosulfate (Blue), or both acetate and thiosulfate (Green) are shaded accordingly. Note that this figure shows a representative period taken from the much longer experiment.....130

Figure 4.6: The bacterial communities composing the inoculant and reactor samples as proportional abundance (%) of taxa of representative class from 16S rRNA gene sequences. 134

Figure 4.7: SEM images of carbonate surfaces colonized by LKC mixed cultures after 3-weeks within a CDC reactor amended with acetate. Microbial community is primarily composed of the SRB *Desulfovibrio*. A, B, C, & D are calcite surfaces with microorganisms attached; note the scale bars are 10µm, 5µm, 20µm, and 10µm, respectively. E & F are Limestone covered in biofilm; note the scale bars are 10µm and 200µm, respectively. G & H are Dolostone covered in biofilm; note the scale bars are 10µm and 200µm, respectively. 138

Figure 4.8: Limestone dissolution is the result of both autotrophy and heterotrophy in *Thiothrix unzii* pure cultures. For each of the specified intervals: Gray is the $\delta^{13}C_{CaCO3}$, yellow is $\delta^{13}C_{Acetate}$, green is $\delta^{13}C_{CO2}$ of the ambient air entering the reactor, orange is the $\delta^{13}C_{CO2}$ of the headspace under abiotic conditions, blue is the mean $\delta^{13}C_{CO2}$ of the biotic reactor, red (-) are the lowest biotic $\delta^{13}C_{CO2}$, black (+) are the highest biotic $\delta^{13}C_{CO2}$. A. Heterotrophy when acetate and thiosulfate are supplied. B. Heterotrophy when acetate is supplied and thiosulfate withheld. C. Autotrophy when thiosulfate is supplied and acetate is withheld. D. Autotrophy when both acetate and thiosulfate are withheld.....143

Figure 4.9: Limestone dissolution is the result of both autotrophy and heterotrophy in the *LKC Mixed* culture reactor. For each of the specified intervals: Gray is the $\delta^{13}C_{CaCO3}$, yellow is $\delta^{13}C_{Acetate}$, green is $\delta^{13}C_{CO2}$ of the ambient air entering the reactor, orange is the $\delta^{13}C_{CO2}$ of the headspace under abiotic conditions, blue is the mean $\delta^{13}C_{CO2}$ of the biotic reactor, red (-) are the lowest biotic $\delta^{13}C_{CO2}$, black (+) are the highest biotic $\delta^{13}C_{CO2}$. Note that there is no $\delta^{13}C_{CO2}$ for the ambient air entering this reactor. A. Heterotrophy when acetate and thiosulfate are supplied. B. Heterotrophy when acetate is supplied and thiosulfate withheld. C. Autotrophy when thiosulfate is supplied and acetate is withheld. D. Autotrophy when both acetate and thiosulfate are withheld.....150

Chapter 1: Introduction

1.1 Motivation and Problem Statement

One of most fundamental and profound aspects of research in the interdisciplinary field of Geomicrobiology is the relationship between microorganisms and natural (mineral and rock) surfaces. This is largely due to the fact that the vast majority of microorganisms exist in biofilms attached to mineral surfaces. This is especially true for subsurface environments, where it has been estimated that 99.9% of microorganisms adhere to this lifestyle (Madigan et al, 2009). In the subsurface, caves, deep marine sediments, deep soils, or any of the other vast and abundant examples of dark, nutrient poor environments, microbes are highly dependent on geochemical interactions with natural surfaces as a source of energy or nutrients (Anderson, 2001; Chapelle et al, 2002; Edwards et al, 2005; Edwards et al, 2012; Stevens, 1997). It is reasonable to hypothesize that, throughout geologic time, the structure and function of these microorganisms would have adapted and evolved to take advantage of geochemical interactions with specific surface types. So I ask if there are genetically engrained affinities for specific surface types and can I detect it? Once I know that these relationships exist I may be able to use that knowledge to exploit the biogeochemical consequences of specific relationships.

Studies have suggested the geochemical composition of solid surfaces and nutrient availability may play a role in distribution of taxa in the subsurface and soils (Carson et al, 2009; Dalton et al, 1994; Huang et al, 1998; Ohashi et al, 1995; Rogers & Bennett, 2004; Rogers et al, 1998; Rogers et al, 2001; Sylvan et al, 2012). These studies have shown correlations between occurrences of specific taxa and specific surfaces types. However, until this study, there has not been a comprehensive study assessing the relative impacts of environmental pressures (carbon source, pH, phosphate availability) and

surface chemistry pressures (buffering ability, nutrient availability) on community structure, phylogenetic diversity, taxonomic diversity, membership, and biofilm accumulation. Additionally, herein I attempt to identify a statistically significant link between phylogenetic diversity of microbial communities to specific natural surface types under a variety of geochemical conditions.

Fundamentally, biofilms attached to surfaces can exert highly localized control on geochemistry of the surrounding microenvironment (Bennett et al, 2000). The effect on geochemistry is highly variable as it is both a function of actively metabolizing microorganisms and a consequence of passive reactions with EPS or even microbial cell walls (Bennett et al, 1996; Ehrlich, 1996). Furthermore, these interactions often results in dissolution of the surface and/or precipitation of secondary minerals (Ehrlich, 1996). There are many suggested mechanisms for this process, for the sake of brevity, two examples include: EPS and cell walls of prokaryotes acting as nucleation sites for mineral precipitation, by binding solutes (Aloisi et al, 2006; Ferris, 2000; Roberts et al, 2004), and microbial metabolism-induced dissolution/precipitation (Engel et al, 2004b; Steinhauer et al, 2010). Due their participation in the global carbon cycle, most biogeochemically-induced dissolution or precipitation reactions involve carbonate minerals, but it has been shown repeatedly that attached microorganisms can facilitate and significantly alter rates of mineral and rock dissolution/precipitation of silicates, hydroxides/oxides, sulfides/sulfates, and phosphates (Schultze-Lam et al, 1996). Despite this, the mechanisms behind the vast majority of these biogeochemical interactions are either not understood or have yet to be documented.

One overt consequence of these interactions is the formation of carbonate karst. Generally, these landscapes form where soluble carbonate rocks dissolve by chemical solution forming distinctive surface features (e.g. sinkholes and dolines) and subsurface

voids features such as caves (White, 1988). Within caves such as Movile Caves (Romania), the Frasassi Caves (Italy), and Lower Kane Cave (LKC, Wyoming, USA) the combination of abiotic autoxidation and microbiological oxidation of H_2S produces SO_4^{2-} and H^+ that promotes limestone dissolution through sulfuric-acid speleogenesis (SAS) (Egemeier, 1981). This happens as a consequence of both abiotic and biotic reaction pathways, but is particularly influenced by the metabolism of chemolithotrophic sulfur oxidizing bacteria (SOB) (Egemeier, 1981; Engel, 2004; Steinhauer et al, 2010).

LKC is situated in the Bighorn River Valley, WY, USA (44°44' N, 108°11' W), and has a single horizontal passage extending ~325 meters along the axial trace of the Little Sheep Mountain Anticline in the Madison Limestone (Stock et al, 2006). The Madison Formation is Mississippian age (~350mya) massive (~150–250m thick) limestone and dolostone with occasional thinly interbedded shale and chert nodules (Peterson, 1984). Recharge water to the LKC stream is a mixture of meteoric water from Madison Limestone and slightly thermal waters from depth (Peterson, 1984). There are 4 sulfidic springs within LKC that serve as the metabolic backbone for filamentous microbial mats that accumulate where the springs enter the cave stream (Egemeier, 1981; Engel et al, 2004a; Peterson, 1984).

The microbial taxonomy within LKC has been previously documented (Engel et al, 2003). In summary, microorganisms belonging to many distinct lineages within the phylum *Proteobacteria* are associated with these spring features. The community is dominated primarily by sulfur-oxidizers of the classes *Gammaproteobacteria* and *Epsilonproteobacteria,* and lesser amounts of *Betaproteobacteria* most closely related to the genera; *Thiothrix*, *Thiobacillus*, *Thiomonas, Thiomicrospira, Thiovulum,* and *Achromatium* (Engel, 2004; Engel et al, 2003). Additionally, I have found that there is a large abundance of sulfur-reducers of the class *Deltaproteobacteria* represented by

members of the genera *Desulfocapsa* and *Desulfovibrio* thriving in oxygen-depleted niches directly beneath or even within sulfur-oxidizing biofilms. However, there have been no extensive studies of the sulfur-reducing populations in these caves. It has only been documented that *Desulfocapsa* has been found within LKC and Frasassi Caves in Italy (Engel et al, 2004a; Macalady et al, 2006).

Sulfur-metabolizing communities are uniquely suited to the experiments described herein, due to the multitude of metabolic pathways provided by the sulfur system. Chemolithoautotrophic SOB gain energy from oxidation of reduced sulfur compounds such as sulfide, thiosulfate, polythionic acids, thiocyanate, carbon disulfide, carbonyl sulfide and methylated sulfur compounds (Kelly et al, 1997; Kelly et al, 1994). CO_2 reduction in the Calvin Cycle is dependent on the electrons provided by sulfur oxidation (Reaction 1) (Kelly, 1999).

$$6CO_2 + 3S_2O_3^{2-} + 9H_2O \rightarrow C_6H_{12}O_6 + 6SO_4^{2-} + 6H^+ \quad (1)$$

In reaction 1, thiosulfate is shown as the electron donor because it was used in the experiments described herein. Additional reactions help to illustrate the effect of sulfur oxidation (both biotic and abiotic) on carbonate dissolution, through either production or consumption of acidity. These reactions include (Kelly, 1999):

$$H_2S + 2O_2 \rightarrow SO_4^{2-} + 2H^+ \qquad \Delta G^o = -714 kJ \bullet mol^{-1} \quad (2)$$

$$HS^- + 0.5O_2 \rightarrow S^o + OH^- \qquad \Delta G^o = -145 kJ \bullet mol^{-1} \quad (3)$$

$$S^o + H_2O + 1.5O_2 \rightarrow SO_4^{2-} + 2H^+ \qquad \Delta G^o = -507 kJ \bullet mol^{-1} \quad (4)$$

$$S_2O_3^{2-} + H_2O + 2O_2 \rightarrow 2SO_4^{2-} + 2H^+ \qquad \Delta G^o = -739 kJ \bullet mol^{-1} \quad (5)$$

Thiothrix unzii and other SOB species oxidize H_2S, $S_2O_3^{2-}$ and S^o to sulfate (Reactions 2, 3, & 5), while many SOB partially oxidize sulfide and store the resulting S^o internally (Reaction 3) where it can later be oxidized (Reaction 4) in times of low sulfide availability (Ehrlich, 1996; Smith & Strohl, 1991).

Generally, the microorganisms within LKC are neutrophilic SOB (Engel et al, 2004a). However, it is clear from reactions 1-5 that most pathways available to neutrophilic SOB generate acidity as a byproduct. The fortuitous presence of highly buffering $CaCO_3$ composing the local limestone host rock consumes this acidity-leading to aggressive corrosion and accelerated speleogenesis. It has long been suspected that these neutrophilic, but acid-producing microorganisms can only exist here because carbonate dissolution acts to stabilize the local pH (Steinhauer et al, 2010). An investigation into the nature of this relationship is presented in Chapter 2 of this dissertation.

Acetate promotes heterotrophic growth and most biological sulfur reduction results from acetate consumption (Sørensen et al, 1981). For example, most sulfur-reducing bacteria (SRB) capable of utilizing acetate with S^o use the tricarboxylic acid (TCA) cycle (Galushko & Schink, 2000) for the following reaction:

$$CH_3COO^- + 4S^o + H^+ + 2H_2O \rightarrow 4H_2S + 2CO_2 \qquad \Delta G^o = -39 kJ \bullet mol^{-1} \quad (6)$$

Other SRB may be capable of utilizing acetate for sulfate reduction:

$$CH_3COO^- + SO_4^{2-} + 3H^+ \rightarrow H_2S + 2CO_2 + 2H_2O \qquad \Delta G^o = -63 kJ \bullet mol^{-1} \quad (7)$$

Whereas the majority of reactions under autotrophic conditions produced acidity leading to increased carbonate corrosion (Reactions 1-5), reactions under heterotrophic conditions might consume acidity leading to decreased carbonate corrosion (Reactions 6 &7). These are purely metabolic consequences on mineral dissolution, but they serve to illustrate the point that a minor change in geochemistry of the local environment can completely alter the community structure and thusly the biogeochemical dynamics of that microbe/surface ecosystem.

1.2 NOVEL QUESTIONS

The goal of this dissertation is to answer or provide insight into the following questions:

1) Do microorganisms select for specific minerals according to their metabolic needs and environmental tolerances?
2) How does surface type affect subsurface biofilm formation and community membership?
3) How does nutrient availability affect biofilm formation and community development?
4) How does electron donor-acceptor availability influence biogeochemical interactions?
5) Does surface type influence phylogenetic similarities between attached biofilm communities?
6) Can changes in microbial community metabolic processes by monitoring trends in simple geochemical parameters (i.e. pH, pCO_2, $^{13}CO_2$, $^{12}CO_2$, Ca^{2+}), be used to infer changes in community membership?

7) How dynamic are the taxonomic compositions of subsurface microbial communities?

8) How do changes in microbial community structure impact carbonate dissolution or precipitation?

9) Are affinities for specific minerals genetically engrained and can I detect them?

1.3 Dissertation Organization

Three chapters of this dissertation are dedicated to addressing the aforementioned questions. The first of these main chapters is already published in a peer reviewed journal (Jones & Bennett, 2014). The second of these chapters is submitted for the peer review process. All three of these chapters are prepared following the peer reviewed journal publication format. Therefore, each chapter has its own abstract, introduction, methods, results, discussion, and conclusion sections. References are collated at the end of this dissertation. Here I present a general description of these dissertation chapters while highlighting independent significance.

Chapter 2 examines the role of rocks and minerals on microbial community structure in dark oligotrophic subsurface environments. I use laboratory flow-through bioreactors inoculated with pure and mixed cultures to investigate microbial biofilm growth and community structure as they colonize a variety of natural surfaces. Analysis of total biomass accumulation, SEM micrographs, and 16S rRNA sequences of attached microorganisms suggests that surface-chemistry influences microbial community structure, biomass accumulation, diversity, and taxonomy. Furthermore, I find that specific microorganisms are better adapted to take advantage of specific minerals/rocks.

Interpretations based on taxonomy of attached communities suggest that microbes select for specific minerals according to their metabolic requirements and environmental tolerances. Specifically, the combination of buffering-capacity, cell wall electronegativity, nutrient content of the rock, and competitive exclusion of some populations control biomass density, α-diversity (local diversity), and β-diversity (global diversity) of the attached communities on mineral and rock surfaces. I suggest that these relationships may be ingrained in the genetics of microorganisms as they have adapted and evolved, largely attached to these surfaces.

Chapter 3 examines the phylogenetic relationship between microorganisms and the natural surfaces they colonize. I use high-throughput pyrosequencing of bacterial 16S rRNA sequences to examine the response of community structure and diversity to environmental stimuli (pH variability, carbon and phosphate limitations/amendments) as biofilms develop on various geochemical surface types (carbonates, silicates, aluminosilicates, planktonic) within laboratory flow-through biofilm reactors. I use phylogenetic distance measures (UniFrac), to cluster the microorganisms according to their genetic diversity. Through permutational multivariate analysis of variance (PERMANOVA) I evaluate the statistical probability that mineralogy and/or environment influence microbial phylogeny and community structure (McArdle & Anderson, 2001). I show that surface type significantly controls ~70-90% of microbial phylogenetic diversity regardless of environmental pressures. Consistent patterns also emerged in the taxonomy of specific guilds (sulfur-oxidizers/reducers, gram-positives, acidophiles) due to variations in media chemistry. I also determine the relative impacts of environmental pressures (carbon source, pH, phosphate availability) on community structure, phylogenetic diversity, taxonomic diversity, membership, and biomass accumulation. There have been studies demonstrating preference of specific taxa to specific surfaces.

However, this study is likely the first to statistically link the phylogenetic diversity of microbial communities to specific natural surface types under a variety of geochemical conditions. Additionally, I coin the term mineraltrophic and define it as microorganisms with a genetically ingrained affinity for specific mineral types.

Chapter 4 is an investigation into the effect of non-photosynthetic communities on stable carbon isotope signatures. I test the viability of using the biogeochemical dynamics of carbon cycling by sulfur metabolizers in sulfuric acid karst environments to infer microbial community structure and function using $\delta^{13}C_{CO2}$. Here I inoculate separate flow-through bioreactors with 1) a pure culture of mixotrophic sulfur-oxidizing *Thiothrix unzii* and 2) a mixed culture (composed of SOB and SRB) from LKC to see if metabolic shifts can be detected by monitoring select geochemical indicators ($\delta^{13}C_{CO2}$, $[CO_2]$, Ca^{2+}, and pH). I find that changes in carbonate solubility are uniquely and adequately sensitive to changes in sulfur metabolizing community function. Carbonate dissolution is ~13X faster than abiotic rates when a reactor community is dominated by autotrophic sulfur-oxidizers. The increased dissolution and preferential reduction of $^{12}C_{CO2}$ over $^{13}C_{CO2}$, causes heavier $\delta^{13}C_{CO2}$ that is enriched up to +3.8‰. Under heterotrophic conditions, sulfate-reduction pathways dominate causing decreased carbonate dissolution rate. The slower rate and preferential oxidation of $^{12}C_{Acetate}$ causes lighter $\delta^{13}C_{CO2}$ values depleted in ^{13}C to values as low as -36‰. Using 16S rRNA sequences of communities, during specific metabolic intervals, I show that this is an ideal system to use stable carbon isotopes to infer community structure and function. Additionally, this study documented the responsiveness of guild composition in a microbial community to geochemical stimuli. Future studies using this method have the potential to resolve microbial community function, composition, and carbon balance to at unprecedented levels of detail.

Chapter 5 is a synthesis of the findings of these investigations with concluding remarks. Specifically this chapter highlights significant findings and scientific impact of each investigation separately and in the context of the whole dissertation. This chapter is also an account of the motivations that connect the separate chapters. Furthermore, this chapter critically evaluates the successes and failures of each investigation as they pertain to potential future investigations.

Chapter 2: Mineral microniches control the diversity of subsurface microbial populations

2.1 ABSTRACT

Rocks and minerals surround the subsurface microbial habitat, yet mineralogy and rock chemistry are rarely considered when characterizing microbial diversity and the microbial ecosystem (Ehrlich, 1996; Konhauser, 2007). Using laboratory biofilm reactors with both a pure culture of *Thiothrix unzii* and a mixed environmental sulfur-metabolizing community I found that the combination of buffering-capacity, cell wall electronegativity, nutrient content of the rock, and competitive exclusion of some populations control biomass density, α-diversity (local diversity), and β-diversity (global diversity) of the attached communities on mineral and rock surfaces. This suggests that different populations are better adapted to, and more competitive on, specific rock types. The primary influence on rock/mineral colonization by sulfur-oxidizing organisms is the acid-buffering capacity of the mineral substratum, with neutrophiles preferentially colonizing highly buffering carbonate rocks, while acidophiles select non-buffering quartz. Beyond chemical controls, *Thiothrix* (often found in mid-ocean ridge environments) demonstrates an affinity for basalt, where it excludes other sulfur-oxidizers. A pure culture of *T. unzii* preferentially colonizes carbonates while all very closely related *Thiothrix* spp. are excluded from these same rock samples in a mixed culture. I report here e[1]xperimental evidence that microorganisms colonize rock surfaces

[1] This chapter has been published as: A.A. Jones, P.C. Bennett, 2014, Mineral microniches control the diversity of subsurface populations, Geomicrobiology Journal, 31: 246-261. Research for this publication was supervised and co-authored by Philip C. Bennett.

according to the rock's chemistry and the organism's metabolic requirements and tolerances. These results suggest that adaptations to specific rocks are retained even when the organism is displaced in time and space from an ancestral rock habitat.

2.2 INTRODUCTION

In the subsurface environment most microorganisms are found attached to rock surfaces (Ehrlich, 1996; Konhauser, 2007), sometimes forming complex biofilm communities, but often simply as scattered individual cells or groups of cells. The traditional view of the association between microorganisms and minerals in the subsurface focuses on attraction forces, surface conditioning, attachment mechanisms, and biofilm development (Banfield & Hamers, 1997; Hazen et al, 1991; Korber et al, 1995), and the mineral matrix is assumed to be a simple, homogeneous and largely unreactive substratum. The microbial community, in contrast, is viewed as a dynamic and complex consortium that is influenced almost exclusively by physicochemical (e.g., temperature, pH, redox potential, salinity) or biochemical (e.g., growth substrate, nutrient or electron acceptor availability) factors (Madigan et al, 2009). Rocks and minerals, however, are neither simple nor homogeneous, and often contain trace elements or other properties that may be either toxic or beneficial to microbial growth, accessory phases containing valuable nutrients, and may provide benefits such as pH buffering or advantageous surface properties.

One overt consequence of subsurface microbe-mineral interactions is the formation of karst porosity and even caves through microbially enhanced limestone corrosion. Generally, karst and cave development (speleogenesis) occurs in soluble

carbonate rocks that dissolve by chemical solution, creating cavernous porosity (caves) in the subsurface as well as distinctive surface features such as sinkholes and dolines (White, 1988). For most karst development the dominant acid generating species is carbon dioxide derived from surface processes, and the process is termed epigenic karst (White, 1988).

For a few caves, however, including Movile Caves (Romania), the Frasassi Caves (Italy), and Lower Kane Cave, acid is generated by the oxidation of hydrogen sulfide to form sulfuric acid that promotes rapid limestone dissolution (Palmer, 1991). This process, termed sulfuric acid speleogenesis, or SAS, is suspected of being implicated in up to 20% of the karst worldwide, and is an important subsurface weathering phenomenon. Early studies of LKC, the type locale for SAS (Egemeier, 1981), assumed that abiotic H_2S autoxidation is the important process and did not consider microbial H_2S oxidation. However, members of our research group have shown that microbial oxidation is likely the predominate pathway (Engel et al, 2004b; Steinhauer et al, 2010). In these systems, chemolithotrophic sulfur-oxidizing bacteria (SOB) take advantage of the redox gradient and generate energy through oxidation of H_2S and other reduced sulfur compounds (Engel et al, 2004a; Engel et al, 2004b; Sarbu et al, 2000; Sarbu et al, 1996).

Previous field experiments suggest differential colonization of rock surfaces (Bennett et al, 2001; Engel et al, 2004a; Rogers & Bennett, 2004), where different minerals sustain different communities, and different amounts of biomass. However, these studies were based largely on morphological characteristics observed by scanning electron microscopy (SEM) of individual mineral specimens from field microcosm

experiments. More recently, indications from long-term field incubations with sulfide minerals suggest community differentiation between different sulfide mineral compositions (Sylvan et al, 2012). Additionally, there appears to be a correlation between microbial community structure and mineralogy in the soil zone (Carson et al, 2009).

The subsurface and other non-photic (dark) biospheres are the largest microbiological habitat on earth and the most poorly understood (Edwards et al, 2012). Research has revealed evidence that microorganisms in these habitats are likely highly dependent on minerals for a variety of functions. These include the dependence of lithoautotrophs living in the Columbia River Basalt Group on the basalts for a series of complex biogeochemical processes (Anderson et al, 2001; Stevens, 1997; Stevens & McKinley, 1995). In both continental aquifers and deep ocean sediments, the interaction of H_2O with Fe^{2+} in the minerals composing basalt generates H_2, which can be used by methanogens or sulfate reducers to generate metabolic energy in the absence of light (Chapelle et al, 2002; Edwards et al, 2005).

We hypothesize that in these complex subsurface microbial communities, factors such as mineral chemistry, buffer capacity, and trace element (nutrient) content, influence microbial diversity and surface colonization, as not every organism will be capable of taking advantage of every mineral surface attribute, giving rise to unique associations between a specific population and specific substratum. Considering that microbes have evolved through time often in contact with mineral surfaces, it is likely that microbes and minerals may have evolved together through geologic time (Hazen et al, 2008) resulting

in microbial communities uniquely adapted to a surface, with each mineral surface being specifically altered by its best-adapted and most competitive community. This study assesses the impact of mineralogy on microbial community structure in the subsurface using laboratory reactors, which allowed microbial colonization of assorted surfaces by both a pure and mixed environmental sulfur-metabolizing microbial inoculant. Variations in microbial community structure were qualified and quantified by optical analysis, measuring total biomass accumulated, and high throughput sequencing technology for analysis of taxonomic diversity. I report here direct laboratory evidence for a selective relationship between rock composition and microbial ecology. The data revealed that under the nutrient-limited conditions common to aquifers and the deep subsurface, the community structure can be differentiated at the scale of individual mineral grains, and that each mineral supports a unique microbial consortium that expresses specific metabolic functions in order to take advantage of, or protect itself from, the unique aspects of that mineral.

2.3 Materials and Methods

To investigate the effect of mineralogy on microbial community structure, I used laboratory flow through biofilm reactors (CDC). Each reactor consisted of eight (8) sterile polypropylene coupon holders suspended in a 1-liter glass vessel with a side-arm discharge port. A liquid media (described herein) was circulated through the vessel while mixing and shear were generated by a magnetic stir vane rotated by a magnetic stir plate at 115 RPM. Sampling of the coupons was conducted by aseptically removing individual

coupon holders and harvesting the coupons. A typical experiment was three weeks in duration.

The reaction solution was prepared by equilibrating DI-H_2O water with finely powdered Iceland spar calcite. Equilibrium status, with respect to calcite, was determined by analysis of DIC, [Ca^{2+}], and pH. This solution was then filtered to 0.2 μm and 8.3 ml of 0.1 N H_2SO_4, 0.1 g $MgSO_4$ and 0.25 g NH_4Cl was added per liter and autoclaved at 121ºC for 45 minutes before adding 2 ml/L and 5 ml/L of filter-sterilized trace metal solution and Wolfe's Vitamin solution, respectively (Burlage, 1998).

The final prepared solution had a pH of ~6.9 and contained (approximately) 0.1 mM HCO_3^-, 0.83 mM $SO_4^=$ and 1.0 mM Ca^{2+}, with a typical saturation state with respect to calcite ($\Omega_{calcite}$) of ~0.01 (SI~-2). Where, $\Omega_{calcite}=IAP/K_{sp}$, IAP is the ion activity product ($aCa^{2+} \cdot aCO_3^{2-}$) and K_{sp} is the calcite solubility product. Six hundred ml of this solution was transferred to a vessel to be combined with the reduced sulfur source, and pumped aseptically through the reactor at 1.2 ml/min. The reduced sulfur electron donor was $S_2O_3^{2-}$ and was prepared from a stock filter sterilized 1M solution of $Na_2S_2O_3$ mixed in-line via a syringe pump to a final concentration of 0.83 mM. Reactor volume was held constant at 400 ml, and the outflow tubing was outfitted with a glass bubble trap to ensure no microbial contamination from drainage.

2.3.1 Mineral Substrata Preparation

Bulk mineral specimens of Iceland spar calcite (calcite), Ontario microcline (microcline), albite, chert, Columbia River basalt (basalt), and quartz were obtained from

Ward's Natural Science Establishment Incorporated, and these minerals have been previously used and characterized (Bennett et al, 2001). Unaltered Mississippian-age Upper Madison Limestone and Upper Madison Dolostone was collected from an outcrop near Lower Kane Cave and characterized by X-Ray powder diffraction (XRD) and environmental scanning electron microscope (ESEM) energy dispersive x-ray analysis (FEI-Philips XL-30 TMP). The limestone is a nearly pure calcite (microsparite) with minor quartz component, and the Madison Dolostone is nearly pure dolomite also with a minor quartz component (Plummer et al, 1990). For ease of reference the general composition, natural geologic setting, potential benefits to microorganisms, and specific attributes of each of these specimens is presented in Table 2.1. Analysis of ammonia and phosphate in dissolved Madison Limestone and Madison Dolostone were done by colorimetry (Chemetrics) after first dissolving 1g of each into concentrated hydrochloric acid.

All samples for use in the biofilm chamber except the Iceland spar calcite were cored with a diamond coring bit on a drill press, cut to ~2 mm thickness with a diamond saw, and polished using thin section preparation techniques both to give a uniform starting surface and to match the dimensions necessary to fit the CDC reactor rods (12.7 mm outer diameter). Iceland spar calcite was prepared to the same specifications by first fracturing the samples to the correct thickness with a razor blade and then hand polishing the samples with 600 grit sandpaper to the correct diameter and circular shape. Prior to the experiment, mineral coupons were rinsed with media solution to remove debris, weighed to 0.1 mg, mounted on the coupon holders and suspended in the reactor, and the

Surface	General Composition and Source	Subsurface Environment	Potential Benefit to Microorganisms
Calcite	$CaCO_3$ Iceland Spar Calcite	Limestone Caves and Karst, Cement in sedimentary rocks	Buffering Capacity[2], Inorganic C, Ca
Madison Limestone	$CaCO_3$ Lower Kane Cave, WY, USA	Caves, Karst, Continental Seafloor, Thick continental deposits	Buffering Capacity[2], Inorganic C, Ca, Trace Nutrients
Madison Dolostone	$CaMg(CO_3)_2$ Lower Kane Cave, WY, USA	Caves, Karst, Continental Seafloor, Thick continental deposits	Buffering Capacity, Inorganic C, Ca, Trace Nutrients
Microcline	$KAlSi_3O_8$ Ontario Microcline[1]	Igneous rocks, Arkose sandstones	Trace Nutrients[1], Competitive Exclusion by Al Tolerant Microorganisms
Albite	$NaAlSi_3O_8$ Ontario Plagioclase[1]	Igneous rocks, Arkose sandstones	Trace Nutrients[1], Competitive Exclusion by Al Tolerant Microorganisms
Chert	SiO_2 Lower Kane Cave, WY, USA	Sandstones, limestones, dolostones, conglomerates	Neutral/Stable Surface, Trace Nutrients[1]
Basalt	Fe, Mg, Ca, Al, Si, O; Columbia River Basalt[1]	Seafloor, Deep Sea Sediments, Rift Zones	Fe Redox, Inorganic P, H_2 source for Methanogens & SO_4^{2-} reducers[3]
Quartz	99.78% SiO_2 Hydrothermal Crystal[1]	Igneous rocks, sandstones, shales, siltstones, mudstones, conglomerates	Neutral/Stable Surface, Trace Nutrients[1]

Table 2.1: General composition, common subsurface environments, potential benefits to microorganisms, and special properties specific to the rocks/minerals used in the biofilm reactor experiments. Superscripts refer to papers with additional information (1-Bennett and Others 2001, 2-Steinhauer and Others 2010, 3-Edwards and Others 2005).

entire apparatus was autoclaved at 121ºC for 45 minutes. Scanning electron microscope (SEM) examination of all starting material specimens was used to compare with coupons run through the experimental processes.

2.3.2 Microbial Inoculant

Thiothrix unzii was used as the pure-culture inoculant for the biofilm experiments. *T. unzii* is a colorless, filamentous, neutrophilic, chemoautotrophic, sulfur-oxidizing member of the *Gammaproteobacteria* class that is known to use both sulfide and thiosulfate as sulfur sources and have the ability to store sulfur intracellularly (Howarth et al, 1999). *T. unzii* is closely related to *Thiothrix* spp. that are known to dominate the biomat community within Lower Kane Cave (Engel, 2004). After the reactor had stabilized with media flowing through it, 15 ml of cultured *T. unzii* was added to the reactor for the experimental run.

A Lower Kane Cave (LKC) biomat was used as the environmental inoculant for the biofilm reactors. LKC is located in the Bighorn River Valley, WY, USA (44º44' N, 108º11' W) and has a single horizontal passage extending about 325 meters into the canyon wall, parallel to the fold axis of the Little Sheep Mountain Anticline in the Madison Limestone (Stock et al, 2006). The Madison Formation is ~150–250 m thick Mississippian-age thin to medium-bedded massive grey limestone and dolomite with occasional chert and shale (Peterson, 1984). The cave has three major and several minor springs that discharge sulfidic water to a single cave stream that discharges at the cave entrance. Spring discharge water is a mixture of meteoric water from Madison Limestone and slightly thermal (~23.5ºC) waters from fractures in the Little Sheep

Mountain Anticline (Peterson, 1984). LKC is near several Madison hosted oil fields, from which sulfidic waters originate (Egemeier, 1981; Peterson, 1984).

The LKC springs support thick biomats dominated by a diverse consortium of SOB from the *Epsilonproteobacteria* and *Gammaproteobacteria* classes as well other members of the *Proteobacteria* lineage (Engel, 2004). Microorganisms belonging to many distinct lineages within the *Proteobacteria* are associated with these spring features that include the following genera: *Thiothrix*, *Thiobacillus*, *Thiomonas, Thiomicrospira, Thiovulum,* and *Achromatium* (Engel, 2004; Engel et al, 2003). The dominant organisms in the microaerophilic stream reaches near discharge outlets belong to lineages within the *Epsilonproteobacteria* class (Engel et al, 2003); as oxygen increases, *Thiothrix* spp. dominate the mat communities (Engel, 2004). Many members of these lineages are known sulfur-oxidizers.

The mixed community was obtained from Lower Kane Cave at 196 meters from the back of the cave at the upper spring location. Samples were collected in the field in sterile falcon tubes with a small amount of stream water, and transported back to the laboratory for use in the experiments. Approximately 15 ml of the raw mat was added to the sterilized and stabilized CDC biofilm reactor for each experiment.

2.3.3 Biomass Accumulation

Specific experiments were run to measure biomass accumulation on the mineral coupons. Three reactor experiments were run under identical input media conditions at pH 6.6, with an additional experiment at pH 8.3 in equilibrium with calcite. Each triplicate set of mineral coupons was weighed, placed in a drying oven overnight at

104ºC, then weighed again. The triplicate coupons were then processed by 3 x 5-minute cycles of alternating sonication and vortexing in a calcite equilibrated (to prevent dissolution) 2% tween 20 solution to remove the biomass, and then dried and weighed again. The difference between the final dry weight with biomass and the dry weight after processing was assumed to be the accumulated biomass. Select chips were also retrieved for imaging on a FEI-Philips XL-30 TMP SEM following previously published methods for chemical critical point drying (Bennett et al, 2006).

2.3.4 Community Analysis

Identical experiments were run specifically for microbial community analysis by 16S rRNA sequencing and analysis. DNA extraction was conducted using methods modified slightly from Engel and others (Engel et al, 2003). Biomass was aseptically removed from the substrata coupons and transferred to a sterilized solution composed of 1 mM EDTA and 0.9X phosphate-buffered saline (PBS) and samples were physically disrupted by freeze-thaw (3 times, -80°C to 65°C) cycles. The samples were then disrupted by 5-minute cycles of alternating sonication and vortexing (3X). The solutions were then transferred into sterile 15 ml tubes and centrifuged at 5000 rpm for 10 minutes, and the supernatant decanted. Genomic DNA was extracted from biomass using an Ultraclean Microbial DNA Isolation Kit (MoBio Laboratories, Inc.; Catalog # 12224-50) and stored at -80°C. Bacterial 16S rRNA genes were amplified using the 28F/519R primer set (Lane, 1991), adaptors and barcodes for 454 pyrosequencing were ligated, and

sequencing on a Roche 454 GS-FLX Titanium™ (454 Life Sciences, Branford, CT, USA) was performed at the Research and Testing Laboratory (Lubbock, TX, USA).

Sequences were depleted of barcodes and primers, and then short sequences <150bp, sequences with ambiguous base calls, and sequences with homopolymer runs exceeding 6bp were all removed. Sequences were then denoised using Ampliconnoise and chimeras removed using Chimera Slayer (Haas et al, 2011; Quince et al, 2011). An average minimum quality score of 25 over a window of 50 bp was used to remove low quality sequences (Bowen De León et al, 2012). For statistical analysis, operational taxonomic units were defined by clustering at 3% divergence (97% similarity) (Barriuso et al, 2011). OTUs were then taxonomically classified using BLASTn against a curated GreenGenes database (DeSantis et al, 2006) and compiled into each taxonomic level with the actual number of sequences and proportional abundances of sequences within each sample that map to the designated taxonomic classification. Due to the shorter length of sequences obtained from 454 pyrosequencing it is generally considered acceptable to resolve taxonomic identity to the genus level. Therefore, the analyses reported herein do not attempt to overreach to the species level.

The resulting dataset was manually processed to reveal both sequence counts and proportional abundances of microbial sequences present on each substratum. To assess the impact of mineralogy on metabolism of attached communities, the taxonomy of sulfur-oxidizing bacteria (SOB, the dominant organism in LKC) was resolved to the genus level and the assigned taxa were compared to extant taxa described in the literature.

Alpha and beta diversity values were calculated on the resulting datasets using Mothur (Schloss et al, 2009). Microbial community alpha diversity for sequences attached to each surface was evaluated in terms of the species richness (S, the total number of OTUs), Simpson dominance index (D, Formula 2.1), Shannon index (H', Formula 2.2), and species evenness (E, Formula 2.3). Inverse-Simpson (1/D) gives more weight to dominant OTUs by expressing the likelihood that two individuals, chosen at random, will belong to different OTUs. The Shannon Weiner index (H') gives more weight to the rare individuals representing low abundance OTUs:

$$D = \sum_{i=1}^{S} \left(\frac{n_i(n_i-1)}{N(N-1)} \right) \quad (2.1)$$

where n_i is the number of sequences assigned to the ith OTU and N is the total number of sequences within the sample (Hill et al, 2003).

$$H' = -\sum_{i=1}^{S} p_i \ln(p_i) \quad (2.2)$$

where p_i is the proportion of sequences assigned to the ith OTU (Hill et al, 2003).

$$E = \frac{H'}{\ln(S)} \quad (2.3)$$

Where H', and S are the Shannon index and species richness, respectively (Hill et al, 2003).

There are several formulas that can be used to calculate beta diversity each with its limitations and specialized applicability (Chao et al, 2005). For this study the abundance-based Sorenson similarity index (β) (Formula 2.4) was used to calculate the fraction of individual sequences that belong to shared OTUs (Chao et al, 2005).

$$S_{abd} = \frac{2UV}{U+V} \quad (2.4)$$

where,

$$U = \sum_{i=1}^{D_{12}} \frac{X_i}{n} + \frac{(m-1)}{m} \frac{f_{+1}}{2f_{+2}} \sum_{i=1}^{D_{12}} \frac{X_i}{n} I\,(Y_i = 1)$$

and

$$V = \sum_{i=1}^{D_{12}} \frac{Y_i}{m} + \frac{(n-1)}{n} \frac{f_{1+}}{2f_{2+}} \sum_{i=1}^{D_{12}} \frac{Y_i}{m} I\,(X_i = 1)$$

In these formulas U and V represent the total abundances of the shared individuals in samples 1 and 2, respectively, D_{12} denotes the number of shared OTUs between sample X and Y, X_i and Y_i are the number of individuals in OTU i of sample X and Y, m and n are the total individuals sampled from samples X and Y, f_{1+} and f_{2+} are the number of shared OTUs with one or two individuals observed in sample X, and f_{+1} and f_{+2} are the number of shared OTUs with one or two individuals observed in sample Y. I (Y_i =1) and I (Y_i =1) are indicator expressions used to account for lower abundance OTUs such that I=1 if the expression is true and I=0 if the expression is false.

This formula was used to circumvent the limitations inherent to classical Jaccard and Sorenson indices as the samples in this study had high abundances of rare OTUs and large discrepancies in sample size (Chao et al, 2005). The abundance-based Sorenson similarity index was then used to assess the proportion of individual sequences that belong to shared OTUs. The resulting values were used to calculate the length and position of the nodes in dendrograms. The resulting .tre file was converted into a dendrogram using FigTree v1.3.1 (http://tree.bio.ed.ac.uk/software/figtree/).

2.4 RESULTS

2.4.1 Biofilm Accumulation

For the 3-week pure culture experiments using *Thiothrix unzii* the greatest biofilm accumulations were found on Madison Limestone (14.4 ± 1.5 mg·cm^{-2}) and Madison Dolostone (25.9 ± 4.1 mg·cm^{-2}) while substantially less biomass was found on the other mineral coupons (Figure 2.1; Table 2.2). Chert had the least accumulation with only 0.4 ± 0.1 mg·cm^{-2}, while the feldspars had nearly identical accumulations (1.2 ± 0.4 mg·cm^{-2}) (Figure 2.1; Table 2.2). Calcite had only 2.3 ± 0.3 mg·cm^{-2} of biomass accumulation (Table 2.2).

Biofilm reactors containing the same substrata but amended with microbial mat collected from LKC also resulted in more growth on the Madison Limestone and Madison Dolostone surfaces, accumulating 17.8 ± 2.3 mg·cm^{-2} and 20.6 ± 6.8 mg·cm^{-2} of biomass respectively after three weeks (Figure 2.1; Table 2.2) with substantially less on pure calcite. More biomass accumulated on basalt compared to calcite and silicate minerals in both pure (3.6 ± 1.0 mg cm^{-2}) and mixed culture (5.4 ± 1.4 mg cm^{-2}) experiments, (Figure 2.1; Table 2.2). Overall, the pure and mixed culture experiments had similar trends in biomass distribution between mineral coupons (Figure 2.1) and the

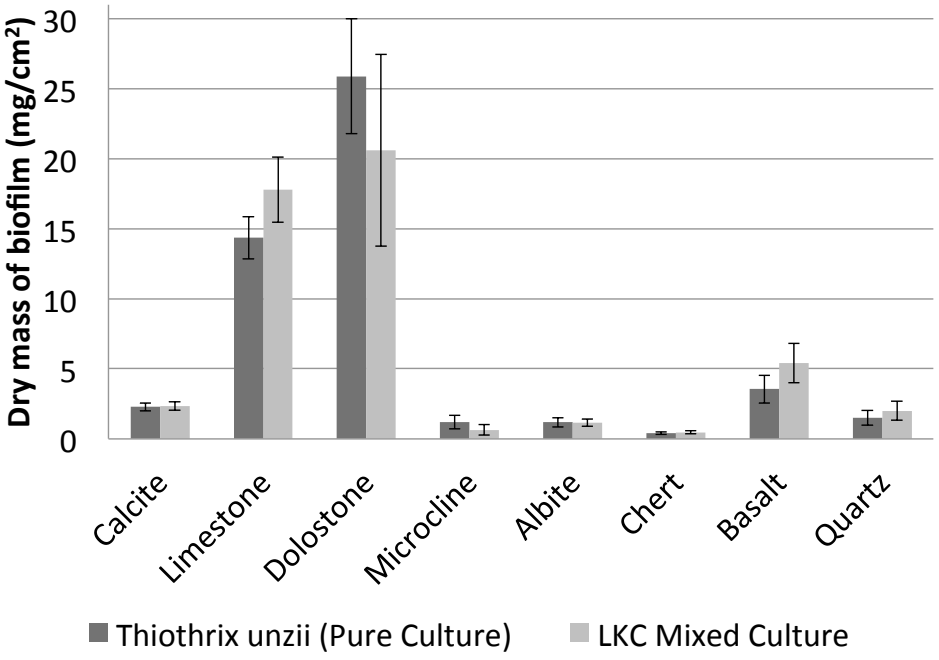

Figure 2.1: Dry weight (mg/cm^2) of biomass accumulation on rock and mineral surfaces for both *Thiothrix unzii* and a mixed culture obtained from Lower Kane Cave. Error bars denote standard deviation, n=3 (see Table 2.2).

	Dry Mass of Biofilm (mg/cm^2)					
Surface	**CDC 1 T.*unzii* pH 6.6**	**CDC 2 Mixed pH 6.6**	**CDC 3 Mixed pH 6.6**	**CDC 4 Mixed pH 8.3**	**Mixed Standard Deviation**	**T. *unzii* Standard Deviation**
Calcite	2.3	2.0	2.4	2.7	0.3	0.3
Limestone	14.4	19.3	18.2	19.3	2.3	1.5
Dolostone	25.9	10.6	22.3	23.6	6.8	4.1
Microcline	1.2	0.6	0.6	0.2	0.4	0.5
Albite	1.2	1.5	0.9	1.1	0.3	0.3
Chert	0.4	0.5	0.4	0.6	0.1	0.1
Basalt	3.6	5.4	5.8	6.9	1.4	1.0
Quartz	1.5	2.9	1.5	2.1	0.7	0.5

Table 2.2: Dry mass of biofilm values and standard deviations. The standard deviation for the pure culture experiment are the result of triplicate experiments with the dry biomass values in the table as the mean of the three. The standard deviations of the mixed culture are for all three mixed culture experiments shown in the table.

biomass accumulation on mineral surfaces did not show a bulk media pH dependency (Table 2.2).

After three weeks within the reactor there were obvious differences in biofilm development. The carbonates and the basalt sample had thick, white, wispy-filamentous accumulations of biofilm, while the remaining silicates appeared to have little or no biofilm accumulation. SEM examination supported the finding that Madison Limestone and Madison Dolostone substratum were consistently, and almost completely, covered by microbial filaments of *Thiothrix unzii* and LKC mixed community, leaving very little of the surface exposed and had more extensive biomass accumulations than silicate minerals or pure Iceland spar calcite in the same reactor (Figure 2.2). Quartz and the feldspars (albite and microcline) have very little coverage with relatively few filaments in pure culture (Figure 2.2a, c, e, g, & i) and no filaments in mixed culture (Figure 2.2b, d, f, h, & j). However, the feldspars accumulated single-celled microorganisms in discrete clumps while the quartz had single-celled organisms that were individually, but homogenously spread over the entire surface (Figure 2.2b & d). These results were consistent with biomass accumulation results, showing homogeneous distributions of *T. unzii* filaments on most substrata (Figure 2.2a, c, e, g, & i), with greatest biomass density on the carbonate rocks. In mixed culture, basalt was the only non-carbonate surface to support substantial accumulations of filamentous sulfur-oxidizers in both pure and mixed cultures (Figure 2.2e & f). However, there are obvious differences in the morphology of the biofilms on these surfaces. The filaments on the carbonate surfaces are coated by

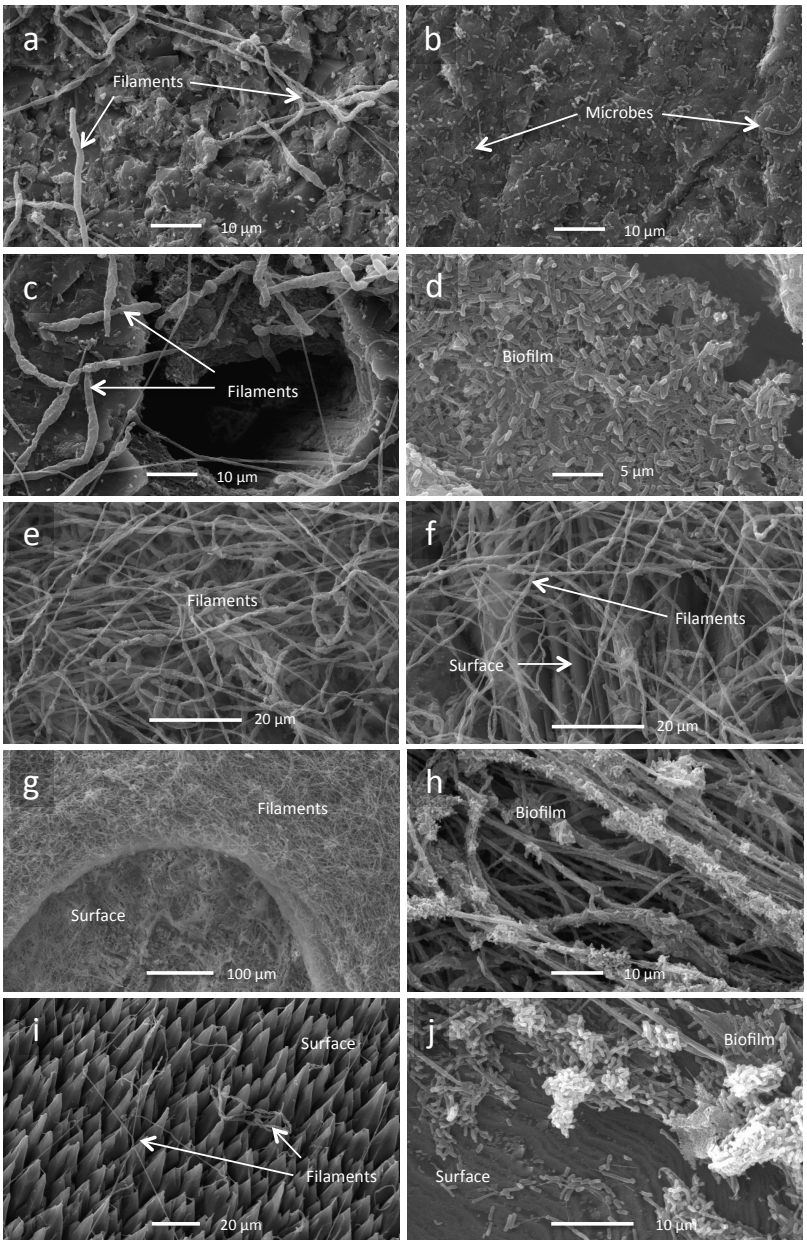

Figure 2.2: SEM images of microbial colonization on surfaces after 3-weeks exposure to *Thiothrix unzii* (a,c, & e, g, & i) and the mixed LKC community (b,d, f, h, & j). (a) & (b) are quartz. (c) is albite and d is microcline. (e) & (f) are images of the biofilm accumulation on the basalt surface. (g) and (h) are Madison Limestone. (i) and (j) are calcite. Note that Madison Dolostone is excluded because it is nearly identical to Madison Limestone. Horizontal white lines are scale bars.

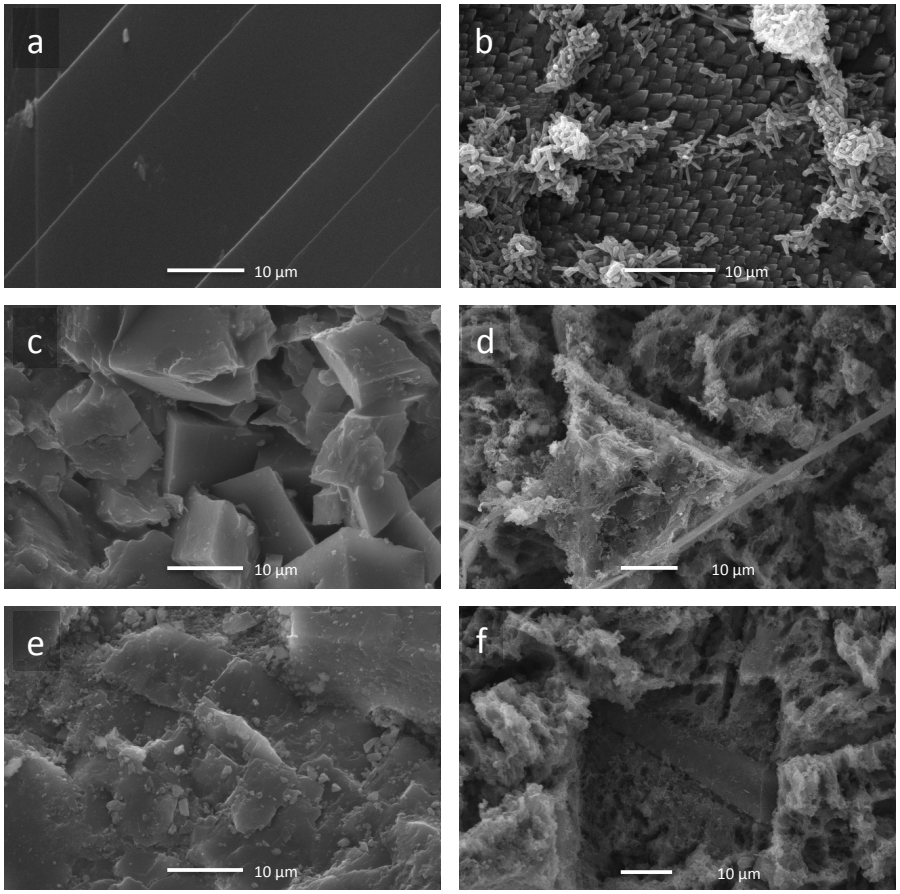

Figure 2.3: SEM images of Abiotic vs. Microbial (LKC mixed culture) carbonate corrosion after 3 weeks within a CDC reactor at pH=6.6: (a) abiotic calcite, (b) microbial calcite, (c) abiotic Madison Limestone, (d) microbial Madison Limestone, (e) abiotic Madison Dolostone, (f) microbial Madison Dolostone. All scale bars are 10 µm.

biofilms composed of single-celled organisms, while the filaments on basalt appear uncoated (Figure 2.2f, j, &f).

Carbonate colonization and the accompanying aggressive sub-biofilm corrosion was examined by SEM imaging. After three weeks in an abiotic reactor with media with a sustained pH of 6.6 there was no obvious corrosion features on any of the carbonate surfaces (Figure 2.3a, c, & e). After three weeks in a reactor inoculated with an LKC mixed community, however, I found that even when the media was close to equilibrium with calcite, aggressive dissolution of carbonate substratum occurred exclusively beneath the biofilm (Figure 2.3 b, d, & f). In regions where the surface was observable through the attached filaments (and regions where the biofilm was removed), the carbonate surface appeared aggressively corroded (Figure 2.3). Specifically, the calcite had a "spikey" corrosion texture that was isolated to regions where biofilm was present (Figure 2.2i, 2.2j, & 2.3b) and both the Madison Limestone and Madison Dolostone showed deeply pitted corrosion textures (Figure 2.3d & f).

2.4.2 Microbial Diversity

At the species level (0.97 similarity cutoff), there was a very large spread in the total OTUs associated with each surface. In terms of richness (S) the number of different OTUs ranged from 21 on albite to 197 on microcline, while the carbonates had a smaller range of 71 on calcite to 87 on the Madison Limestone (Table 2.3). Similarly, measures of diversity Inverse-Simpson's dominance index (1/D) and Shannon Weiner index (H') are commensurate with species richness. The carbonates, quartz, and albite all had a

small range of H' (from 2.41 to 2.80) and 1/D (from 7.03 to 10.61) values (Table 2.3). The outliers were basalt with the lowest diversity (H'=1.63 & 1/D=2.22) and microcline with the highest diversity (H'=4.39 & 1/D=42.97)(Table 2.3).

A majority of the microbes in the original LKC inoculant came from two dominant classes representing ~97.1% of the total sequences (Table 2.4). *Epsilonproteobacteria* represented ~62.4% and *Gammaproteobacteria* was found to represent ~34.7% of the community. *Deltaproteobacteria* represented only ~0.5% of the community (Table 2.4). At the genus level, these major lineages were nearly completely composed of *Sulfurovum* spp. (~62.3%) and *Thiothrix* spp. (~34.7%), respectively (Table 2.4).

Despite this dominance of *Epsilonproteobacteria* in the inoculant, *Epsilonproteobacteria* were almost exclusively found on the carbonates as the representative genus *Sulfurovum* (Table 2.4, Figure 2.4). *Gammaproteobacteria* were proportionally abundant on the carbonates (>23%) and basalt (~70%); and less abundant on albite (~20%), microcline (~16%), basalt (~9%) and quartz (~1.8%) (Table 2.4, Figure 2.4). *Deltaproteobacteria* were rare on every surface, but most abundant on albite (~4%) as the genus *Desulfococcus* (Table 2.4, Figure 2.4). *Alphaproteobacteria* were proportionally abundant on the carbonates (>57%) and albite (>56%) and less abundant on microcline (~24%), basalt (~9%), and barely detected on quartz (Table 2.4, Figure 2.4).

Surface	No. Sequences	No. Sequences Subsampled	No. OTUs (S)	Shannon Wiener (H')	Evenness (E)	Simpson's Index (D)	Inverse Simpson (1/D)
Calcite	7962	6261	71	2.52	0.59	0.14	7.16
Limestone	6261	6261	87	2.80	0.63	0.11	8.79
Dolostone	7604	6261	79	2.79	0.64	0.09	10.61
Basalt	1152	1152	41	1.63	0.44	0.45	2.22
Quartz	2695	2695	125	2.49	0.52	0.14	7.03
Albite	396	396	21	2.41	0.79	0.13	7.52
Microcline	881	881	197	4.39	0.83	0.02	42.97

Table 2.3: Alpha microbial community diversity from 16S rRNA based classification of microorganisms attached to solid surfaces after 3-weeks within the reactor. Measures of alpha diversity: Simpson's dominance index (D), which favors OTUs with more sequences, and Shannon Weiner index (H'), which favors OTUs with fewer sequences (rare OTUs), Number of OTUs (species richness (S)), and Species Evenness (E).

Molecular characterization of the biofilm community on the mineral surfaces revealed a high degree of similarity between the carbonate surface microbial assemblages. The overlap in bacterial community membership between two samples (β-diversity), based on the fraction of sequences that belonged to shared operational taxonomic units (OTUs), was estimated by the abundance-based Sorenson similarity index (β). Here I defined OTUs at the 0.03 distance level, so sequences with ≥ 97% similarity were designated by a single OTU. β-diversity analysis of the carbonates revealed that Madison Limestone, Madison Dolostone and calcite had a high degree of similarity with $\beta > 0.98$, where $\beta = 0$ indicates no similarity and $\beta = 1$ indicates that samples are completely similar (Chao et al, 2005). The majority of the community on the carbonates was composed of *Alphaproteobacteria* (~57-67%) and *Gammaproteobacteria* (~24-38%)(Figure 2.4; Table 2.4). The basalt community structure was most closely related to the carbonates with $\beta \sim 0.69$. Basalt was dominated by *Gammaproteobacteria* (~70%), primarily represented by microorganisms most closely related to the genus *Thiothrix* (~66%) (Table 2.4).

Microbial taxonomic similarities between silicate substrata were far less than their carbonate counterparts (Figure 2.4). Microcline and albite had the greatest similarity between taxon distribution ($\beta \sim 0.35$). The community on microcline was composed mostly of *Alphaproteobacteria* (~25%), *Gammaproteobacteria* (~16%), and had the largest proportional abundance of *Actinobacteria* (~25%). Similarly, the community on albite was dominated by *Alphaproteobacteria* (~57%) and *Gammaproteobacteria* (~20%), but had no detectable *Actinobacteria* (Table 2.4). The Gram-positive

microorganisms of the Phyla *Firmicutes* and *Actinobacteria* were found almost exclusively on silicate surfaces and were most abundant on the feldspars (Table 2.4). Of the silicates, the community on microcline and albite were most closely related to quartz with β~0.03 and β~0.025, respectively. Quartz had the least similar community structure to any other mineral surface with β~0.035 when compared to sequences represented within OTUs assigned to carbonate surfaces (Figure 2.4). This lack of similarity was evident as quartz was the only surface to not accumulate significant *Alphaproteobacteria* (<1%) while also being the only surface to accumulate significant *Betaproteobacteria* (~44%) and *Nitrospira* (~15%).

At the genus level, there were nine taxonomic groups that are likely SOB (Table 2.4). These genera are *Bosea, Thioclava, Halothiobacillus, Thiothix, Thobacillus, Thiomonas, Sulfurovum, Acidithiobacillus,* and *Acidithiobacillus*. The carbonates accumulated a community with a large proportional abundance (~17-45%) of potential sulfur-oxidizing microorganisms with representatives of *Bosea, Thioclava, Halothiobacillus, Thiothrix, Thiobacillus,* and *Sulfurovum* (Table 2.4). Additionally, quartz accumulated ~15% potential SOB composed almost entirely of *Acidithiomicrobium* (~13%), with representatives of *Acidithiobacillus* (1%) and *Thiobacillus* (~1%) (Table 2.4). Basalt had the largest proportional abundance of SOB with ~65% representatives of the genus *Thiothrix*. The feldspars, microcline had <1% SOB and albite had ~6% potential SOB (Table 2.4).

Representative *Class*	Representative *Genus*	LKC Inoculant	Calcite	Madison Limestone	Madison Dolostone	Microcline	Albite	Quartz	Basalt
Alphaproteobacteria		**0.1**	**58.9**	**67.0**	**57.4**	**25.4**	**56.7**	**0.5**	**9.2**
	Ensifer	0.0	29.4	30.4	14.7	6.0	29.2	0.0	4.7
	Azospirillum	0.0	6.6	8.3	11.5	1.3	16.4	0.0	2.5
	Bosea	0.0	5.6	3.0	12.9	0.2	6.5	0.0	0.0
	Thioclava	0.0	6.0	3.1	7.1	0.1	0.0	0.0	0.0
	Defluvibacter	0.0	2.9	1.1	0.6	0.1	1.4	0.0	0.1
	Sphingopyxis	0.0	2.5	12.6	5.3	3.2	0.0	0.0	0.4
	Sphingomonas	0.0	0.0	0.0	0.0	3.2	0.2	0.0	0.0
	Acidisphaera	0.0	0.0	0.0	0.0	0.0	0.0	0.3	0.0
Gammaproteobacteria		**34.7**	**37.6**	**23.7**	**28.8**	**16.0**	**20.1**	**1.8**	**70.1**
	Acinetobacter	0.0	22.6	3.5	4.0	2.0	0.0	0.2	0.1
	Halothiobacillus	0.0	9.1	5.6	14.5	0.3	0.0	0.0	0.0
	Thermomonas	0.0	4.4	12.5	7.7	0.2	5.1	0.0	0.0
	Pseudomonas	0.0	0.8	0.4	0.4	4.5	10.4	0.0	0.0
	Thiothrix	34.7	0.0	0.2	0.2	0.0	0.0	0.0	65.5
	Stenotrophomonas	0.0	0.0	0.0	0.1	1.4	1.6	0.0	3.7
	Acidithiobacillus	0.0	0.0	0.0	0.0	0.0	0.0	1.2	0.0
Betaproteobacteria		**0.2**	**1.5**	**4.0**	**11.0**	**2.9**	**1.4**	**44.1**	**0.6**
	Thiobacillus	0.0	0.3	0.5	0.7	0.0	0.0	1.2	0.0
	Methyloversatilis	0.1	0.2	0.9	0.9	0.0	0.0	26.4	0.0
	Zoogloea	0.0	0.0	0.0	0.0	0.0	0.0	3.5	0.0
	Thiomonas	0.0	1.0	2.5	9.1	0.0	0.0	0.0	0.0
Epsilonproteobacteria		**62.4**	**1.2**	**2.6**	**0.7**	**0.9**	**0.0**	**0.0**	**0.0**
	Sulfurovum	62.3	1.2	2.6	0.7	0.3	0.0	0.0	0.0
Actinobacteria		**0.1**	**0.1**	**0.3**	**0.4**	**24.6**	**0.0**	**13.1**	**8.6**
	Acidithiomicrobium	0.0	0.0	0.0	0.0	0.0	0.0	12.6	0.0
	Rubrobacter	0.0	0.0	0.0	0.0	3.9	0.0	0.0	0.0
	Propionibacterium	0.0	0.1	0.1	0.1	0.8	0.0	0.2	4.7
Bacilli		**0.0**	**0.1**	**0.2**	**0.4**	**6.7**	**6.5**	**0.0**	**4.9**
	Lactobacillus	0.0	0.1	0.1	0.2	0.2	0.9	0.0	3.8
Clostridia		**0.9**	**0.1**	**0.1**	**0.1**	**3.6**	**7.9**	**2.1**	**3.5**
Sphingobacteria		**0.0**	**0.0**	**0.0**	**0.0**	**2.1**	**0.2**	**4.2**	**0.0**
Acidobacteria		**0.0**	**0.0**	**0.0**	**0.0**	**1.6**	**0.0**	**0.0**	**0.0**
		0.0	0.0	0.0	0.0	0.0	0.0	0.0	0.0
Deltaproteobacteria		**0.5**	**0.1**	**0.4**	**0.2**	**0.9**	**3.7**	**1.7**	**0.4**
	Desulfococcus	0.0	0.0	0.2	0.0	0.0	3.7	0.0	0.0
	Desulfomonile	0.0	0.1	0.0	0.1	0.0	0.0	0.0	0.4
Deinococci	***Meiothermus***	**0.0**	**0.0**	**0.0**	**0.0**	**0.0**	**0.0**	**9.4**	**0.7**
Nitrospira	***Thermodesulfovibrio***	**0.0**	**0.0**	**0.0**	**0.0**	**0.0**	**0.0**	**15.4**	**0.1**
***Class* <1% Proportional Abundance**		**0.5**	**0.5**	**1.8**	**1.1**	**15.3**	**3.5**	**7.8**	**2.0**
Total Proportion SOB		**97.0**	**23.3**	**17.4**	**45.2**	**0.9**	**6.5**	**15.1**	**65.5**

Table 2.4: Proportional abundance (%) of representative class (Bold) and representative genera from 16S rRNA gene sequence taxonomic classification for microorganisms in the LKC inoculant and those removed from each surface after 3-weeks within the biofilm reactor. Potential sulfur-oxidizing genera and total proportion of sulfur-oxidizing genera are shaded.

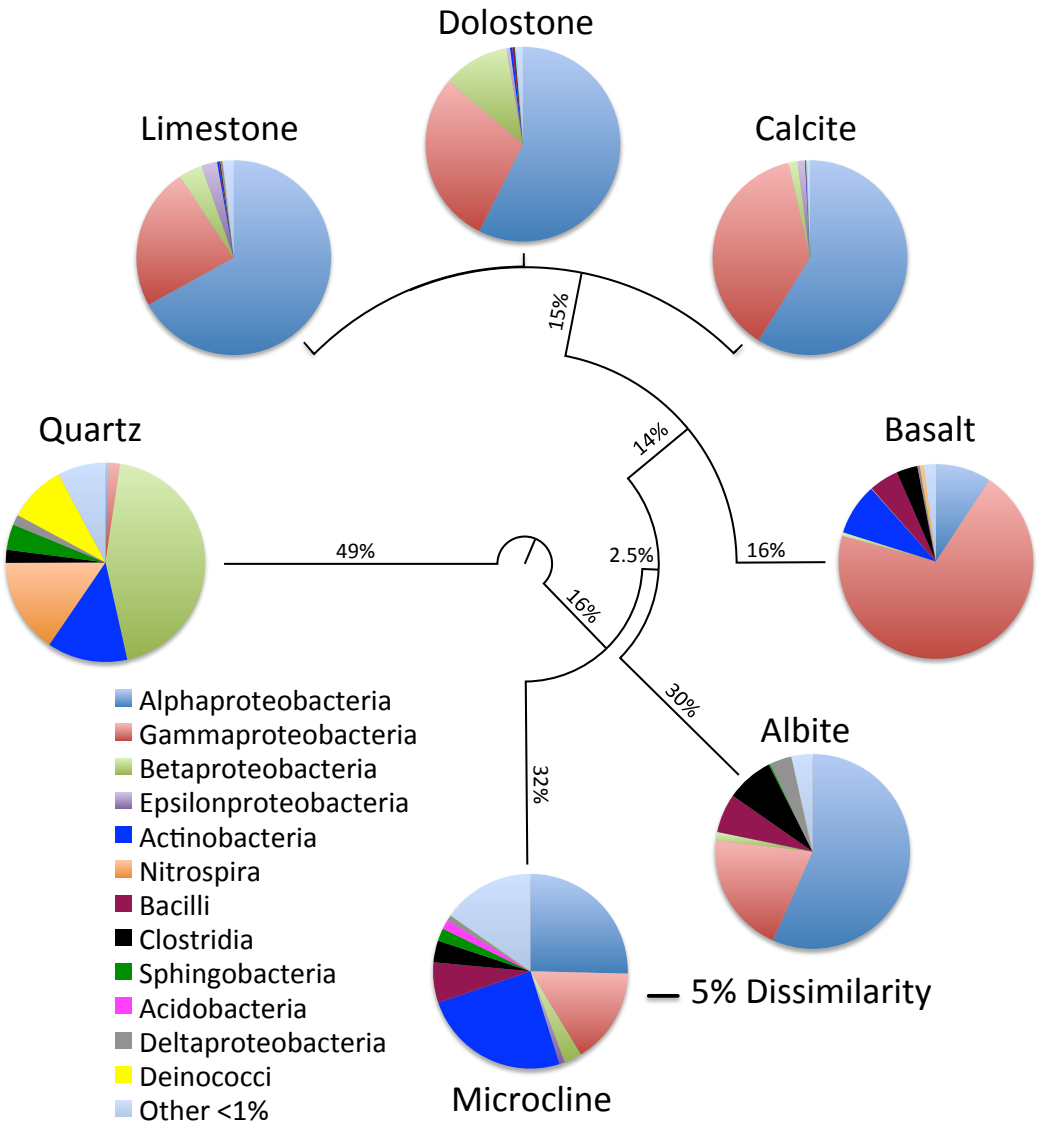

Figure 2.4: Dendrogram of bacterial β-diversity displaying the overlap in bacterial communities colonizing various solid surfaces. The key (bottom left) contains class level taxonomy associated with each mineral surface (see Table 2.4 for proportional abundances). The scale bar represents 0.05 (5%) dissimilarity in sequences isolated from each mineral/rock surface (proportion of sequences belonging to unshared OTUs). Dissimilarity increases with branch length in the outward direction. Each of the carbonate branches are ≤2% in length. Branch lengths were calculated using the abundance based Sorenson similarity index wherein OTUs were assigned at ≥ 97% similarity in sequences.

2.5 DISCUSSION

Microbes influence mineral dissolution, alteration, and precipitation (Ehrlich, 1996), and a variety of mechanisms have been implicated, including acid or alkali production, changing redox conditions, or the production of chelating biomolecules (Bennett et al, 2000; Bennett et al, 2001; Hiebert & Bennett, 1992). Often these observations are interpreted as a coincidental outcome of microbial metabolic processes, but increasingly I find that microbes benefit by interacting with minerals. Specific examples include access to mineral electron acceptors (Lovley & Phillips, 1986), buffering of excess acidity (Engel et al, 2004b), dissolution of apatite to release P (Jansson, 1987; Rogers & Bennett, 2004), and sulfide and ferromagnesian silicate dissolution for enzyme cofactors (Banfield et al, 1999) such as copper for the particulate form of methane monooxygenase (Knapp et al, 2007; Semrau et al, 2010). Even subtle differences in the chemistry of similar minerals or glasses result in dissimilar surface biofilms, based on the presence or absence of a limiting nutrient or toxic element (Rogers & Bennett, 2004).

As an alternative to analyzing sequences of nearly full-length PCR amplicons of homologous genes from environmental DNA samples, sequence fragments from hypervariable regions in rRNA can provide measures of richness and relative abundance for OTUs in microbial communities providing information about taxonomic identity and microbial diversity that has previously been unobtainable (Sogin et al, 2006). This technological advance offers a novel method for statistical comparison of complex microbial communities (Schloss et al, 2009). Combining this information with

environmental biogeochemical variability allows researchers to isolate the impact of this variability on microbial community structure.

In this study, 16S rRNA analysis of microorganisms attached to mineral surfaces revealed substantial variability in microbial community structure on different minerals. However there was a large discrepancy in the total number of sequences that could be used to analyze diversity. While this should have had a minimal effect on α-diversity values, adjustments were required for β-diversity calculations. With this in mind, all calculations were normalized to the smallest dataset for each analysis and the remaining samples were randomly sampled in order to maximize the entire breadth of the dataset (6261 using only the carbonates, 2695 including the quartz, 1152 including the basalt, 881 including microcline, and 396 including albite). The diversity values were normalized to the number of sequences subsampled (Anderson et al, 2011). When examining variations in community structure, proportional abundance is important and should not be ignored in these types of studies, as quantitatively dominant species will likely play a larger role in biogeochemical processes within the community (Anderson et al, 2011).

LKC is host to a very diverse microbial community and previous studies provide details of the microbial taxonomy and phylogeny of the biomass (Engel et al, 2003). LKC hosts microbial mats dominated by putative autotrophic, sulfur-oxidizing bacteria (SOB) of the *Epsilonproteobacteria* and *Gammaproteobacteria* classes, with sulfate-reducing *Deltaproteobacteria* dominating the associated anaerobic community (Engel et al, 2003; Engel et al, 2004a). Consistent with previous studies, the environmental inoculant used in

this study was also dominated by *Gammaproteobacteria* (34.7%) and *Epsilonproteobacteria* (62.4%) (Table 2.4). In the inoculant, these two lineages were composed almost exclusively of the genera *Thiothrix* spp. and *Sulfurovum* spp., respectively. *Sulfurovum* spp. are known to be mesophilic microaerobes that use sulfur species as electron donors capable of using either nitrate or oxygen as the electron acceptor (Huber et al, 2007). *Epsilonproteobacteria* have recently been recognized as important filamentous, sulfur-oxidizing members of deep-sea hydrothermal vent communities (Campbell et al, 2001; Corre et al, 2001). Lower Kane Cave was the first nonmarine natural system that was found to be dominated by the acitivity of *Epsilonproteobacteria* (Engel et al, 2003). However, *Epsilonproteobacteria* were poorly represented in microbial communities colonizing mineral surfaces and were limited to calcite and Madison Limestone surfaces (Table 2.4). The lack of representation of filamentous *Epsilonproteobacteria*, which dominate in waters with high sulfide to oxygen ratios, is likely due to this oxygen sensitivity (Macalady et al, 2008). The reactor conditions maintained relatively low sulfide and high oxygen, which not only favors *Thiothrix* but also maintains a higher energy environment that favors greater diversity (Engel et al, 2004a; Macalady et al, 2008). *Epsilonproteobacteria* are commonly found associated with deep sea hydrothermal features such as chimneys that are primarily composed of carbonate minerals (Brazelton et al, 2010). Although limited, their representation on carbonate surfaces (calcite (1.2%), Madison Limestone (2.6%), Madison Dolostone (0.7%)) and near exclusion from non-carbonates supports a

hypothesis that mineralogy controls microbial community composition and that neutrophilic SOB preferentially colonize highly-buffering carbonates (Table 2.4).

As a result of the oxidation of sulfur compounds and production of mineral acidity, SOB corrode carbonate minerals (Barton & Luiszer, 2005; Davis et al, 2007; Engel et al, 2004b; Macalady et al, 2007; Steinhauer et al, 2010), and I find there is a link between microbial community composition and mineral weathering reactions. In biofilm reactors, all sulfur-oxidizing genera that colonized carbonate surfaces were neutrophilic (~17% to ~45% of the representative sequences; Table 2.4), and had a much greater affinity for carbonate rocks over silicates. This association reflects the advantage of colonizing a buffering mineral surface for neutrophilic but acid-producing bacteria, whereby dissolution of carbonate minerals neutralizes excess acidity generated by the oxidation of both S^o and $S_2O_3^{2-}$:

$$2CaCO_3 + S^o + 1.5O_2 + H_2O \Leftrightarrow SO_4^{2-} + 2HCO_3^- + 2Ca^{2+}$$

$$2CaCO_3 + S_2O_3^{2-} + 2O_2 + H_2O \Leftrightarrow 2SO_4^{2-} + 2HCO_3^- + 2Ca^{2+}$$

These biogeochemical dependencies cause the carbonates (Madison Limestone, Madison Dolostone, and calcite) to accumulate nearly identical communities ($\beta>0.98$) while having relatively low β-diversity values when compared to non-buffering basalt ($\beta<0.69$), albite ($\beta<0.60$), microcline ($\beta<0.50$), and quartz ($\beta<0.035$) (Figure 2.4). This indicates that the microbial communities on carbonates are nearly identical at the species level. Additionally, this dependency results in aggressive dissolution of the carbonate mineral, producing a characteristic weathered surface texture (Figure 2.3). These textures

have been documented in past studies and are indicative of biofilm mediated carbonate corrosion (Jones, 2010; Steinhauer et al, 2010). This aggressive corrosion was observed when the bulk media pH was 6.6 and 8.3 and appears to be independent of bulk media pH (Figure 2.3). This suggests highly localized control of biogeochemical conditions by microbes within a biofilm.

Similarly, each mineral surface reacts uniquely to the metabolic production of acidity by attached microorganisms resulting in geochemical microniches. Specifically, each mineral has the capacity to: 1) buffer the produced acidity (i.e. carbonates), 2) enhance local acidity (i.e. pyrite), or 3) remain relatively unreactive (i.e. quartz). These variable pH microniches have the potential to benefit microbial communities that are uniquely adapted to take advantage of specific geochemical conditions. While neutrophilic SOB dominated the carbonates, there were few found on the silicates. The classifiable microbial community on quartz was composed of ~15% SOB, with ~91% of those sequences associated with acidophilic sulfur-oxidizing genera (Table 2.4), including *Gammaproteobacteria Acidithiobacillus* and *Actinobacteria Acidithiomicrobium* which represented the only acidophilic SOB found in samples collected from LKC. Both micoorganisms are autotrophic aerobes that require reduced sulfur to grow; *Acidithiobacillus* is an obligate acidophile with an optimum pH of <4.0 (Kelly & Wood, 2000a) and *Acidithiomicrobium* is a facultative acidophile with an optimum pH ~2 (Stackebrandt & Schumann, 2006). Acidophilic acid-producing organisms would have an advantageous position on quartz due to the low acid-buffering

capacity of this mineral that does not interfere with the maintenance of an acidic microenvironment.

Additionally, the quartz surface is the only surface to accumulate microorganisms of the class *Nitrospira* (Table 2.4). Generally, members of this class are categorized as metabolically diverse aerobic chemolithotrophs capable of oxidizing nitrite to nitrate and of dissimilatory sulfate reduction (Garrity & Holt, 2001). At the genus level, these sequences are most similar to *Thermodesulfovibrio*, which is the one representative genus of this lineage that is thermophilic, anaerobic, and obligately acidophilic (Garrity & Holt, 2001). Furthermore, the acidophilic sulfur-reducer *Thermodesulfovibrio* were found together with the acidophilic sulfur-oxidizers (*Acidithiobacillus* and *Acidithiomicrobium*) in similar amounts at ~15% each (Table 2.4). This suggests a symbiotic relationship between these two types of organisms that may both be taking advantage of the low-acid buffering capacity of quartz.

Members of the genus *Meiothermus* were found in high abundance on the quartz surface. *Meiothermus* has recently been implicated as a major cause of biofouling in paper producing machinery where it accumulates in large quantities on machinery that operate at pH below 6 (Kolari et al, 2003). It is likely that the affinity of *Meiothermus* for quartz is due to this acidophilic behavior.

Gram-positive bacteria were almost completely excluded from colonization of the carbonate surfaces, but were found in relatively high abundance on all of the silicate surfaces (Table 2.4). Specifically, microcline had the highest abundance of members of the Phyla *Actinobacteria* (~25%) and albite had the highest abundance of the Phyla

Firmicutes (~14% as Bacilli and Clostridia). Although, bacterial cell walls of both Gram-negative and Gram-positive are predominantly electronegative, the Gram-positive cell has a higher surface area to volume ratio resulting in regions of the outermost wall with greater concentrations of COO^- groups and a net greater electronegativity (Beveridge, 1988). This increased electronegativity has been implicated in a greater incidence of mineral nucleation (particularly silicate) through anion binding to positive sites created by multivalent metal cations which salt-bridge silica ions to the wall and thus play a direct role in silicate binding by microorganisms (Mera & Beveridge, 1993). Additionally, Gram-positive microorganisms generally possess a large concentration of electropositive amino groups and a proton motive force that extrudes protons into the cell wall that causes a greater concentration of electropositive sites surrounding Gram-positive cells (Beveridge, 1981). Both of these processes would benefit from a lower pH as abundant H^+ ions would occupy negatively charged carboxyl radicals and reduce the electrostatic repulsive forces for anions (Mera & Beveridge, 1993). In fact, it is under acidic conditions, such as those achievable on non-buffering silicate surfaces, that these microorganisms most effectively form metal silicate minerals (Mera & Beveridge, 1993). Therefore, Gram-positive bacteria may have a competitive advantage over Gram-negative bacteria as the electronegativity of their cell walls provides a more stable connection to silicate mineral surfaces.

The quartz surface had the largest proportion of *Betaproteobacteria* (~44%), largely represented by the genus *Methyloversatilis* (Table 2.4). Members of this genus are Gram-negative, non-motile rods, that are facultative methanotrophs capable of

growing on single or multi-carbon compounds (Kalyuzhnaya et al, 2006). Methanotrophy has been implicated previously as an important part of carbon cycling within sulfidic caves such as Movile Cave in Romania by actively converting CH_4 into complex organic compounds, which help to sustain a diverse microbial community (Chen et al, 2009). Low dissolved methane within LKC (<80 μmol L^{-1}) is likely prohibitive to growth of methanotrophs and low population sizes of methanogens have been indicated within LKC (Engel et al, 2004a). However, within the laboratory reactor, it appears that the quartz surface provided some advantage to these microorganisms (Table 2.4). The large proportion of *Methyloversatilis* on quartz is probably tied to populations of methanogenic Archaea that are likely present, but whose genes were not sequenced in these experiments or previous experiments.

Quartz is also stable in acidic conditions without mobilizing potentially toxic aluminum, as is the case for feldspars (Bousserrhine et al, 1998; Flis et al, 1993; Wood, 1995). There is a very low abundance of putative neutrophilic sulfur-oxidizing genera (0.7%) on microcline and (~6%) on albite (Table 2.4), which have a low buffer capacity and the potential for mobilizing aluminum via acid-catalyzed hydrolysis (Chou & Wollast, 1985). The presence of toxic aluminum and lack of buffering in microcline and albite both restrict microbial growth (Figure 2.1) and increase α-diversity to the highest observed diversity of any surface (Table 2.3) as colonizing microbes struggle to thrive and gain a competitive advantage. This result is consistent with recent studies that showed that the number of bacterial and fungal ribotypes attached to a natural surface was positively correlated with aluminum concentration of that surface (Gleeson et al,

2005; Gleeson et al, 2006). However, the effect is nullified on the albite surface due to the presence of the sulfur-reducing *Desulfococcus,* which could act to neutralize some of the generated acidity and release of toxic aluminum, decreasing the effect of aluminum on α-diversity of the attached communities (Table 2.4). Alternatively, higher diversity in microbial communities has been negatively correlated to dissolution rate of mineral surfaces (Uroz et al, 2011). It has been suggested that this might cause non-specific colonization by bacterial communities that can dissolve the mineral and extract mineral bound nutrients and are thus well adapted to poor-nutrient conditions (Uroz et al, 2011).

Some microorganisms have the capacity to neutralize local aluminum toxicity. The feldspar surfaces were host to a relatively large abundance of members of the genus *Pseudomonas* (Table 2.4). Species of *Pseudomonas* (specifically, *P. fluorescens*) have been shown in previous studies to have the ability to neutralize toxic aluminum by a variety of mechanisms (Appanna et al, 1995; Hamel & Appanna, 2003; Singh et al, 2005; Singh et al, 2009).

Members of the genus *Ensifer* colonize all surfaces, except quartz, in relatively high proportional abundance with an apparent lack of discrimination (Table 2.4). The type species *Ensifer adherens* is a known bacterial predator that attaches endwise to a host cell where it can cause lysis (Balkwill, 2005; Casida, 1982). Additionally, *Ensifer* has a symbiotic relationship with *Bacillus,* as *Ensifer* promotes *Bacillus* spore germination and receives vital nutrients that are produced during spore activation (Balkwill, 2005). This may explain the ubiquity of this microorganism on each surface as discrimination is not due to the surface type, but to the type and quantity of "food" (other

microorganisms) that is attached to the surface. The absence of *Ensifer* on quartz is possibly due to the locally adverse conditions imparted by the acidophilic inhabitants, discussed herein. This lysogenicity is also common in *Azospirillum* species, which show the similar trends in colonization ubiquity as *Ensifer*, and exclusion from quartz, but at lower proportional abundance (Döbereiner & Pedrosa, 1987).

There are also more subtle controls on community and growth. The α-diversity values (Simpson's dominance index (D), Shannon diversity index (H'), and Evenness (E)), are all consistent with a relatively diverse and highly similar (β~0.98) microbial community on the carbonate surfaces (Chao et al, 2005). Despite similarities in community structure, (β-diversity, Figure 2.4), far less biomass accumulated on calcite compared to environmental carbonate surfaces (i.e. Madison Limestone & Madison Dolostone) in both pure and mixed cultures composed primarily of neutrophilic, autotrophic, acid-producing organisms (Figure 2.1; Table 2.2) even though the substrata have essentially equivalent buffering capacity. This suggests that acid buffering is not the sole factor influencing microbial accumulation, and other variables such as mineral-derived nutrient availability and competition between populations within the sulfur-oxidizing guild are potentially important.

We hypothesize that when allowed to choose between a pure calcite, limestone or dolostone rocks, there was preferential colonization of the Madison Dolostone and then Madison Limestone due to the availability of trace P in these rocks (~2905 μmol kg^{-1} and ~736.8 μmol kg^{-1} respectively) that was not detected in calcite. Ortho-phosphate is an essential macronutrient for microbial growth and development, but mineral sources of P

such as apatite are relatively insoluble (Goldstein, 1986). Microbially generated inorganic and organic acids are primarily responsible for the solubilization of mineral-bound P (Banik & Dey, 1982; Craven & Hayasaka, 1982; Goldstein et al, 2003; Leyval & Berthelin, 1989). The difference in P concentration is therefore likely responsible for the greater biofilm growth on Madison Dolostone than Madison Limestone and calcite, but mineral buffering capacity is the controlling factor for community composition (Figure 2.1, Figure 2.4).

Additionally, increased calcium concentration has been shown to have a positive effect on cell viability in acidic pHs (Dilworth et al, 1999; Draghi et al, 2010; Indrasumunar et al, 2012). Ca^{2+} appears to directly protect cellular components from degradation under low pHs (as low as 4) as well as increase the production of EPS (Dilworth et al, 1999). In our study, microorganisms were found in large proportional abundance on the highly corroded carbonate surfaces, where Ca^{2+} would be locally abundant (Figure 2.1).

Similarly, colonization of silicates, by both pure and mixed cultures, was preferential towards P-bearing basalt over the other silicates that had no detectable inorganic P (Table 2.2). Our laboratory experiments were maintained in a phosphate-limited condition (similar to the cave stream environment) while the basalt used for these experiments had abundant phosphate (~3000 μmol/kg) in the form of apatite (Bennett et al, 2001). In the pure culture experiment, the preferred substrates were the carbonate rock samples Madison Limestone and Madison Dolostone. In contrast, with the mixed culture experiments *Thiothrix* spp. overwhelmingly selected the basalt, with few

sequences found on the Madison Limestone and Madison Dolostone (Table 2.4). As a result, the basalt-hosted biofilm had a low α-diversity with ~66% abundance of a filamentous organism closely associated with *Thiothrix unzii* (>99% similarity, Engel 2004), which competitively excluded all other SOB from colonizing the basalt surface (Table 2.4). Therefore, I hypothesize a relationship based on nutrient limitations, mineral nutrient sources, and competition by other SOB populations.

Initially, the abundance of *Thiothrix unzii and Thiothrix* spp. on basalt appears to reflect a less-than-ideal environment for dominance by neutrophilic, acid-producing microorganisms. However, in nature *Thiothrix unzii* grows on sulfide, thiosulfate, or sulfur, and is found in association with mid-ocean basalts (Dulov et al, 1991; Jannasch & Mottl, 1985; Kalanetra et al, 2004; Moyer et al, 1995; Schauer et al, 2011). The overwhelming dominance by *Thiothrix* spp. was surprising and suggests an adaptive ability of these microorganisms to tolerate basalt and efficiently extract limiting nutrients, namely P. This attribute may not be shared by other organisms in the consortium and may indicate an adaptation to that rock substratum that is expressed when that mineral is introduced, even when there is no basalt present in the region where that organism was collected.

2.6 CONCLUSIONS

Subsurface environments are composed of a diverse array of minerals with varying chemical compositions. Core sampling often targets for specific physical (temperature) or geochemical (redox) conditions under the assumption that the associated

microbial community is homogeneously distributed. However I argue that this is not the case. By inoculating laboratory reactors containing a variety of minerals with a microbial community from a cave with a deep (hypogenic) energy source (H_2S) I found that subsurface microbial communities have specific associations to specific minerals. Phylotypes closely related to neutrophilic sulfur-oxidizing microorganisms have an affinity for acid-buffering carbonate surfaces and accumulate significantly greater biomass on carbonates with abundant mineral bound nutrients. Phylotypes closely related to acidophilic acid-producing microorganisms are exclusively associated with non-buffering minerals such as quartz, even though growth is not abundant due to mineral-bound nutrient limitations. However, acid producing phylotypes, both acidophilic and neutrophilic, do not colonize aluminosilicates as their metabolism would release toxic aluminum. Additionally, there appear to be specific associations, such as *Thiothrix* (a microorganism commonly found associated with mid-ocean ridge basalts) with basalt, where it competitively excludes all other SOB. This indicates an adaptation to that rock substratum that is expressed when that mineral is introduced, even when there is no basalt present in the region where that organism was collected.

Our results show that under the nutrient-limited conditions common to aquifers and the deep subsurface, the community structure can be differentiated at the scale of individual mineral grains, and that each mineral supports a unique microbial consortium that expresses specific metabolic functions in order to take advantage of, or protect itself from, the unique aspects of that mineral. Even grains of a polymineralic rock such as basalt can support a different community on different mineral exposures, at the scale of a

few microns (Rogers & Bennett, 2004). The results of this study, in context with previous research summarized above, describes a fundamental property of microbe-mineral interactions in the subsurface biome. This association has been evolving over ~3.5 billion years and a relationship between mineral and biochemical reactions may be critical to the origin of the first functional cell (Hazen, 2006; Smith, 1998). I propose that bacteria evolved predominantly on or in close association with minerals, and that successful growth is significantly influenced by mineralogy that gives particular microorganisms, a population or consortium, a competitive advantage and therefore directly impacts both local and global microbial diversity. Our results and recent findings suggest that minerals have also evolved through time due to the influence of living microorganisms (Barskov, 2008). Therefore, I argue that this is in fact a co-evolutionary relationship based on fundamental and preferential associations between microorganisms and minerals.

Chapter 3: Revealing hidden diversity: investigating the impact of minerals on biofilm community structure and diversity

3.1 ABSTRACT

Throughout geologic time, microorganisms evolved in direct contact with mineral surfaces. It stands to reason that the pliant and inconstant nature of these environments likely caused dynamic ecological shifts in these microbial communities that should be detectable in the phylogenetics of attached communities. I used laboratory biofilm reactors (inoculated with a diverse subsurface community) to explore the phylogenetic and taxonomic variability in microbial communities as a function of surface type (carbonate, silicate, aluminosilicate), media pH, and carbon and phosphate availability. Using high-throughput pyrosequencing, I found that surface type significantly controlled ~70-90% of the variance in phylogenetic diversity regardless of environmental pressures. Consistent patterns also emerged in the taxonomy of specific guilds (sulfur-oxidizers/reducers, Gram-positives, acidophiles) due to variations in media chemistry. Media phosphate availability was key property associated with variation in phylogeny and taxonomy of whole reactors and was negatively correlated with biofilm accumulation and α-diversity (species richness and evenness). However, mineral-bound phosphate limitations were correlated with less biofilm. Carbon added to the media was correlated with a significant increase in biofilm accumulation and overall α-diversity. Additionally, planktonic communities were phylogenetically distant from those in biofilms. All reactors harbored structurally (taxonomically and phylogenetically) distinct microbial communities.

3.2 INTRODUCTION

The vast majority of microorganisms in the subsurface exist in biofilms attached to solid surfaces; it is estimated that the attached community represents up to 99.9% of the total biomass of microorganisms in a subsurface environment (Madigan et al, 2009). Unlike laboratory growth experiments the subsurface mineral assemblage is complex and heterogeneous with many different minerals contributing many different surface chemistries that offer a wide range of advantages or disadvantages to each microbial population. These mineral attributes could contribute to growth, present challenges, or influence community membership or biofilm diversity, while the attached community will directly perturb the mineral surface, forming a coupled biogeochemical system, with that perturbation dependent on the community composition. While the diversity in bulk sediments and soils has been characterized in a variety of settings, each environment likely contains uniquely complex mineralogical habitats with dramatic microscale spatial heterogeneities in associated microbial communities. The purpose of this study is to directly characterize the mineralogical contribution to microbial diversity, and test that contribution under a range of media types and environmental conditions.

Several factors have been suggested to control dynamic diversity and growth, and stimulate specific biogeochemical survival strategies employed by attached biofilm communities. These include physical properties (hydrodynamics) of the bulk fluid (Kugaprasatham et al, 1992), physical and chemical nature of the solid substratum (Carson et al, 2009; Dalton et al; Rogers & Bennett, 2004; Rogers et al, 1998; Sylvan et al, 2012), composition of the microbial community (Lawrence et al), and nutrient availability (primarily carbon, phosphorous, and nitrogen) (Huang et al, 1998; Ohashi et al, 1995; Rogers et al, 2001). pH is often identified as a key factor controlling microbial community composition (Chu et al, 2010; Fierer & Jackson, 2006; Lauber et al, 2009;

Siciliano et al, 2014; Winsley et al, 2014). Biofilm and EPS production are both influenced by the nutrient content of the growth medium with respect to available carbon, or limitations in K or P that affect biofilm development (Ellwood et al, 1982; Matin et al, 1989; Wrangstadh et al, 1990. Nutrient limitations, for example, stimulate the production of extracellular polysaccharides (EPS) (EPS) (Ellwood et al, 1982; Matin et al, 1989; Wrangstadh et al, 1990) (Eboigbodin et al, 2007; Zisu & Shah, 2003). However, few studies examine complex natural communities on natural surfaces. In oligotrophic environments, such as those in the subsurface, microorganisms are likely to be highly dependent on minerals ("mineraltrophic") as they support a variety of biogeochemical processes (Anderson, 2001; Chapelle et al, 2002; Edwards et al, 2005; Edwards et al, 2012; Stevens, 1997).

Previously, using flow-through biofilm reactors inoculated with biomass from a microbial mat gathered from the sulfidic cave Lower Kane Cave (LKC), located in Bighorn River Valley, WY, USA. I found that specific clades appeared to have an affinity for specific mineral types according to their metabolic requirements and environmental tolerances (Jones & Bennett, 2014). The motivation of those experiments, however was specifically to evaluate the role of mineralogy in selecting for neutrophilic, but acid-producing sulfur-oxidizers (SOB) in subsurface karst environments. As such, experiments were designed to mimic the nutrient-limited environment found within LKC, where sulfidic water serves as the metabolic backbone for a diverse microbial community within the cave (Egemeier, 1981; Engel et al, 2004a). This led me to hypothesize that phylogenetically similar microorganisms would still show an affinity for specific natural surface types (e.g. carbonates, silicates, aluminosilicates) even under variable nutrient limitations.

For this study I utilize high-throughput 454-pyrosequencing (Margulies et al, 2005) of bacterial 16S rRNA sequences to examine the response of community structure and diversity to environmental stimuli (pH variability, carbon and phosphate limitations/amendments) as biofilms develop on mineral surfaces within flow-through biofilm reactors. I use phylogenetic distance measures (UniFrac), to account for the relationships among populations attached to the various surfaces (Lozupone & Knight, 2005). The UniFrac distances were then subjected to permutational multivariate analysis of variance (PERMANOVA) in order to evaluate mineralogical and environmental influence on microbial community structure (McArdle & Anderson, 2001). Additionally, I re-evaluate the 16S rRNA sequences from Jones & Bennett (2014) using more robust methodology with this new hypothesis in mind. I can then evaluate if surface type significantly impacts microbial community structure, and biofilm accumulation under a variety of environmental conditions. I then use taxonomy to identify consistent responses to variations in media and surface chemistry among specific guilds (SOB, SRB, Gram-positives, Acidophiles), which I can use to interpret the ecological role of the detected taxa.

3.3 Materials and Methods

3.3.1 Flow through Biofilm Reactor (CDC)

For these experiments I used a modified CDC biofilm reactor (Biosurface Technologies, Bozeman, MT, USA): a 1-liter glass vessel with a ported polyethylene top that supports 8 polypropylene rods each holding up to three coupons (12.7 mm OD disks ~3 mm thick). The reactor was operated as a continuous-flow stirred reactor at

1.5ml/min liquid medium flow. Consistent shear and mixing at all positions within the reactors was maintained using a stir vane rotated by a magnetic stir plate.

Samples were collected in the field at Lower Kane Cave (LKC) (WY, USA) in sterile falcon tubes. The mixed environmental inoculant for these experiments was identical to that used in Jones & Bennett (2014). The inoculum is a consortium composed primarily of autotrophic sulfur-oxidizing members of lineages *Gammaproteobacteria* (34.7%) of the genus *Thiothrix*, and *Epsilonproteobacteria* (62.4%) of the genus *Sulfurovum* (Engel et al, 2003; Engel et al, 2004a; Jones & Bennett, 2014), but with many other Bacterial lineages at lower abundance. Approximately 15 ml of the raw mat was added to the sterilized CDC biofilm reactor for each experiment.

Synthetic cave water was prepared by equilibrating DI-H_2O water with finely powdered Iceland spar calcite to equilibrium. The solution was filtered to 0.2 μm and 0.1 g $MgSO_4$ and 0.25 g NH_4Cl were added per liter and autoclaved at 121°C for 45 minutes before adding 2 ml/L and 5 ml/L of filter-sterilized trace metal solution and Wolfe's Vitamin solution, respectively (Burlage, 1998). The reduced sulfur electron donor was $S_2O_3^{2-}$ prepared from a stock filter-sterilized 1M solution of $Na_2S_2O_3$ mixed in-line via a syringe pump to a final concentration of 0.83 mM.

Amendments (P, C, or both) were then added to this basic liquid media or pH adjusted to examine the influence of environmental conditions (Table 3.1). Specifically, the carbon/phosphorus-limited (CP-Limited) media used in Jones & Bennett (2014) was this basic liquid media with sterile 0.1 N H_2SO_4 added to achieve a final pH of 6.9 (Jones and Bennett 2014). The C-Amended medium was prepared by amending the basic medium with 5 mM Na-Acetate, 5 mM Na-Lactate and filter sterilized 0.1 N H_2SO_4 added to a final pH of 6.9. The P-Amended media was prepared with 0.53 g/L KH_2PO_4 and 0.12 g/L $K_2H_2PO_4$ and filter sterilized NaOH added to a final pH of 8.3. The no

limitation medium (CP-Amended) was amended with 5 mM Na-Acetate, 5 mM Na-Lactate, 5 mM Na-Formate, 0.53 g/L KH_2PO_4, 0.12 g/L $K_2H_2PO_4$, and 0.1 N H_2SO_4 added to achieve a final pH of 6.9 (Table 3.1).

3.3.2 Mineral Substrata Preparation

Mineral/rock substrata were selected to represent the lithology of a variety of geologic environments (Table 3.2). The surfaces were broadly categorized into mineral types (carbonates, silicates, aluminosilicates, planktonic (none)). Each of the selected specimens offers potential advantages and disadvantages to microorganisms equipped to exploit (or defend against) them and are described briefly in Table 3.2. Specimens of calcite, microcline, albite, basalt, and quartz were obtained from Ward's Natural Science Establishment Incorporated, and these minerals have been previously characterized (Bennett et al, 2001)(Jones & Bennett, 2014). Unaltered Mississippian-age Upper Madison Limestone, Upper Madison Dolostone and the contained chert, were collected from an outcrop near Lower Kane Cave. The Madison limestone is nearly pure calcite (microsparite) with a minor quartz component, and the Madison Dolostone is nearly pure dolomite also with a minor quartz component (Plummer et al, 1990). Mineral coupons were prepared using previously published methods (Jones & Bennett, 2014).

Composition of Medias (L^{-1})				
Component	**CP-Limited**	**C-Amended**	**P-Amended**	**CP-Amended**
Calcite (Eq.) DI	1000 ml	1000 ml	1000 ml	1000 ml
$Na_2S_2O_3$	10 mM	10 mM	10 mM	10 mM
$MgSO_4$	0.25 g	0.25 g	0.25 g	0.25 g
NH_4Cl	0.1 g	0.1 g	0.1 g	0.1 g
Trace Metals	2.1 ml	2.1 ml	2.1 ml	2.1 ml
Wolfe's Vitamins	5.3 ml	5.3 ml	5.3 ml	5.3 ml
KH_2PO_4	-	-	0.53 g	0.53 g
$K_2H_2PO_4$	-	-	0.12 g	0.12 g
Na-Lactate	-	5 mM	-	5 mM
Na-Acetate	-	5 mM	-	5 mM
Na-Formate	-	-	-	5 mM
pH initial	6.9	6.9	8.3	6.9
pH reactor	5.7	7.5	7.9	7.8

Table 3.1: Media recipes for each of the four reactor conditions. (-) represents none added.

Surface Type	Surface	General Composition & Origin	Biogeochemical Significance
Carbonates	**Calcite**	$CaCO_3$ Iceland Spar Calcite	High-Buffering Capacity[2], No Trace Nutrients
	Madison Limestone	$CaCO_3$ Lower Kane Cave, WY, USA	High-Buffering Capacity[2], Trace Nutrients, High-PO_4^{2-}
	Madison Dolostone	$CaMg(CO_3)_2$ Lower Kane Cave, WY, USA	High-Buffering Capacity, Trace Nutrients, High-PO_4^{2-}
Aluminosilicates	**Microcline**	$KAlSi_3O_8$ Ontario Microcline[1]	Low-Buffering Capacity, Low-Trace Nutrients[1], Potentially Toxic Al
	Albite	$NaAlSi_3O_8$ Ontario Plagioclase[1]	Low-Buffering Capacity, Low-Trace Nutrients[1], Potentially toxic Al
Silicates	**Chert**	SiO_2 Lower Kane Cave, WY, USA	Low-Buffering Capacity, Low-Trace Nutrients[1]
	Basalt	Fe, Mg, Ca, Al, Si, O Columbia River Basalt[1]	Low-Buffering Capacity, High-PO_4^{2-}, H_2 source for Methanogens & SO_4^{2-} reducers[3]
	Quartz	99.78% SiO_2 Hydrothermal Crystal[1]	Low-Buffering Capacity, No-Trace Nutrients[1]

Table 3.2: Surface types, general compositions, and biogeochemical significance of the rocks/minerals used in these biofilm reactor experiments. This table is modified from Jones & Bennett 2014. Superscripts refer to papers with additional information.[1]Bennett et al, 2001 [2]Steinhauer et al, 2010 [3]Edwards et al, 2005.

3.3.3 Biomass measurement and extraction

To measure biomass accumulation after 3 weeks, triplicate mineral coupons were weighed (wet, biofilm attached), dried overnight at 104°C, weighed again (dry, biofilm attached), processed by 3 x 5-minute cycles of alternating sonication and vortexing in a calcite equilibrated (to prevent dissolution) 2% tween 20 solution to remove biomass, dried overnight again, and weighed again (dry, biofilm removed). The dry weight of biomass accumulated is the difference between the final dry weight with biomass and the dry weight after processing.

Biofilm growth curves were constructed in order to determine the standard duration (3-weeks) of each experiment. Curves were constructed for both pure and mixed culture reactors under CP-Limited, C-Amended, and P-Amended conditions. For these experiments, limestone was the sole surface type occupying all 24 coupon spaces. Two limestone coupons (chosen randomly) were sacrificed at 48-hour intervals and biomass was measured according to the method described above. The resulting curves are shown in Figure 3.1a.

For DNA extraction, biomass was aseptically isolated from mineral coupons in 1 mM EDTA and 0.9X phosphate-buffered saline (PBS with physical disruption by freeze-thaw (3 times, -80°C to 65°C) cycles followed by alternating sonication and vortexing (3 X 5-minutes) (Jones & Bennett, 2014). The biomass was isolated from solution by centrifugation at 5000 rpm for 10 minutes, and the supernatant decanted. DNA extraction from biomass was conducted using an Ultraclean Microbial DNA Isolation Kit (MoBio Laboratories, Inc.; Catalog # 12224-50). DNA samples were quantified and qualified using a Nanodrop spectrophotometer (Nyxor Biotech, Paris, France). Bacterial tag-encoded FLX-titanium amplicon pyrosequencing (bTEFAP) was used to evaluate the bacterial populations removed from the mineral surfaces at MR DNA Lab

(www.mrdnalab.com, Shallowater, TX, USA). The bTEFAP procedures are based on Research and Testing Laboratory protocols http://www.researchandtesting.com and are previously described (Dowd et al, 2008). Briefly, the 16S universal Eubacterial primers 27F (5'-AGRGTTTGATCMTGGCTCAG-3') and 519R (5'-GTNTTACNGCGGCKGCTG-3') were used to amplify the v1-v3 region of 16S rRNA genes using 30 cycles of PCR. HotStarTaq Plus Master Mix Kit (Qiagen) was used for PCR under the following conditions: 94°C for 3 min, followed by 28 cycles of 94°C for 30 s; 53°C for 40 s and 72°C for 1 min after which a final elongation step at 72°C for 5 min was performed. After PCR, all amplicon products from the different samples were mixed in equal volumes and purified using Agencourt Ampure Beads (Agencourt Bioscience Corporation, Beverly, Ma). Adaptors and barcodes for 454 pyrosequencing were ligated, and sequencing on a Roche 454 GS-FLX Titanium™ (454 Life Sciences, Branford, CT, USA).

Sequences were preprocessed using the open source software package QIIME version 1.9 (http://qiime.sourceforge.net), (Caporaso et al, 2010). QIIME was also used for identification of operational taxonomic units (OTUs), taxonomic assignment, and community structure statistical analyses and comparisons. In preprocessing, we remove from further analysis: sequences < 200 bp or > 550 bp, sequences with ambiguous base calls (>6 bp), sequences with homopolymer runs (>6 bp), low quality scores (<25 bp), sequences with primer mismatches, and barcode errors (>1 bp). Additionally, noisy sequences were discarded using the "denoise_wrapper" script (Reeder & Knight, 2010). Chimeric sequences were removed using ChimeraSlayer with the QIIME default settings after OTU-picking and taxonomic assignment.

The uclust method was used to pick de novo OTUs at 3% (genus level) divergences. Representative sequences for each OTU were then aligned with PyNAST

and taxonomy was assigned with the uclust consensus taxonomy assigner using the greengenes_13_8 reference database. Potential contaminants and OTUs with less than 4 members were then filtered from the resulting OTU table. After taxonomy was determined and OTUs were assigned, this dataset was manually processed to reveal both sequence counts and proportional abundances of microbial sequences present on each substratum. Assigned taxa were compared with extant taxa described in the literature, at the genus level, to infer the putative ecological role of these microorganisms.

3.3.4 Biodiversity Metrics and Statistical Analysis

Community diversity was evaluated using both standard statistical analysis on OTUs (e.g. Species Richness, Shannon-Wiener, Simpson's) and phylogenetic analysis (Bohannan & Hughes, 2003). α and β-diversity values were calculated on the resulting datasets using QIIME with selective manual calculations for validation (Caporaso et al, 2010; Hill et al, 2003). Due to the different number of sequences among samples, the data was normalized for diversity analysis using rarefaction curves. Rarefaction curves of the observed richness were calculated in QIIME using 100000-fold resampling without replacement (Figure 3.1b). Estimates of α-diversity were based on evenly rarefied OTU abundance matrices and included observed species richness (S), the reciprocal of the Simpson dominance index (D), Shannon-Weiner index (H'), and species evenness (E) (Hill et al, 2003). Sampling effort was estimated using Good's coverage (Good, 1953). The reciprocal Simpson dominance index (D) gives more weight to dominant OTUs by expressing the likelihood that two individuals, chosen at random, will belong to different OTUs. The effect of geochemical (pH_{in}, pH_{out}, C-P Availability) and mineralogical (mineral geochemistry, P-Availability, Buffering Capacity) variations on microbial

community diversity was assessed at rarefication depths according to the smallest sample within each subset.

Beta diversity (global diversity) both between communities on multiple surfaces and between reactors was assessed using weighted UniFrac (phylogenetic) distance matrices at sequence divergences of 3% (Lozupone et al, 2011) between samples were calculated after rarefying all samples. The effect of geochemistry on microbial/mineral associations was depicted using UniFrac distance based 3D Principal Coordinate Analysis (PCoA) plots (Borg & Groenen, 2005), and UPGMA trees (Felsenstein, 2004).

To assess the statistical significances in microbial community dissimilarity between particular groups, the UniFrac distance matrix generated in QIIME was analyzed with R statistical software (R foundation for Statistical Computing, Vienna, Austria). Statistical significance was considered at $P<0.05$. Alpha diversity metrics were compared within and between reactor types using Wilcoxon signed rank test. Testing for the presence of a significant effect of sample type on beta diversity metrics was done using permutational multivariate analysis of variance (PERMANOVA) and the 'Adonis' function from the R package 'vegan', which partitions the distance matrix among sources of variation, fits linear models to distance matrices and uses a permutation test (10^5) with pseudo-F ratios to obtain *P*-values (McArdle & Anderson, 2001). Data sets for the effect of phosphate and carbon on microbial biomass were analyzed by analysis of variance (ANOVA) with significance at $P<0.05$.

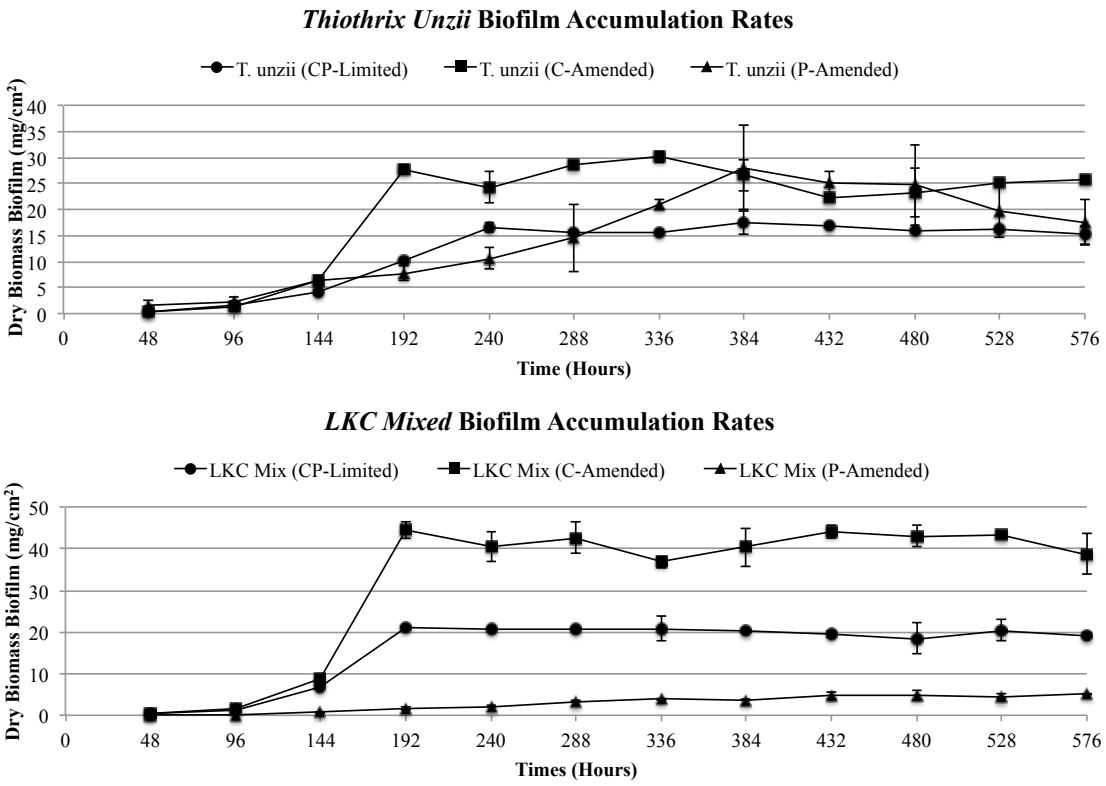

Figure 3.1a: Growth curves for biofilm accumulated on limestone surfaces in pure culture (*Thiothrix unzii*) and *LKC mixed culture* reactors under CP-Limited, C-Amended, and P-Amended media conditions. Error bars represent duplicate experiments.

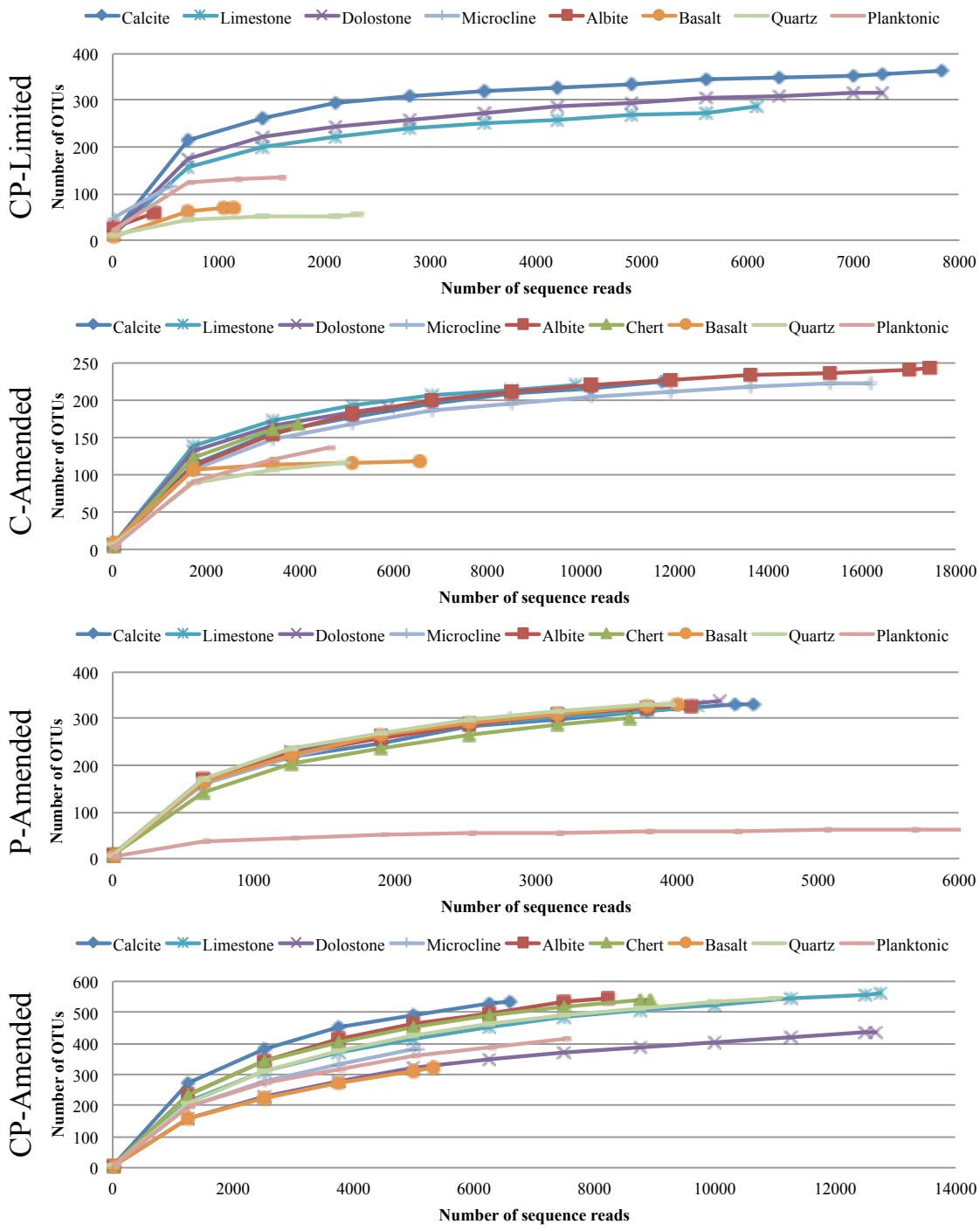

Figure 3.1b: Rarefaction curves of 16S rRNA sequences. OTUs were defined at 97% similarity cutoff. The figure depicts the comparison between samples from all four reactors.

3.4 RESULTS

3.4.1 Effect of reactor conditions on bacterial diversity

There were 578,969 total raw sequences obtained from all samples and all the four reactors. Of those, a total of 209,973 (CP-Limited – 27,173 total with an average of 3397 ± 3133 per sample, C-Amended – 66,383 total with an average of 7376 ± 5662 per sample, P-Amended – 34,847 total with an average of 4205 ± 934 per sample, CP-Amended – 78,570 total with and average of 8730 ± 2900 per sample) bacterial 16S high-quality sequences with an average read length of 440 bp were obtained for the 35 samples (9 samples per reactor except 8 for CP-Limited).

Rarefactions were performed for each reactor independently at the maximum subsampling depth that would allow the inclusion of all samples within that reactor. Accordingly, the CP-Limited reactor was rarefied to a depth of 396 reads, C-Amended to 594 reads, P-Amended to 2820 reads, and CP-Amended to 5077 reads. Overall, the mean species richness was 275.8 species. However the mean species richness varied greatly per reactor: CP-Limited, 175.1 species; C-Amended, 145.0; P-Amended, 294.7; CP-Amended, 477.2. Additionally, the total unique OTUs varied greatly per reactor: CP-Limited, 349; C-Amended, 386; P-Amended, 459; CP-Amended, 757. Rarefaction curves for richness of 33 (except CP-Limited microcline and albite) of the 35 samples approach a plateau at their respective maximum sampling depth, indicating an adequate sampling procedure (Figure 3.1). Additionally, the overall average Good's coverage is 98.4 ± 0.9% including CP-Limited microcline and albite with Good's coverage values of 95.1% and 95.7%, respectively, indicating an adequate sampling procedure.

The reactor conditions (C, P, and pH) and the surface types were all significant drivers of variation in bacterial β-diversity and taxonomy. The overall bacterial communities were between 40.6% and 67.5% UniFrac (phylogenetically) similar. These

differences are evident when plotted in PCoA and were statistically significant between all reactors (P<0.001; Figure 3.2). All four reactor systems formed distinct clusters in the ordination space. The clusters were quantitatively supported by high dissimilarity values and PERMANOVA and 'Adonis' analyses. Overall, the effect of separate reactor conditions as a whole on β-diversity was confirmed by 'Adonis' with an R^2 value of 0.456 (45.6%, P<0.001) of the variation in distances is explained by grouping the samples into their respective reactors (Figure 3.2, Table 3.3). The effect overall reactor conditions had on community structure was comprised of the effect of phosphate amendment contributing 23.2%, carbon amendment contributing 16.5%, and media pH buffering contributing 20.1% of the variability in β-diversity between reactors (P<0.001; Table 3.3).

The effects of reactor conditions on α-diversity were statistically less robust, although significant shifts were still detected (Table 3.4). The reactor conditions only had a significant effect on α-diversity when comparing specific reactors (Table 3.4). Differences in both α-diversity were most significantly driven by whether the reactor was amended with phosphate or not as both P-Limited reactors have the lowest species richnesses and both C-Limited reactors have the highest Shannon diversity (Table 3.4). For a complete list of α-diversity values see (Table 3.5).

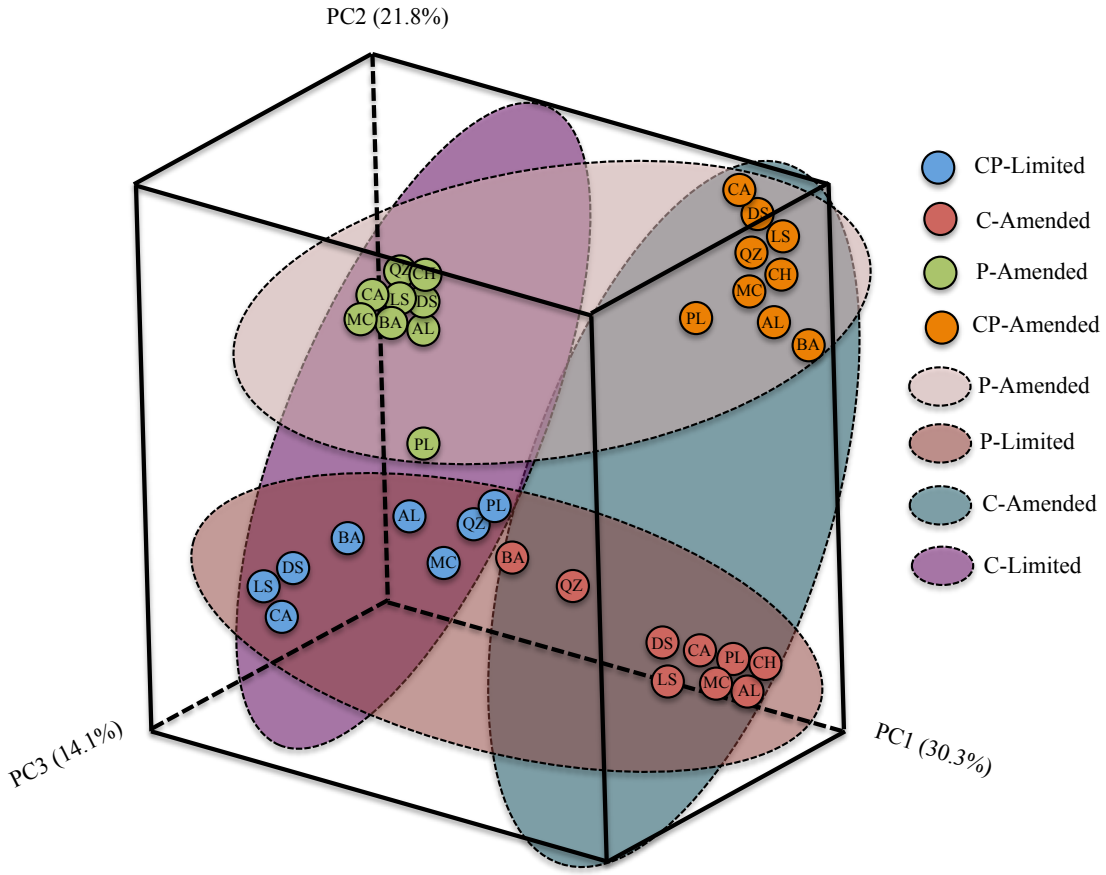

Figure 3.2: Principal coordinate analysis (PCoA) plot based on the relative abundances and phylogenetic diversity of 16S rRNA gene sequences using a UniFrac weighted distance matrix, colored according to reactor conditions and labeled according to solid substrate type; blue, CP-Limited; green, P-Amended; orange, CP-Amended; red, C-Amended. Percentage of the diversity distribution explained by each axis is indicated in the figure. The colored ellipses encircle variations in reactor conditions.

Surface Controlling Variables[a]	CP-Limited			C-Amended			P-Amended			CP-Amended		
	F	*P*	(R^2)	F	*P*	(R^2)	F	*P*	(R^2)	F	*P*	(R^2)
Buffering Capacity	**2.3**	**0.036**	**12.3**	0.1	0.929	Neg	0.8	0.537	10.7	**29.3**	**0.012**	**73.4**
Mineral Type	**3.1**	**0.009**	**69.8**	0.8	0.609	32.3	**10.2**	**0.035**	**85.9**	**12.5**	**0.003**	**88.3**
Mineral Phosphate	1	0.344	8.8	**3.1**	**0.034**	**30.9**	0.651	0.613	8.5	0.1	0.784	1.9

Reactor Controlling Variables[b]	F	*P*	(R^2)
Media Carbon	**6.5**	**<0.001**	**16.5**
Media Phosphate	**9.9**	**<0.001**	**23.2**
Media pHin	**2.4**	**<0.001**	**6.7**
Media pHout	**8.3**	**<0.001**	**20.1**
Reactors[c]	t	P_{adjust}	$Ø_{sim}$
CP-Limited vs. C-Amended	**2.6**	**0.029**	**46.9**
CP-Limited vs. P-Amended	**5.8**	**<0.001**	**55.8**
CP-Limited vs. CP-Amended	**4.4**	**<0.001**	**40.6**
C-Amended vs. P-Amended	**4.1**	**<0.001**	**55.1**
C-Amended vs. CP-Amended	**6.3**	**<0.001**	**48.1**
P-Amended vs. CP-Amended	**8.6**	**<0.001**	**67.5**

Table 3.3: Effects of reactor conditions and surface type on bacterial β-diversity. [a]Effects of surface type and [b]reactor conditions as assessed by multivariate permutational analysis of variance (PERMANOVA). Surface factors are buffering capacity (high vs. low based on whether surface is a carbonate or non-carbonate), mineral type (carbonate, silicate, aluminosilicate, planktonic), and mineral phosphate (high vs. low). Reactor correlation factors are carbon amendment (yes vs. no), phosphate amendment (yes vs. no), media pHin (high vs. low), and media pHout (high vs. Low). Values represent the pseudo-F ratio (F), the permutation-based level of significance (*P*), and the 'adonis' (R^2). Values at $P<0.05$ are shown in bold. Negative variance components (Neg) can result from underestimations of small or zero variances. [c]Pairwise comparisons between reactors. Values represent the univariate t-statistic (t) and the between reactor UniFrac (phylogenetic) similarity ($Ø_{sim}$). The permutation-based level of significance was adjusted for multiple comparisons using the Benjamini-Hochberg procedure (P_{adjust}). Values at $P_{adjust}<0.05$ are shown in bold.

	CP-Limited		C-Amended		P-Amended		CP-Amended	
Surface[a]	Species Richness (S)	Shannon Diversity (H')	Species Richness (S)	Shannon Diversity (H')	Species Richness (S)	Shannon Diversity (H')	Species Richness (S)	Shannon Diversity (H')
Calcite	362	6.38	195	2.41	332	6.49	534	6.53
Limestone	289	6.20	149	3.74	326	6.57	561	5.28
Dolostone	318	6.10	129	3.69	337	6.69	435	4.14
Basalt	71	3.04	115	5.21	332	6.55	323	4.27
Quartz	55	3.67	54	3.80	332	6.68	548	5.23
Albite	57	4.96	210	2.57	329	6.65	547	5.78
Microcline	116	6.33	190	2.27	301	6.43	381	5.00
Chert	0	0	143	2.93	300	6.18	542	5.55
Planktonic	133	5.79	120	1.90	63	2.24	424	5.65
Whole Reactor	349	6.63	386	3.56	459	6.54	757	5.63
Mean ± s.e.	175 ± 127	5.31 ± 1.30	145 ± 49	3.17 ± 1.04	295 ± 88	6.05 ± 1.44	477 ± 88	5.27 ± 0.74
Surface Correlation Factors[b]	F (*P*)	F (*P*)	F (*P*)	F (*P*)	F (*P*)	F (*P*)	F (*P*)	F (*P*)
Buffering Capacity	**7.6 (0.024)**	**3.2 (0.036)**	1.1 (0.328)	0.8 (0.461)	0.9 (0.461)	0.7 (0.566)	0.8 (0.399)	0.1 (0.892)
Mineral Type	5.6 (0.556)	1.1 (0.624)	3.9 (0.606)	2.2 (0.420)	0.4 (0.996)	0.3 (0.991)	0.6 (0.996)	0.2 (0.884)
Mineral Phosphate	0.7 (0.461)	0.18 (0.834)	0.2 (0.863)	**4.3 (0.007)**	0.9 (0.602)	1.0 (0.428)	1.3 (0.201)	1.7 (0.061)

Reactor Correlation Factors[b]	Species Richness F (*P*)	Shannon Diversity F (*P*)
Carbon Amendment	1.1 (0.278)	**3.1 (0.006)**
Phosphate Amendment	**6.9 (0.0001)**	**3.2 (0.004)**
Media pHin	**2.8 (0.011)**	**3.2 (0.003)**
Media pHout	1.1 (0.301)	0.3 (0.758)
Reactors[c]	Species Richness F (*P*)	Shannon Diversity F (*P*)
CP-Limited vs. C-Amended	0.4 (0.892)	**3.2 (0.048)**
P-Amended vs. CP-Amended	0.1 (0.887)	1.7 (0.656)
P-Amended vs. C-Amended	**5.1 (0.002)**	**4.2 (0.008)**
P-Amended vs. CP-Limited	**3.6 (0.042)**	1.8 (0.709)
CP-Limited vs. CP-Amended	**4.5 (0.005)**	0.7 (0.997)
C-Amended vs. CP-Amended	**7.2 (0.001)**	**3.7 (0.006)**

Table 3.4: Bacterial α-diversity and effects of mineralogy and reactor conditions on α-diversity. [a]Measures of species richness (S) and Shannon Diversity (H') for each surface and each reactor. Values are based on rarefied data sets in order to allow comparisons across reactors.

Table 3.4 caption continued: [b]Impact of surface factors and reactor conditions assessed by PERMANOVA. Surface factors are buffering capacity (high vs. low based on whether surface is a carbonate or non-carbonate), mineral type (carbonate, silicate, aluminosilicate, planktonic), and mineral phosphate (high vs. low). Reactor correlation factors are carbon amendment (yes vs. no), phosphate amendment (yes vs. no), media pHin (high vs. low), and media pHout (high vs. Low). Values are the pseudo-F ratio (F) and the level of significance (*P*). Values at $P < 0.05$ indicate a significant differences in a factor and are shown in bold. [c]Pairwise comparisons of overall alpha diversity between reactors using PERMANOVA as described above.

Reactor	Surface	High-Quality Seqs.	Species Richness (S)	Shannon Diversity (H')	Evenness (E)	Simpson's Index (1-D)	Inverse Simpson (1/(1-D))	Good's Coverage
CP-Limited	Calcite	7829	362	6.38	1.08	0.03	35.31	99.7%
	Limestone	6095	289	6.20	1.09	0.03	39.63	99.4%
	Dolostone	7279	318	6.10	1.06	0.03	34.65	99.5%
	Basalt	1136	71	3.04	0.71	0.35	2.84	98.7%
	Quartz	2315	55	3.67	0.91	0.15	6.89	99.8%
	Albite	396	57	4.96	1.23	0.05	22.05	95.7%
	Microcline	546	116	6.33	1.33	0.02	55.25	95.1%
	Planktonic	1577	133	5.79	1.18	0.05	21.86	99.6%
	Whole Reactor	27173	349	6.63	0.98	0.02	56.85	99.9%
	Mean	3397	175	5.31	1.08	0.09	27.31	98.4%
	Standard Dev	3133.3	126.9	1.30	0.19	0.12	17.42	1.9%
C-Amended	Calcite	10894	195	2.41	0.46	0.47	2.15	99.5%
	Limestone	5604	149	3.74	0.75	0.22	4.64	99.6%
	Dolostone	2792	129	3.69	0.76	0.22	4.57	99.2%
	Basalt	6555	115	5.21	1.10	0.07	13.80	99.8%
	Quartz	594	54	3.80	0.95	0.14	7.03	99.5%
	Albite	16531	210	2.57	0.48	0.43	2.32	99.8%
	Microcline	15484	190	2.27	0.43	0.48	2.08	99.8%
	Chert	3484	143	2.93	0.59	0.38	2.66	98.6%
	Planktonic	4445	120	1.90	0.40	0.54	1.86	99.0%
	Whole Reactor	66383	386	3.56	0.78	0.22	4.47	100.0%
	Mean	7376	145	3.17	0.66	0.33	4.57	99.4%
	Standard Dev	5662.3	48.5	1.04	0.25	0.17	3.86	0.4%
P-Amended	Calcite	4538	332	6.49	1.12	0.02	42.00	98.1%
	Limestone	4146	326	6.57	1.14	0.02	42.70	98.2%
	Dolostone	4302	337	6.69	1.15	0.02	49.14	98.1%
	Basalt	3997	332	6.55	1.13	0.02	43.20	97.8%
	Quartz	3945	332	6.68	1.15	0.02	45.02	98.2%
	Albite	4099	329	6.65	1.15	0.02	47.43	97.9%
	Microcline	2820	301	6.43	1.13	0.03	36.03	96.5%
	Chert	3668	300	6.18	1.08	0.04	27.78	97.5%
	Planktonic	6332	63	2.24	0.54	0.39	2.56	99.8%
	Whole Reactor	37847	459	6.54	0.97	0.03	33.74	99.9%
	Mean	4205	295	6.05	1.06	0.07	37.32	98.0%
	Standard Dev	933.8	87.9	1.44	0.20	0.12	14.53	0.9%
CP-Amended	Calcite	6589	534	6.53	1.04	0.04	25.15	97.7%
	Limestone	12751	561	5.28	0.83	0.10	10.43	98.9%
	Dolostone	12674	435	4.14	0.68	0.20	5.12	99.1%
	Basalt	5340	323	4.27	0.74	0.16	6.15	97.4%
	Quartz	11016	548	5.23	0.83	0.11	9.38	98.8%
	Albite	8230	547	5.78	0.92	0.07	14.73	98.0%
	Microcline	5077	381	5.00	0.84	0.11	9.09	96.9%
	Chert	8936	542	5.55	0.88	0.09	11.55	98.4%
	Planktonic	7957	424	5.65	0.93	0.06	17.25	98.2%
	Whole Reactor	78570	757	5.63	0.92	0.08	12.15	99.9%
	Mean	8730	477	5.27	0.86	0.10	12.10	98.1%
	Standard Dev	2899.6	88.0	0.74	0.11	0.05	6.20	0.7%

Table 3.5: Bacterial α-diversity on each surface and for each whole reactor. High-quality sequences are the total sequences that were used in diversity analyses. Table also includes measures of species richness (S), Shannon Diversity (H'), Evenness (E), Simpson's diversity index (1-D), and Good's Coverage (%) for each surface and each reactor. Values are based on rarefied data sets for sequences from surfaces within each reactor and then for whole reactors in order to allow comparisons across reactors.

3.4.2 Effect of mineralogy on bacterial diversity

To quantify the effect of mineralogy (surface chemistry) on bacterial diversity, surfaces were categorized by whether they contained mineral bound phosphate, buffering capacity (carbonate vs. silicate) and overall mineral type (carbonate, silicate, or aluminosilicate, or no mineral/planktonic). Although variable in magnitude, the effect of surface chemistry on microbial diversity (both phylogenetic and taxonomic) was statistically significant, in all reactors, regardless of environmental pressures (Table 3.3). Visualizing β-diversity with Unweighted Pair Group Method with Arithmetic mean (UPGMA) clustering as tree constructed from the UniFrac distance matrix reinforces this statistical clustering according to mineral type (Figure 3.3). Phylogenetically, surface type controlled ~70-90% of the diversity, meaning that organisms attached to similar surfaces were significantly more genetically similar. The only exception is the C-Amended reactor where mineral phosphate is the most statistically significant variable, but some clustering by mineral type is still apparent (Figure 3.3b).

Specifically, when samples from the CP-Limited reactor were grouped as carbonates and non-carbonates, 12.3% (P=0.036) of the variation in phylogenetic β-diversity distances was explained and that overall mineral type accounted for 69.8% (P=0.009) of the variability. In the tree, the carbonates cluster together and are the most closely related phylogenetically ($Ø_{sim}$>93%), then the aluminosilicates ($Ø_{sim}$>85%), and the silicates ($Ø_{sim}$>48%). Finally, sequences from the planktonic microorganisms are most closely related to the silicate cluster, but $Ø_{sim}$<36% similar phylogenetically (Figure 3.3a).

Similarly, when sequences in the CP-Amended reactor were grouped I found an even greater impact on phylogenetic distances from carbonate vs. non-carbonates (R^2=73.4, P<0.012) and overall mineral type (R^2=88.3, P<0.003). Viewing the tree, the

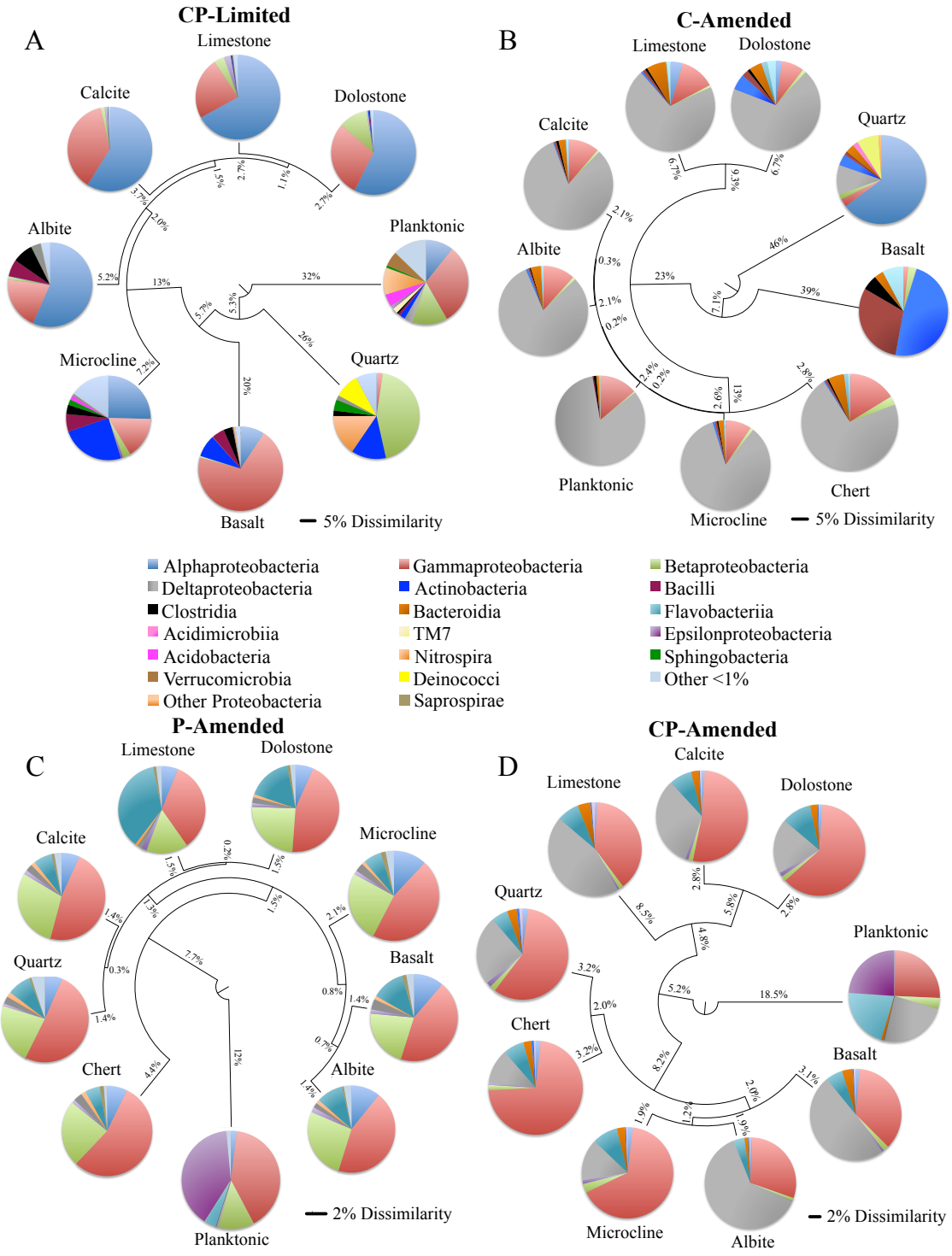

Figure 3.3: Caption on next page:

Figure 3.3: Unweighted pair group method with arithmetic mean (UPGMA) trees constructed using weighted UniFrac (phylogenetic) distance matrix constructed from 16S rRNA sequences clustered at 97% similarity for each of the four reactors (CP-Limited, P-Amended, C-Amended, CP-Amended). The trees display the phylogenetic overlap in bacterial communities colonizing various solid surfaces within each reactor. The key (center) contains the class level taxonomy associated with each mineral surface (see S-TableTaxonomy for proportional abundances). The scale bars for the CP-Limited and C-Amended reactors represents 0.05 (5%) dissimilarity in 16S rRNA sequences isolated from each surface and the scale bars for the P-Amended and CP-Amended reactors 0.02 (2%) dissimilarity. Note that although the taxonomy of the CP-Limited reactor is the same as Jones and Bennett 2014, the UPGMA tree here is based on UniFrac distances, while the tree in Jones and Bennett 2014 (Fig. 4) used the OTU based Sorenson similarity index.

sequences in the CP-Amended reactor cluster according to mineral type (Figure 3.3d). In the CP-Amended reactor carbonates are less closely related ($Ø_{sim}$>80%) than in the CP-Limited reactor. However, the silicates ($Ø_{sim}$>86%) and the aluminosilicates ($Ø_{sim}$>96%) are more closely related than in the CP-Limited reactor. Additionally, the planktonic sample is equally related to, but substantially different from, every mineral type cluster ($Ø_{sim}$~63%).

In the C-Amended reactor, mineral phosphate availability accounted for 30.9% (P=0.034) of the phylogenetic variability, but mineral type had no statistically significant impact on phylogenetic relatedness. Again the carbonates cluster together with limestone and dolostone more closely related ($Ø_{sim}$>86%) and calcite ($Ø_{sim}$~68%). However, the sequences from calcite are more similar to albite ($Ø_{sim}$~96%), microcline ($Ø_{sim}$~95%), chert ($Ø_{sim}$~94%), and the planktonic ($Ø_{sim}$~95%) samples. Furthermore, basalt and quartz have very low phylogenetic similarity to all other samples in the C-Amended reactor, with <8% similarity to each other, basalt <23% related to any other sample, and quartz <9% similar to all other samples (Figure 3.3b).

Finally, 85.9% (P=0.035) of the phylogenetic variability in the P-Amended reactor was controlled by overall variations in mineral chemistry, but mineral buffering (carbonate vs. non-carbonate) and mineral phosphate availability had no significant impact. The UPGMA tree reveals clustering similar to, but less significant than that of the CP-limited and CP-Amended reactors (Figure 3.3). The P-Amended reactor had the least amount of phylogenetic variability between surface attached communities of all reactors. The carbonate samples are >95% similar, but all surface samples are >91% similar. The planktonic sample is the least similar sample to all other samples in the P-Amended reactor ($Ø_{sim}$>75%).

Within the CP-Limited reactor there was a significant difference in species richness between carbonates and non-carbonates (P=0.024). Additionally, there was a significant difference in Shannon diversity between carbonates and non-carbonates (P=0.036). Within the C-Amended reactor Shannon diversity was significantly impacted by mineral phosphate concentration (P=0.007, Table 3.4).

Although there were no statistically significant differences in Shannon diversity or species richness of communities within the other reactors, there were notable differences in these parameters. In terms of species richness (S), samples from the C-Amended reactor had a total of 386 unique OTUs. The number of OTUs varied from 54 on quartz to 210 on albite (Table 3.4). Although there was large variability in species richness it could not be significantly tied to a correlation factor. Within the C-Amended reactor microcline, albite, and calcite had the least diverse attached communities (H'=2.27, 2.57, & 2.41 respectively). However, the planktonic community had the lowest diversity (H'=1.90). In the CP-Limited reactor basalt had the lowest Shannon diversity, but in the C-Amended reactor had the highest Shannon diversity (H'=3.04 vs. 5.21, respectively).

Within both the P-Amended and CP-Amended reactor, differences in alpha-diversity values among attached microorganisms were statistically small and not significant. However, as whole reactors, the two P-Amended reactors had significantly higher species richnesses. Therefore, species richness was significantly tied to whether the reactor was P-Amended (P=0.0001) and the pH_{in} (P=0.011) of the reactor. Additionally, the P-Amended reactors had significantly higher overall and individual Shannon diversity values. The overall Shannon diversity of each reactor was tied to mineral phosphate availability (P=0.001), whether or not the reactor was C-amended (P=0.006), whether or not the reactor was P-amended (P=0.004), and the pHin of the

media into the reactor (P=0.003). Additionally, the planktonic community within the P-Amended reactor was significantly less diverse than the attached communities within that reactor (Table 3.4).

3.4.3 Taxonomic composition and condition sensitive taxa

The taxonomic complexity of communities within each reactor and shared between reactors is visualized in Figure 3.4 and a complete list of all detected bacterial taxa, summarized at the class and genus level, is provided in Tables 3.6-3.9. Upon taxonomy assignment, these OTUs represented 280 unique bacterial genera. 73 genera, out of the 280, had a relative abundance of more than 1% in any given sample and these are listed in Tables 3.6-3.9. At this level, the composition of microbial communities included 11 bacterial phyla: *Acidobacteria, Actinobacteria, Bacteroidetes, Chloroflexi, Firmicutes, Nitrospirae, Planctomycetes, Proteobacteria, Thermi, TM7,* and *Verrucomicrobia*. *Proteobacteria* was the most abundant phylum across all 35 samples with the exception of basalt in the C-Amended reactor. The composition of microbial communities included 20 bacterial classes: *Alphaproteobacteria, Betaproteobacteria, Deltaproteobacteria, Gammaproteobacteria, Epsilonproteobacteria, Acidobacteria, Acidomicrobiia, Actinobacteria, Bacilli, Bacteroidia, Clostridia, Coriobacteriia, Cytophagia, Deinococci, Flavobacteria, Nitrospira, Opitutae, Saprospirae, Sphingobacteria,* and *TM7*.

OTUs classified at lower taxonomic levels (genus) contain more information relevant to inferring their putative ecological role in each unique bioreactor ecosystem. Once I classified the sequences at the genus level, I was able to examine individual responses of these OTUs and identify guilds that respond similarly to geochemical

variables. Taxonomically, there is very little overlap between overall reactor communities (Figure 3.4). All reactors harbored structurally, taxonomically, and phylogenetically distinct microbial communities. At the genus level, there are no common taxa shared between all 4 reactors or between the CP-Limited, C-Amended, and P-Amended taken together (Figure 3.4). The C-Amended, P-Amended, and CP-Amended share only members of the genus *Cloacibacterium*. Further responses of genera to geochemical variability is summarized in these results, followed by a more detailed discussion in the context of extant literature in the Discussion section, herein.

Sequencing of the inoculant revealed only ~10 OTUs due to the overwhelming dominance of *Gammaproteobacteria* (34.7%) and *Epsilonproteobacteria* (62.4%) composed primarily of the genera *Thiothrix* spp. and *Sulfurovum* spp., respectively (Jones & Bennett, 2014). By providing a variety of potential selective advantages I revealed the presence hundreds of OTUs representing a consortium of microorganisms. Furthermore, *Epsilonproteobacteria* were poorly represented in the microbial communities colonizing mineral surfaces in all reactors despite their relative abundance in the inoculant (Tables 3.6-3.9). However, *Epsilonproteobacteria* were detected in abundance in planktonic samples from the P-Amended and CP-Amended reactors (Figure 3.3c & d).

Taxonomically, surfaces within the CP-Limited reactor had distinct lineages, which also appeared to be constrained by mineralogy and mineral buffering capacity. Many of the details of the distribution of taxonomies were discussed thoroughly in a previous study (Jones & Bennett, 2014). In summary, I found that the taxonomy of communities associated with carbonates were nearly identical; primarily composed of *Alphaproteobacteria* (57-67%), *Gammaproteobacteria* (23-38%) and *Betaproteobacteria* (1.5-11%). The communities also had minor amounts (<3% proportional abundance) *Epsilonproteobacteria, Actinobacteria, Bacilli, Clostridia,* and *Deltaproteobacteria*

(Table 3.6). These communities were substantially dominated by putative neutrophilic sulfur oxidizers (SOB) (*Thioclava*, *Halothiobacillus*, *Thiothrix*, *Sulfurovum*, and *Bosea*) in relatively large proportional abundances (17-45%) when compared to other communities within the same reactor (Table 3.6). Quartz was colonized by a large proportion of putative acidophilic organisms (*Acidisphaera*, *Meiothermus*, *Acidithiomicrobium*, *Acidithiobacillus* and *Thermodesulfovibrio*) that are found only in the quartz sample. Additionally, sequences isolated from the basalt surface were closely related to members of the genus *Thiothrix* (~66%). Furthermore, gram-positive microorganisms (*Actinobacteria, Bacilli, Clostridia,* and *TM7*) were found almost exclusively on silicates and aluminosilicates, but particularly on aluminosilicates (Table 3.6).

The planktonic community is both phylogenetically and taxonomically distinct from any of the attached communities (Figure 3.3a). The primary differences taxonomically are the significant abundance of *Acidithiobacillus*, *Chloroacidobacterium*, *Acidisphaera*, *Thiobacillus*, and *Thermodesulfovibrio*) which supports the phylogenetic assessment that these organisms are most similar to those found on quartz, but still significantly different ($Ø_{sim}$<36% to quartz, P<0.05).

The CP-Amended reactor had the least variable community across the mineral surfaces (Figure 3.3), and consisted of minor phylogenetic variability in populations primarily composed of *Gammaproteobacteria* (*Halothiobacillus* 29.8-72.3%) and *Deltaproteobacteria* (*Desulfovibrio* 11.9-61.4%; Table 3.7). The planktonic community also had high abundances of these genera, but also had nearly equal abundances of *Flavobacteria* (*Cloacibacterium,* 21.4%) and *Epsilonproteobacteria* (*Sulfurospirillum,* 23.9%) in the planktonic sample (Table 3.7). Gram-positive bacteria were nearly absent

(<1%) on all surfaces in the CP-Amended reactor, and not detectable in the planktonic sample (Table 3.7).

Most surfaces within the C-Amended (P-Limited) reactor were dominated by members of the class *Deltaproteobacteria* (*Desulfovibrio* 69.1-84.5%). These surfaces had nearly identical community memberships with minor representation from members of the lineages *Gammaproteobacteria* (8.1-16.0%), *Bacilli* (0.6-2.4%), *Actinobacteria* (0.4-48.0%), *Bacteriodia* (2.0-7.2%), and *Clostridia* (0.4-1.0%) (Table 3.8). However, *Desulfovibrio* spp. was not dominant on either quartz (10.1%) or basalt (0.2%) (Table 3.8). Quartz was dominated by *Alphaproteobacteria* (64.8%); primarily of the genus *Bradyrhizobium* (45.3%) (Table 3.8). Basalt was dominated by gram-positive *Actinobacteria* (48.0%); primarily of the genus *Propionibacterium* (35.7%) and a variety of members of the lineage *Bacilli* (30.5%) represented by members of the genera *Staphylococcus* (9.4%), *Alicyclobacillus* (7.3%), and *Streptococcus* (8.9%); all of which are nearly exclusive to the basalt surface (Table 3.8). Quartz had low representation from *Actinobacteria* (4.2%) represented by members of the genera *Propionibacterium* (2.6%) and *Acidomicrobiales* (1.9%), *Bacilli* (1.3%) composed completely of the genus *Bacillus,* *Bacteroidia* (3.2%) composed completely of the genus *Blvii28,* and was the only community to contain members of the candidate division TM7 (8.0%) (Table 3.8). The microbial community on basalt contained members of the lineage *Bacteroida* as *Blvii28* (3.2%), *Clostridia* as *Anerococcus* (5.6%), and was the only community to contain members of the class *Cytophagia* as *Adhaeribacter* (1.2%) and *Coriobacteriia* as *Atobium* (2.7%) (Table 3.8).

Surfaces within the C-Limited (P-Amended) reactor had nearly identical community structures dominated by *Gammaproteobacteria* (34.2-54.9%) represented primarily by the genus *Thiothrix* (26.4-48.9%), with lesser abundance of members of the

genera *Thermonas* (0.7-2.6%), *Aquimonas* (1.6-4.5%), *Thioalkalivibrio* (0.3-1.1%), *Rheinheimera* (0.3-2.1%), and *Lysobacter* (0.5-2.7%) (Table 3.9). The other dominant lineage was *Betaproteobacteria* (16.0-32.1%) represented primarily by the genus *Hydrogenophaga* (4.8-11.8%), with lesser representations from the genera *Mitsuaria* (1.4-4.3%), *Vogesella* (0.4-6.3%), *Ideonella* (1.4-5.1%), *Pelomonas* (0.6-2.9%), *Thiomonas* (0.6-3.3%), and *Thiobacillus* (0.4-2.0%) on all surfaces with representatives of the genus *Acidovorax* (0.2-1.0%) excluded from the surfaces of calcite, microcline, and basalt (Table 3.9). *Alphaproteobacteria* (6.3-12.6%) and *Flavobacteria* (7.1-38.6%) represent the next most abundant lineages on all surfaces and gram-positive bacteria were almost completely absent from the reactor (Table 3.9).

Epsilonproteobacteria was poorly represented within the P-Amended reactor with between 1.1-2.0% proportional abundance across all surfaces as members of the genera *Sulfurovum* spp. and *Sulfurospirillum* spp. (Table 3.9). However, similar to the CP-Amended reactor, *Epsilonproteobacteria* was found in high abundance (39.5%) as members of the planktonic community, closely related to *Sulfuricurvum*. Within the *Alphaproteobacteria* lineage, the genera *Thioclava* (2.7-5.6%) and *Pannonibacter* (1.3-2.8%) were the most dominant (Table 3.9). Within the *Flavobacteria* lineage, the genera *Bergeyella* (3.9-21.1%) and *Flavobacterium* (0.9-14.8%) are the most dominant (Table 3.9). *Deltaproteobacteria* (1.2-3.4%) are poorly represented on all surfaces and primarily composed of representatives of the genus *Corallococcus* (Table 3.9).

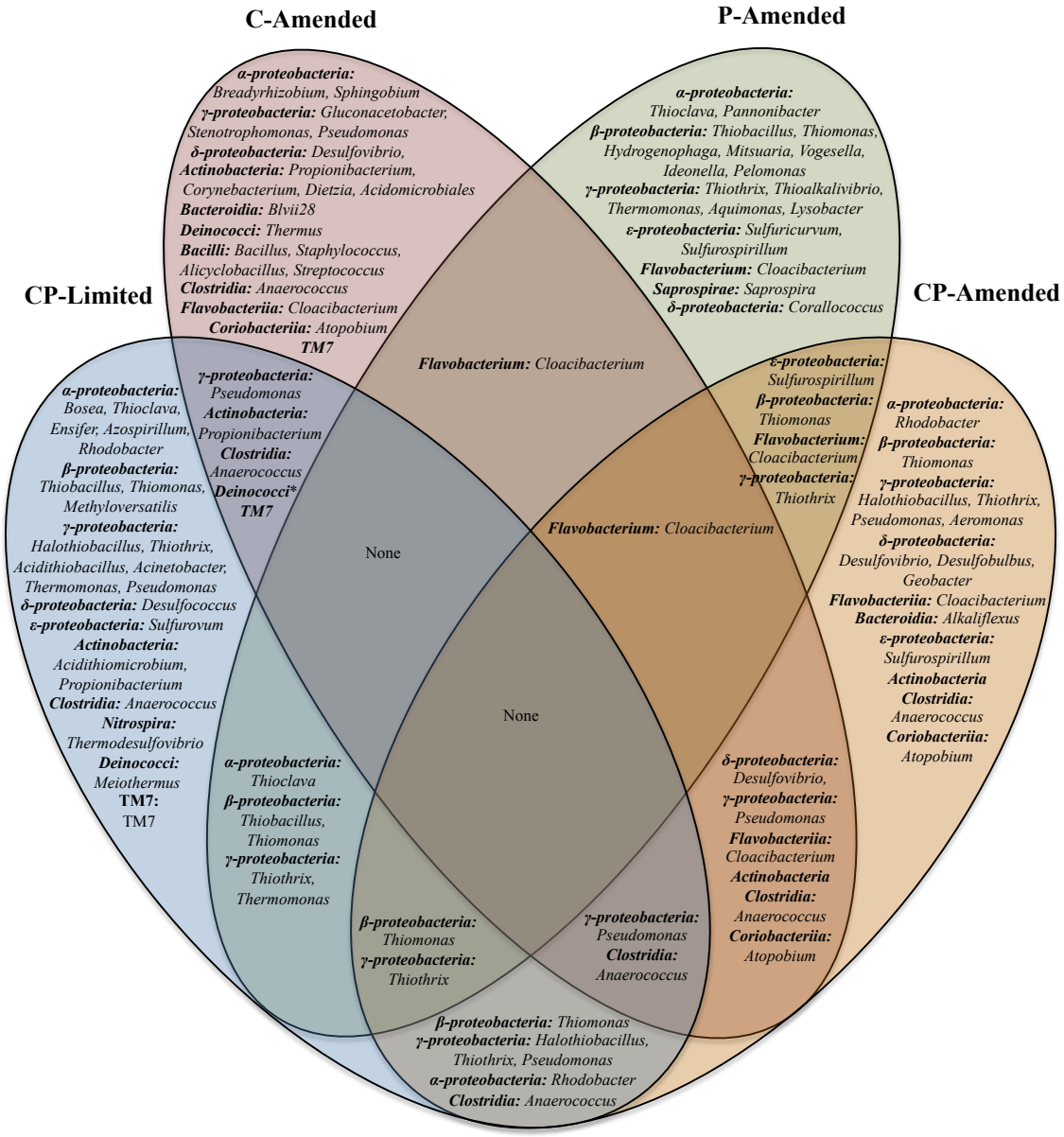

Figure 3.4: Venn diagram of the shared bacterial genera found in the four reactors (CP-Limited, P-Amended, C-Amended, CP-Amended). Overlaps between the reactors are indicated by overlaps in the diagram.

Representative *Class*	Representative *Genus*	LKC Inoculant	Calcite	Madison Limestone	Madison Dolostone	Microcline	Albite	Quartz	Basalt	Planktonic
α-proteobacteria		**0.1**	**58.9**	**67.0**	**57.4**	**25.4**	**56.7**	**0.5**	**9.2**	**10.7**
	Ensifer	0	29.4	30.4	14.7	6.0	29.2	0	4.7	0
	Azospirillum	0	6.6	8.3	11.5	1.3	16.4	0	2.5	0
	Bosea	0	5.6	3.0	12.9	0.2	6.5	0	0	0
	Thioclava	0	6.0	3.1	7.1	0.1	0	0	0	0
	Defluvibacter	0	2.9	1.1	0.6	0.1	1.4	0	0.1	0.1
	Sphingopyxis	0	2.5	12.6	5.3	3.2	0	0	0.4	0
	Sphingomonas	0	0	0	0	3.2	0.2	0	0	0.1
	Acidisphaera	0	0	0	0	0	0	0.3	0	3.1
	Rhodobacter	0	0	0	0	0	0	0	0	1.5
γ-proteobacteria		**34.7**	**37.6**	**23.7**	**28.8**	**16.0**	**20.1**	**1.8**	**70.1**	**31.1**
	Acinetobacter	0	22.6	3.5	4.0	2.0	0	0.2	0.1	0
	Halothiobacillus	0	9.1	5.6	14.5	0.3	0	0	0	0
	Thermomonas	0	4.4	12.5	7.7	0.2	5.1	0	0	0
	Pseudomonas	0	0.8	0.4	0.4	4.5	10.4	0	0	0.2
	Thiothrix	34.7	0	0.2	0.2	0	0	0	65.5	0.2
	Stenotrophomonas	0	0	0	0.1	1.4	1.6	0	3.7	0
	Acidithiobacillus	0	0	0	0	0	0	1.2	0	25.9
	Nitrosococcus	0	0	0	0	0	0	0	0	2.2
β-proteobacteria		**0.2**	**1.5**	**4.0**	**11.0**	**2.9**	**1.4**	**44.1**	**0.6**	**13.5**
	Thiobacillus	0	0.3	0.5	0.7	0	0	1.2	0	5.9
	Methyloversatilis	0.1	0.2	0.9	0.9	0	0	26.4	0	0.4
	Zoogloea	0	0	0	0	0	0	3.5	0	2.5
	Thiomonas	0	1.0	2.5	9.1	0	0	0	0	0
ε-proteobacteria		**62.4**	**1.2**	**2.6**	**0.7**	**0.9**	**0**	**0**	**0**	**1.4**
	Sulfurovum	62.3	1.2	2.6	0.7	0.3	0	0	0	0
Actinobacteria		**0.1**	**0.1**	**0.3**	**0.4**	**24.6**	**0**	**13.1**	**8.6**	**2.1**
	Acidithiomicrobium	0	0	0	0	0	0	12.6	0	0.5
	Rubrobacter	0	0	0	0	3.9	0	0	0	0.1
	Propionibacterium	0	0.1	0.1	0.1	0.8	0	0.2	4.7	0
	Microthrix	0	0	0	0	0	0	0	0	1.5
Bacilli		**0**	**0.1**	**0.2**	**0.4**	**6.7**	**6.5**	**0**	**4.9**	**0.9**
	Lactobacillus	0	0.1	0.1	0.2	0.2	0.9	0	3.8	0.0
Clostridia	***Anaerococcus***	**0.9**	**0.1**	**0.1**	**0.1**	**3.6**	**7.9**	**2.1**	**3.5**	**0.7**
Sphingobacteria		**0**	**0**	**0**	**0**	**2.1**	**0.2**	**4.2**	**0**	**0.9**
Acidobacteria		**0**	**0**	**0**	**0**	**1.6**	**0**	**0**	**0**	**4.7**
	Chloroacidobacterium	**0**	**0**	**0**	**0**	**0**	**0**	**0**	**0**	**4.7**
δ-proteobacteria		**0.5**	**0.1**	**0.4**	**0.2**	**0.9**	**3.7**	**1.7**	**0.4**	**3.1**
	Desulfococcus	0	0	0.2	0	0	3.7	0	0	0
	Desulfomonile	0	0.1	0	0.1	0	0	0	0.4	0
Deinococci	***Meiothermus***	**0**	**0**	**0**	**0**	**0**	**0**	**9.4**	**0.7**	**0**
Nitrospira	***Thermodesulfovibrio***	**0**	**0**	**0**	**0**	**0**	**0**	**15.4**	**0.1**	**10.4**
Opitutae	***Opitutus***	**0**	**0**	**0**	**0**	**0**	**0**	**0**	**0**	**5.7**
TM7	***TM7***	**0**	**0**	**0**	**0**	**0**	**0**	**0**	**0**	**2.0**
***Class* <1% Abundance/Unclassified**		**0.5**	**0.5**	**1.8**	**1.1**	**15.3**	**3.5**	**7.8**	**2.0**	**12.8**
Total Proportion SOB		**97.0**	**23.3**	**17.4**	**45.2**	**0.9**	**6.5**	**15.0**	**65.5**	**32.5**
Total Proportion Netrophilic SOB		**97.0**	**23.3**	**17.4**	**45.2**	**0.9**	**6.5**	**1.2**	**65.5**	**6.1**
Total Proportion Acidophilic SOB		**0**	**0**	**0**	**0**	**1.6**	**0**	**13.8**	**0**	**26.4**
Total Proportion Acidophilic		**0**	**0**	**0**	**0.9**	**0**	**0**	**38.9**	**0.8**	**44.6**
Total Proportion SRB		**0**	**0.1**	**0.2**	**0.1**	**0**	**3.7**	**15.4**	**0.5**	**10.4**
Total Proportion Gram Positive		**1.0**	**0.3**	**0.6**	**0.9**	**34.9**	**14.4**	**15.2**	**17.0**	**5.7**

Table 3.6: CP-Limited reactor samples as proportional abundance (%) of taxa of representative class (bold) and genera from 16S rRNA gene sequences in the LKC inoculant, for each surface, and the planktonic sample after 3-weeks within the CP-Limited reactor. Potential sulfur-oxidizing genera (SOB), sulfur reducing genera (SRB), acidophilic genera, and gram-positive genera are highlighted (Adapted from Jones and Bennett 2014).

Representative Class	Representative Genus	Calcite	Madison Limestone	Madison Dolostone	Microcline	Albite	Quartz	Basalt	Chert	Planktonic
γ-proteobacteria		**52.1**	**39.0**	**62.4**	**66.0**	**29.8**	**58.5**	**36.1**	**72.3**	**25.4**
	Pseudomonas	36.3	5.3	9.0	13.2	6.2	16.2	6.4	18.5	9.8
	Thiothrix	2.2	0.5	2.5	0.4	0.6	0.4	0.8	0.3	0.1
	Halothiobacillus	9.6	29.3	45.9	49.5	21.4	38.7	24.7	49.5	11.4
	Aeromonas	2.4	3.0	3.1	1.5	0.8	1.8	3.0	2.0	0.1
δ-proteobacteria		**32.3**	**44.2**	**19.5**	**14.9**	**62.3**	**24.5**	**48.8**	**11.9**	**24.0**
	Desulfovibrio	28.8	44.1	19.4	14.4	61.4	24.1	48.3	11.6	22.1
	Desulfobulbus	3.3	0.0	0.1	0.1	0.9	0.0	0.3	0.1	0.0
	Geobacter	0.1	0.1	0.0	0.4	0.0	0.4	0.2	0.2	1.8
Flavobacteriia		**8.1**	**7.8**	**10.6**	**9.1**	**3.9**	**5.8**	**6.0**	**7.1**	**21.4**
	Cloacibacterium	7.4	7.4	10.3	8.9	3.7	5.4	5.9	6.9	21.4
Bacteroidia		**2.7**	**4.4**	**2.6**	**3.0**	**1.3**	**3.4**	**3.7**	**2.7**	**1.0**
	Alkaliflexus	1.5	2.4	1.9	2.0	0.6	2.1	2.2	1.6	0.9
β-proteobacteria		**1.6**	**1.5**	**1.8**	**3.1**	**1.1**	**2.1**	**2.0**	**1.9**	**4.0**
	Thiomonas	0.0	0.1	0.5	0.4	0.2	0.5	0.4	0.2	0.0
	Comamonas	0.5	0.3	0.2	1.0	0.2	0.4	0.6	0.4	2.7
ε-proteobacteria		**1.1**	**0.7**	**1.4**	**1.2**	**0.2**	**1.8**	**0.8**	**0.8**	**23.9**
	Sulfurospirillum	1.0	0.7	1.4	1.2	0.2	1.7	0.8	0.8	23.9
α-proteobacteria		**1.0**	**0.8**	**1.1**	**1.9**	**0.6**	**1.9**	**1.4**	**1.8**	**0.3**
	Rhodobacter	0.8	0.6	0.9	1.4	0.3	1.5	0.8	1.2	0.1
Actinobacteria		**0.3**	**0.3**	**0.3**	**0.2**	**0.3**	**0.8**	**0.3**	**0.8**	**0.0**
Clostridia		**0.0**	**0.1**	**0.1**	**0.1**	**0.0**	**0.1**	**0.1**	**0.1**	**0.0**
	Clostridium	0.0	0.1	0.1	0.1	0.0	0.1	0.1	0.1	0.0
Class <1% Abundance/Unclassified		**0.7**	**1.2**	**0.3**	**0.5**	**0.4**	**1.2**	**0.8**	**0.6**	**0.0**
Total Proportion SOB		11.9	29.9	48.9	50.2	22.2	39.6	25.8	50.0	11.5
Total Proportion SRB		33.1	44.9	20.9	15.7	62.4	25.8	49.4	12.5	46.0
Total Proportion G+		0.4	0.4	0.4	0.3	0.3	0.9	0.4	0.8	0.0

Table 3.7: CP-Amended reactor samples as proportional abundance (%) of taxa of representative class (bold) and genera from 16S rRNA gene sequences for each surface and the planktonic sample after 3-weeks within the CP-Amended reactor. Potential sulfur-oxidizing genera (SOB), sulfur reducing genera (SRB), acidophilic genera, and gram-positive genera are highlighted.

Representative Class	Representative Genus	Calcite	Madison Limestone	Madison Dolostone	Microcline	Albite	Chert	Quartz	Basalt	Planktonic
δ-proteobacteria		**82.1**	**70.4**	**69.1**	**84.5**	**80.8**	**71.6**	**10.5**	**0.2**	**82.8**
	Desulfovibrio	82.1	70.4	69.1	84.5	80.8	71.6	10.1	0.2	82.8
α-proteobacteria		**0.2**	**4.5**	**2.3**	**0.1**	**0.0**	**0.2**	**64.8**	**0.0**	**0.1**
	Sphingobium	0.0	2.1	1.5	0.0	0.0	0.0	10.5	0.0	0.0
	Blastomonas	0.0	0.2	0.3	0.0	0.0	0.0	4.6	0.0	0.0
	Novosphingobium	0.0	0.1	0.0	0.0	0.0	0.0	3.0	0.0	0.0
	Bradyrhizobium	0.0	0.1	0.4	0.0	0.0	0.0	45.3	0.0	0.0
γ-proteobacteria		**11.1**	**12.7**	**8.1**	**9.4**	**11.6**	**16.0**	**3.0**	**1.8**	**13.8**
	Gluconacetobacter	5.2	8.4	6.4	3.1	5.3	4.0	1.3	0.0	6.6
	Stenotrophomonas	2.8	3.7	0.4	4.2	4.2	7.5	1.1	0.0	1.7
	Pseudomonas	1.4	0.2	0.7	1.2	0.9	2.0	0.0	0.0	4.5
β-proteobacteria		**0.8**	**0.9**	**1.3**	**1.1**	**1.1**	**3.0**	**2.0**	**2.9**	**0.5**
	Diaphorobacter	0.0	0.7	0.2	0.0	0.0	0.0	0.7	2.6	0.0
	Janthinobacterium	0.5	0.0	0.2	0.7	0.8	2.7	0.0	0.0	0.4
Actinobacteria		**0.4**	**0.7**	**5.8**	**0.7**	**0.9**	**0.5**	**4.2**	**48.0**	**0.0**
	Propionibacterium	0.0	0.2	1.6	0.0	0.0	0.0	2.6	35.7	0.0
	Acidomicrobiales	0.0	0.0	0.0	0.0	0.0	0.0	1.9	0.0	0.0
	Corynebacterium	0.0	0.0	2.4	0.0	0.0	0.0	0.7	2.5	0.0
	Dietzia	0.0	0.0	0.0	0.0	0.0	0.0	0.0	8.1	0.0
Bacilli		**0.8**	**1.2**	**2.4**	**0.8**	**0.6**	**0.8**	**1.3**	**30.5**	**0.4**
	Bacillus	0.2	0.6	2.2	0.5	0.1	0.3	1.3	0.0	0.2
	Staphylococcus	0.0	0.3	0.0	0.0	0.0	0.0	0.0	9.4	0.0
	Alicyclobacillus	0.0	0.0	0.0	0.0	0.0	0.0	0.0	7.3	0.0
	Streptococcus	0.0	0.0	0.1	0.0	0.0	0.0	0.0	8.9	0.0
Bacteroidia		**2.6**	**7.2**	**4.6**	**2.0**	**3.7**	**5.3**	**3.2**	**3.4**	**0.9**
	Blvii28	2.5	7.2	4.4	2.0	3.6	5.2	3.2	3.3	0.9
Cytophagia	***Adhaeribacter***	**0.0**	**0.0**	**0.0**	**0.0**	**0.0**	**0.0**	**0.0**	**1.2**	**0.0**
Clostridia		**0.9**	**0.8**	**1.0**	**0.5**	**0.4**	**0.6**	**0.0**	**5.6**	**1.0**
	Anaerococcus	0.0	0.0	0.0	0.0	0.0	0.0	0.0	5.5	0.9
Coriobacteriia	***Atopobium***	**0.0**	**0.0**	**0.0**	**0.0**	**0.0**	**0.0**	**0.0**	**2.7**	**0.0**
Deinococci		**0.0**	**0.0**	**2.0**	**0.0**	**0.0**	**0.0**	**0.0**	**0.0**	**0.0**
	Thermus	0.0	0.0	1.8	0.0	0.0	0.0	0.0	0.0	0.0
TM7	***TM7***	**0.0**	**0.0**	**0.0**	**0.0**	**0.0**	**0.0**	**8.0**	**0.0**	**0.0**
Flavobacteriia	***Cloacibacterium***	**0.3**	**0.3**	**2.1**	**0.3**	**0.4**	**1.5**	**0.0**	**0.0**	**0.5**
Acidimicrobiia	***Unclassified***	0.0	0.0	0.0	0.0	0.0	0.0	1.9	0.0	0.0
Class <1% Abundance/Unclassified		**0.8**	**1.3**	**1.3**	**0.6**	**0.5**	**0.5**	**1.1**	**3.7**	**0.0**
Total Proportion SRB		**82.1**	**70.4**	**69.1**	**84.5**	**80.8**	**71.6**	**10.5**	**0.2**	**82.8**
Total Proportion SOB		**0.0**	**0.0**	**0.0**	**0.0**	**0.0**	**0.0**	**0.0**	**0.0**	**0.0**
Total Proportion Gram Positive		**2.1**	**2.7**	**9.2**	**2.1**	**1.9**	**1.8**	**13.5**	**86.8**	**1.4**
Total Proportion Acidophilic		**0.0**	**0.1**	**0.4**	**0.0**	**0.0**	**0.0**	**47.2**	**0.0**	**0.0**

Table 3.8: C-Amended reactor samples as proportional abundance (%) of taxa of representative class (bold) and genera from 16S rRNA gene sequences for each surface and the planktonic sample after 3-weeks within the C-Amended reactor. Potential sulfur-oxidizing genera (SOB), sulfur reducing genera (SRB), acidophilic genera, and gram-positive genera are highlighted.

Representative Class	Representative Genus	Calcite	Madison Limestone	Madison Dolostone	Microcline	Albite	Chert	Quartz	Basalt	Planktonic
α-proteobacteria		**6.7**	**6.1**	**6.7**	**12**	**10.8**	**7.2**	**6.5**	**11.2**	**2.0**
	Thioclava	2.7	2.9	3.2	3.3	5.6	3.1	3.5	4.5	1.5
	Pannonibacter	2.6	1.4	1.4	6.0	2.8	2.8	1.3	4.6	0.0
β-proteobacteria		**29.4**	**15.4**	**24.3**	**25.3**	**26.5**	**23.7**	**22.4**	**21.6**	**11.7**
	Hydrogenophaga	11.8	4.8	7.2	11.8	6.8	6.8	5.9	8.0	3.7
	Mitsuaria	4.3	3.1	2.9	1.4	2.5	2.1	2.8	2.5	0.0
	Vogesella	0.4	1.5	1.3	1.6	6.3	5.3	0.5	1.4	1.5
	Ideonella	5.1	1.4	3.6	3.7	2.6	2.7	3.8	2.3	0.0
	Pelomonas	2.9	0.6	1.9	1.0	2.5	1.8	2.0	1.5	0.0
	Thiomonas	1.0	0.6	1.3	1.8	1.4	3.3	2.7	3.2	0.9
	Thiobacillus	1.6	0.9	2.0	1.2	1.0	0.4	1.3	0.5	0.4
γ-proteobacteria		**47.4**	**34.2**	**44.4**	**45.6**	**44.1**	**54.9**	**50.8**	**43.6**	**40.3**
	Thiothrix	38.0	26.4	34.6	37.6	35.5	48.9	40.8	34.2	35.2
	Thermomonas	1.1	2.3	1.5	2.4	2.6	0.7	2.1	2.6	3.4
	Aquimonas	4.5	1.7	3.8	1.8	1.6	2.0	2.0	1.9	0.0
	Thioalkalivibrio	0.9	0.8	0.7	1.0	0.8	0.3	1.1	0.8	0.0
	Rheinheimera	1.0	0.6	1.9	1.4	2.1	2.1	1.9	0.3	1.2
	Lysobacter	1.4	0.9	0.5	1.3	1.1	0.6	2.2	2.7	0.1
δ-proteobacteria		**2.6**	**1.7**	**2.2**	**3.1**	**1.8**	**3.2**	**2.7**	**3.9**	**1.0**
	Corallococcus	0.9	0.6	0.6	0.9	0.5	1.5	0.7	1.5	0.7
ε-proteobacteria		**1.6**	**2.1**	**1.4**	**1.4**	**2.0**	**1.2**	**1.0**	**1.6**	**39.5**
	Sulfuricurvum	1.0	1.1	1.2	1.1	1.6	0.9	0.8	1.1	39.4
	Sulfurospirillum	0.1	0.8	0.1	0.1	0.0	0.2	0.1	0.2	0.0
Other Proteobacteria		**1.6**	**1.0**	**1.2**	**1.2**	**1.5**	**1.7**	**1.9**	**1.3**	**0.0**
Flavobacteriia		**6.9**	**36.4**	**16.6**	**6.5**	**9.9**	**5.4**	**8.8**	**12.4**	**4.0**
	Flavobacterium	0.1	0.7	1.2	0.0	0.2	0.4	0.0	0.0	0.0
	Cloacibacterium	6.0	32.7	15.3	6.5	7.2	5.0	8.8	12.3	3.9
Saprospirae	***Saprospira***	**1.0**	**1.0**	**1.1**	**1.7**	**0.7**	**1.5**	**0.8**	**1.5**	**0.0**
Class <1% Abundance/Unclassified		**2.7**	**2.1**	**2.1**	**3.0**	**2.9**	**1.2**	**5.1**	**2.9**	**1.5**
Proportion SOB		**45.2**	**32.7**	**43.0**	**46.0**	**46.0**	**56.9**	**50.2**	**44.3**	**77.4**
Proportion SRB		**1.0**	**1.4**	**0.7**	**1.0**	**0.5**	**1.7**	**0.8**	**1.7**	**0.0**
Proportion Gram-positive		**0.1**	**0.1**	**0.1**	**0.1**	**0.1**	**0.0**	**0.2**	**0.2**	**0.0**
Proportion Alkaliphiles		**28.1**	**13.3**	**20.2**	**26.9**	**25.6**	**23.6**	**18.2**	**20.6**	**6.4**

Table 3.9: P-Amended reactor samples as proportional abundance (%) of taxa of representative class (bold) and genera from 16S rRNA gene sequences for each surface and the planktonic sample after 3-weeks within the P-Amended reactor. Potential sulfur-oxidizing genera (SOB), sulfur reducing genera (SRB), acidophilic genera, and gram-positive genera are highlighted.

3.4.4 Biofilm Abundance

Biomass accumulation on the mineral coupon surfaces was measured (in triplicate) after 3-weeks within each reactor. I found significant discrepancies in biofilm growth both among reactors and between surfaces within each reactor. These trends are visualized in Figure 3.5 and the actual values can be found in Table 3.10. In summary, the total dry mass of biofilm for the CP-Limited, C-Amended, P-Amended, and CP-Amended reactors was 50.5 $mg \cdot cm^{-2}$, 110.1 $mg \cdot cm^{-2}$, 12.8 $mg \cdot cm^{-2}$, and 25.4 $mg \cdot cm^{-2}$, respectively (Figure 3.5).

Previously, I found that in a CP-Limited reactor limestone and dolostone accumulated substantially greater biomass than any other surface, including calcite (Jones & Bennett, 2014). This correlation was observed in both pure cultures of the mixotrophic, sulfur-oxidizing *Thiothrix unzii* and the mixed cultures. Furthermore, these trends were observed within both high and low-pH bioreactors. I concluded that greater biomass was accumulated on surfaces with greater concentrations of phosphate, as phosphate rich basalt also accumulated significantly greater biomass (Jones & Bennett, 2014).

ANOVA analysis revealed that the addition of phosphate and carbon affected overall (total) attached microbial biomass, with significantly lower biofilm biomass ($P<0.002$) recorded in reactors where phosphate was added and, to a lesser degree, significantly higher biofilm biomass ($P<0.04$) recorded in reactors where carbon was added. Additionally, I was able to assess the potential impact of pH on biomass accumulation by comparing these new results with those found in previous experiments (Jones & Bennett, 2014). Previously I conducted bioreactor experiments under conditions identical to CP-Limited, but at a constant pH=8.3. ANOVA analysis of those

triplicate results, combined with those from these reactors revealed that pH was not significantly correlated to biofilm accumulation.

Within each reactor biomass distribution was tied to mineral phosphate concentration, albeit to varying degrees dependent on the media phosphate and carbon amendments (Figure 3.5). In the CP-Limited reactor, High-P surfaces (limestone, dolostone, and basalt) accumulated between ~3-40X that of low-P surfaces while those in the C-Amended reactor were between ~2-10X higher. However, within the C-Amended reactor the total biomass on every surface was ~2-10X higher than the CP-Limited reactor and the standard deviation of biofilm accumulation on each surface was nearly double that of the CP-Limited reactor (~15.2 $mg \cdot cm^{-2}$ vs. ~8.0 $mg \cdot cm^{-2}$) (Table 3.10).

The P-Amended reactor had the lowest biofilm accumulation on every surface. However, the high-P surfaces accumulated between ~3-60X higher biomass than low-P surfaces. Although this is the largest discrepancy, the actual variation in total biomass (SD ~2.3 $mg \cdot cm^{-2}$) was lowest in the P-Amended reactor (Table 3.10).

In the CP-Amended reactor, as with all other reactors, there was substantially more biofilm on high-P surfaces than on low-P surfaces (~2-24X; Figure 3.5). Overall, the CP-Amended reactor only accumulated more biomass than the P-Amended reactor. Additionally, the CP-Amended reactor had the second lowest standard deviation (~3.8 $mg \cdot cm^{-2}$) in biomass accumulated between surfaces.

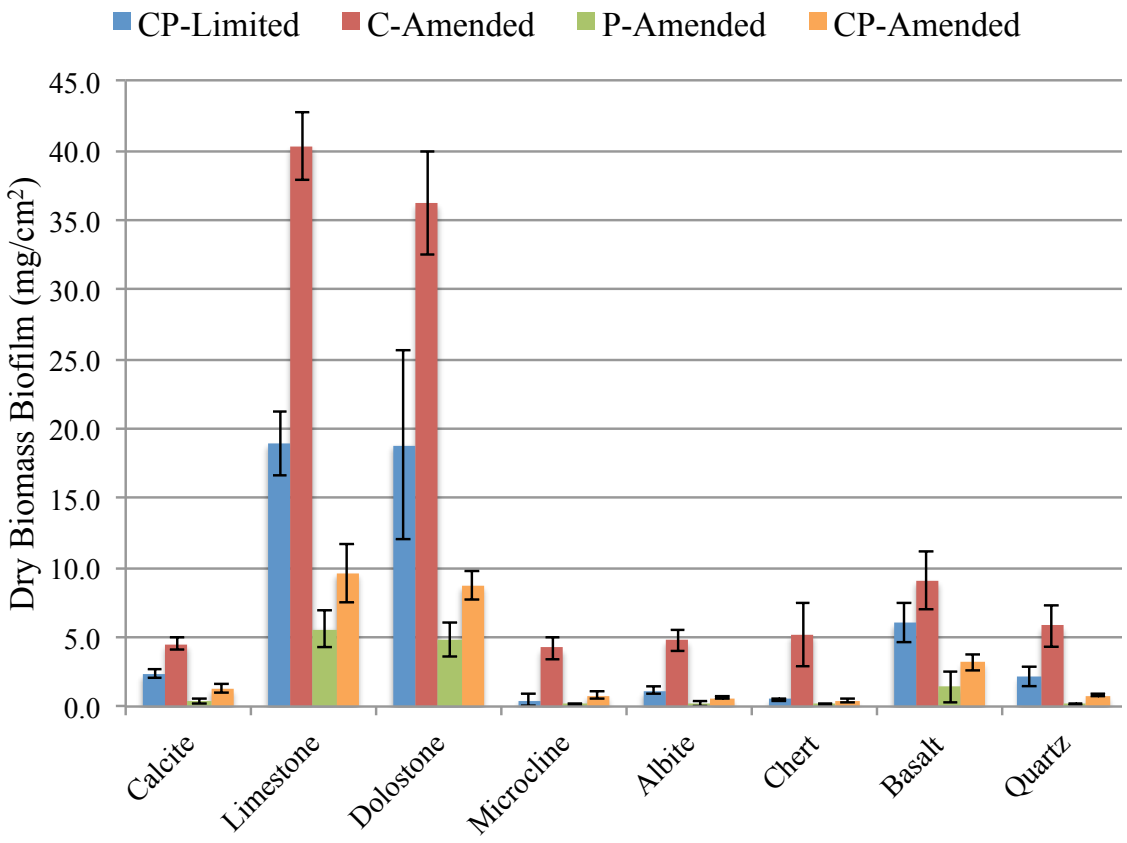

Figure 3.5: Dry weight (mg/cm2) of biomass accumulation on surfaces for each reactor. Error bars denote standard deviation, n=3. See Table 3.10 for numerical values.

	Dry Mass of Biofilm (mg/cm^2)			
Surface	CP-Limited[c]	C-Amended	P-Amended	CP-Amended
Calcite	2.4 ± 0.3	4.5 ± 0.4	0.4 ± 0.2	1.3 ± 0.3
Limestone	18.9 ± 2.3	40.3 ± 2.4	5.6 ± 1.4	9.6 ± 2.1
Dolostone	18.8 ± 4.1	36.2 ± 3.7	4.8 ± 1.2	8.7 ± 1.0
Microcline	0.5 ± 0.4	4.2 ± 0.8	0.1 ± 0.1	0.8 ± 0.3
Albite	1.2 ± 0.3	4.8 ± 0.8	0.2 ± 0.2	0.6 ± 0.1
Chert	0.5 ± 0.1	5.2 ± 2.3	0.1 ± 0.1	0.4 ± 0.1
Basalt	6.0 ± 1.4	9.1 ± 0.8	1.4 ± 1.1	3.2 ± 0.6
Quartz	2.2 ± 0.7	5.8 ± 1.5	0.2 ± 0.1	0.8 ± 0.1
Whole Reactor[a]	50.5	110.1	12.8	25.4
Standard Deviation[b]	8.0	15.2	2.3	3.8

Table 3.10: Dry mass of biofilm values and standard deviations. The standard deviations for all experiments are the result of triplicate experiments with the dry biomass values as the mean of the three. [a]Sum of the mean values of dry biomass for each reactor. [b]Standard deviation in for dry biomasses on surfaces within each reactor. [c]Dry biomass of biofilm values for CP-Limited reactor from Jones and Bennett 2014.

3.5 DISCUSSION

These laboratory reactor experiments represent a unique study evaluating the influence of natural surface types on microbial community structure and taxonomic and phylogenetic disparity between both attached and planktonic communities under varying environmental pressures (pH, TOC, Nutrients, surface chemistry). Multivariate analysis showed that the effect of surface chemistry on microbial β-diversity was significant, in all reactors, regardless of macroenvironmental pressures. Within each reactor UniFrac (phylogenetic) analysis revealed that microorganisms on similar surface types (carbonates, silicates, or Al-silicates) were more phylogenetically similar (Figure 3.3).

Previously, researchers have observed that different mineral type can exert strong control on microbial community structure of attached communities in both soils and surface outcrops (Carson et al, 2009; Gleeson et al, 2006). Very recently, Hartmann et al. (2015) went much further, showing that soil chemistry and local environmental chemistry both play an integral role in microbial community structure (phylogeny and taxonomy) in both nutrient-limited and nutrient-rich soils (Hartmann et al, 2015). Here, I show that while media pH, phosphate amendments, and carbon amendments significantly impacted the overall community membership within every reactor, the distribution of that community among surfaces is ultimately controlled by surface type. Additionally, I show that phosphate amendments, carbon amendments, surface phosphate availability all significantly impacted biofilm accumulation. In fact, mineral phosphate concentration exerted significant control on biomass accumulation under all reactor conditions (Figure 3.5). Overall taxonomy and proportional abundance were significantly sensitive to variations in media and surface chemistry with consistent patterns emerging among specific guilds (SOB, SRB, Gram-positives, acidophiles).

Principal coordinate analysis (PCoA) along with permutative multivariate analysis (PERMANOVA) of UniFrac (phylogenetic) similarity matrixes and taxonomic assignment reveal that all four reactor systems harbored structurally, taxonomically, and phylogenetically distinct microbial communities (Figures 3.2 & 3.4). Structurally, phosphate amendments in the media had the largest impact on overall species richness with both P-Amended reactors having ~2-3 fold higher richness values than either of the P-Limited reactors (Table 3.4). Additionally, media phosphate had the greatest impact on β-diversity, as the P-Amended reactors were 67.5% phylogentically similar. Both phosphate and carbon amendments have a significant, but opposite impact on Shannon diversity. P-Amended media has higher Shannon diversity and C-Amended media has lower Shannon diversity (Table 3.4). Concurrently the pH_{in} of the media was significantly correlated with increases in both the species richness and overall Shannon diversity of reactor communities (Table 3.4). However, pH_{in} had very little impact on similarity of microbial communities between reactors, but pH_{out} had the second greatest impact (Table 3.3). As I will discuss, pH_{out} is largely a function of the metabolism of the taxa present within each reactor, which is statistically controlled by both carbon and phosphate amendments to the media (Table 3.3).

3.5.1 Sulfur-Metabolizers

Although PERMANOVA and UniFrac analyses reveal the phosphate-amended (P-Amended and CP-Amended) reactors to be most phylogenetically similar ($Ø_{sim}$=67.5% Table 3.3), the taxonomic shift caused by carbon-amendments has the most dynamic geochemical consequences (Figure 3.3, Tables 3.6-3.9). In both C-Limited reactors (CP-Limited and P-Amended) neutrophilic, but acid producing sulfur-oxidizing

microorganisms were dominant (Tables 3.6 & 3.9). In the CP-Limited reactor, these SOB preferentially colonized highly-buffering carbonates (Table 3.6). In Jones and Bennett 2014, I hypothesized that SOB would benefit from this preference as the carbonates would buffer the acidity generated by sulfur-oxidation to sulfate:

$$2CaCO_3 + S° + 1.5O_2 + H_2O \rightarrow SO_4^{2-} + 2HCO_3^{-} + 2Ca^{2+}$$

$$2CaCO_3 + S_2O_3^{2-} + 2O_2 + H_2O \rightarrow 2SO_4^{2-} + 2HCO_3^{-} + 2Ca^{2+}$$

This caused aggressive dissolution of the carbonates (Calcite, Madison Limestone, and Madison Dolostone) which was confirmed by SEM analysis (Jones & Bennett, 2014). In the CP-Limited reactor, potential SOB were identified as members of the genera *Thiothrix, Thioclava, Halothiobacillus, Thiobacillus, Bosea, Thiomonas*, and *Sulfurovum* (Jones & Bennett, 2014). It should be noted that our previous investigation was limited to interpretation of taxonomic similarities of the microbial communities within the CP-Limited reactor. Here I reveal significant phylogenetic and taxonomic similarities between those communities (Jones & Bennett, 2014).

Within the P-Amended reactor, media buffering reduced the dependence of neutrophilic SOB on mineral buffering of metabolically generated acidity. As a result, potential SOB were found ubiquitously on every surface, represented by the genera *Thiothrix* (26.4-48.9%), *Thioalkalivibrio* (0.3-1.1%), *Thiomonas* (0.6-3.3%), and *Thiobacillus* (0.4-2.0%). Also, the P-Amended reactor had the least phylogenetic variability between surface attached communities. UniFrac analysis showed that all communities were very similar (>91% similar) (Figure 3.3c). Despite this high degree of similarity, 85.9% (P=0.035) of the phylogenetic variability in the P-Amended reactor was controlled by overall variations in mineral chemistry. Regardless, both of these reactor

communities were composed of chemoautotrophic microorganisms, as the reactor media was carbon limited.

Similarly, SOB were ubiquitous on every surface within the CP-Amended reactor, as members of the genera *Halothiobacillus* (9.6-49.5%), *Thiothrix* (0.3-2.5%), and *Thiomonas* (0-0.5%). However, the addition of a carbon source (in the form of acetate, lactate, and formate) to the media promotes chemoheterotrophic growth. In fact, both of the C-Amended reactors have significant quantities of *Deltaproteobacteria* (0.2-84.5% in C-Amended, 11.6-61.4% in CP-Amended), represented by members of the genus *Desulfovibrio* (Tables 3.7 & 3.8). *Desulfovibrio* is a motile, vibrio-shaped, heterotrophic, sulfur-reducing bacteria capable of growth on a variety of sulfur substrates (as the terminal electron acceptor) as well as lactate, pyruvate, acetate, propionate, and butyrate (as electron donor and carbon source) (Cypionka, 2000; Liu & Peck, 1981). Until recently, members of the genus *Desulfovibrio* were thought to be anaerobic, but now are known to not only tolerate, but actively grow and metabolize in aerobic environments (Abdollahi & Wimpenny, 1990; Cypionka, 2000; Eschemann et al, 1999).

Metabolic sulfate reduction by SRB generally causes an increase in pH (Dupraz et al, 2009; Lyons et al, 1984; Van Lith et al, 2003; Walter et al, 1993). The geochemical consequences of sulfur-reduction by *Desulfovibrio* are localized consumption of acidity by paired acetate (shown below), lactate, or formate oxidation with reduction of inorganic sulfur compounds.

$$CH_3COO^- + S_2O_3^{2-} + H^+ \rightarrow 2HS^- + 2CO_2 + H_2O$$

$$CH_3COO^- + SO_4^{2-} \rightarrow HS^- + 2CO_2 + 2OH^-$$

Also, in aerobic environments, several species of *Desulfovibrio* have been shown to pair sulfur-reduction with O_2 reduction to H_2O (Cypionka, 2000).

$$CH_3COO^- + S_2O_3^{2-} + O_2 + 2H^+ \rightarrow S° + SO_3^{2-} + 4CO_2 + 4H_2O$$

This reaction will also consume acidity resulting in a localized increase in pH. Within the C-Amended reactor, the metabolism of SRB allows more favorable conditions to be established on feldspars (albite & microcline) where consumption of local acidity decreases the mobility of potentially toxic mineral-bound aluminum. This has the added effect of decreasing the overall species richness (alpha-diversity) as well as increasing the amount of shared species (beta-diversity) between the surfaces (Figure 3.3b, Table 3.4). Overall, the dominance of these organisms was statistically correlated with lower Shannon diversity and β-diversity with less phylogenetic diversity between surfaces within C-Amended reactors (Table 3.4, Figure 3.3b & d). Decreased species richness has been documented to be a function of increasing carbon concentration (Larson & Passy, 2013). However, decrease in species diversity, in attached communities, as a function of carbon limitation across multiple surfaces is previously undocumented.

3.5.2 Acidophiles

Previously, I found that, in a CP-Limited system, although neutrophilic SOB dominated the carbonates, few were found on silicates (Jones & Bennett, 2014). The community on quartz in the CP-limited system was largely composed (~39%) of acidophilic and acid-tolerant microorganisms, including the SOB genera *Acidithiobacillus* and *Acidithiomicrobium,* the acidophilic SRB *Thermodesulfovibrio,* and

other potentially acid-tolerant microorganisms which were all found exclusively on quartz (Jones & Bennett, 2014).

Significant proportions of potentially acidophilic microorganisms were only found in the CP-Limited and C-Amended reactors as the sustained pH in these reactors provided a selective advantage on specific surfaces. In the C-Amended system, members of the genus *Bradyrhizobium* were found in very high abundance (45.3%) almost exclusively on the quartz surface (Table 3.8). Members of the genus *Bradyrhizobium* are Gram-negative, aerobic, non-spore-forming rods, motile by a single subpolar flagellum (Leon-Barrios et al, 1991). Most members of this lineage grow best at pH ~6.0 and poorly or not at all at pH>8.0 (Leon-Barrios et al, 1991). However, most *Bradyrhizobium* strains are commonly found in ultisols (acidic soils with a pH range of 4-5) and are indigenous to podzolic soils with a pH of 4.6 (Ozawa et al, 1999). Recently, the highly acid-tolerant *Bradyrhizobium canariense* was isolated and shown to grow well at pHs as low as 4.2 (Vinuesa et al, 2005). Additionally, acidophilic *Acidomicrobiales* was found exclusively associated with quartz (Table 3.8).

Furthermore, TM7, a recently described candidate division of the domain *Bacteria,* was found exclusively on the quartz surface (Table 3.8). TM7 is only the third bacterial lineage recognized to have gram-positive representatives and exist in a wide variety of terrestrial and aquatic habitats (Hugenholtz et al, 2001). It should be noted that candidate phylum TM7 has recently been renamed as phylum Candidatus Saccharibacteria (Albertsen et al, 2013). Members of this candidate division have recently been found as abundant representatives of acidophilic communities in acid mine drainage with pH ~3.0 and therefore may be an acid tolerant lineage (Hao et al, 2007). Recently, a study in to the geographical distribution of TM7 found that it displays correlations with acidic, highly-siliceous (high SiO_2) sediments (Winsley et al, 2014).

Additionally, TM7 was found in the planktonic sample from the CP-Limited reactor, which also had a significant proportion (~45%) of acidophilic microorganisms (Table 3.6).

3.5.3 Gram-positives and other potential biophysical/mineral relationships

Gram-positive organisms were more abundant in the two reactors where a lower pH was maintained (Tables 3.6-3.9). Within these reactors, Gram-positive organisms trended towards surfaces with lower buffering capacity (non-carbonates). Specifically, in the C-Amended reactor, Gram-positive *Actinobacteria, Bacilli,* and *Clostridia* composed a large proportion (86.8%) of the microbial community associated with basalt (Table 3.8). *Actinobacteria* in particular represented 48.0% of the total community. *Actinobacteria* have been implicated in previous studies to have a significant role in the weathering of volcanic rocks, particularly basaltic rocks and is found commonly in nature as one of the dominant lineages present in biofilms on basaltic outcrops (Cockell et al, 2013; Gomez-Alvarez et al, 2007; Kelly et al; Weber & King, 2010). The dominance of *Actinobacteria* on basalt is also consistent with a study of microorganisms associated with volcanic ash and basalt deposits in Kilauea Volcano, Hawaii, USA where it was the only phylum present at all of the sites investigated (Gomez-Alvarez et al, 2007). Additionally, a multitude of studies of microbial communities within basaltic lava caves reveal *Actinobacteria* as the one of the dominant and most ubiquitous genera within biofilms attached to basalts (Hathaway et al, 2014; Howarth, 1981; Northup et al, 2011; Staley & Crawford, 1975). Consistent with our observed trends, despite this ubiquity in lava cave biofilms, Northup et al 2011 found a lack of *Actinobacteria* on secondary mineral and non-basaltic surfaces within lava caves.

In the CP-Limited reactor, I found *Actinobacteria* (specifically *Propionibacterium* spp.) associated with basalt in high abundance (Jones & Bennett, 2014), but it is significantly more dominant in the C-Amended reactor (Table 3.8). Recent studies demonstrated that the ability of *Actinobacteria* to weather basaltic materials in order to access mineral bound nutrients is increased significantly when provided a carbon source (Cockell et al, 2013). This diverse phylum is thought to have evolved ~2.7 BYA and it has been hypothesized that this ability to efficiently derive nutrients from volcanic rocks has led to it's longevity and dominance (Cockell et al, 2013). Therefore, I hypothesize that the dominance of *Actinobacteria* on basalt in the C-Amended reactor is largely due to this long-lived evolutionary advantage over other lineages to derive mineral bound nutrients in otherwise nutrient limited systems.

Similarly, the Gram-positive Phylum *Firmicutes,* which contains the classes *Bacilli* and *Clostridia* is commonly found on and in basaltic rocks and soils (Kelly et al; Weber & King, 2010). Once again, this association was observed in a CP-Limited reactor (Jones & Bennett, 2014). Beyond this, not as much attention has been paid to this association in the literature. Although, it has been suggested that the presence of the Gram-positive peptidoglycan layer is an ancestral function of early terrestrial growth habitats (Battistuzzi & Hedges, 2009). However, I propose that research into this common association may yield similar results to that conducted on *Actinobacteria*.

In the CP-Limited, Gram-positive microorganisms were negligible on the carbonate surfaces (0-1%), but abundant on all silicate surfaces (14.4-34.9%) (Table 3.6). Previously, I hypothesized that Gram-positive bacteria may have a competitive advantage in low pH environments (non-buffering surfaces) as the electronegativity of their cell walls is adheres better to silicate surfaces (Jones & Bennett, 2014). Additionally, Gram-positive bacteria such as Bacillus spp. and TM7 are more attracted to silicate surfaces in

low pH environments due to pyoverdine siderophores (Gordienko & Kurdish, 2007; Winsley et al, 2014). In both of the low-pH (and low P) reactors (CP-Limited and C-Amended) there is a clear bias for Gram-positive bacteria on silicate surfaces (Tables 3.6 and 3.8). The increase in ubiquity of Gram-positive organisms within the C-Amended reactor is likely because the Gram-positive organisms present in the reactor are heterotrophic. Furthermore, Gram-positives are negligible on all surfaces in the high-pH/C-limited reactor (P-amended). This signifies that pH and C may be the controlling factors on Gram-positive membership in microbial biofilm communities and additionally explains the lack of Gram-positive organisms within either of the reactors (P-Amended and CP-Amended) where a high pH was sustained (Tables 3.7 & 3.9).

The cell wall of Gram-negative bacteria is composed of the cytoplasmic membrane, the peptidoglycan layer, and the outer membrane. The inner leaflet of the outer membrane is composed of only phospholipids, while the outer leaflet is usually composed of lipopolysaccharides (LPSs) (Lüderitz et al, 1982). Microorganisms in the genus *Sphingomonas* were originally described as strictly aerobic, chemoheterotrophic, Gram-negative, rod-shaped bacteria that differ from other Gram-negatives as they lack LPS and instead contain glycosphingolipids (GSLs) as cell envelope components (Yabuuchi et al, 1990). In 2001, the genera *Sphingobium, Novosphingobium, Sphingopyxis,* and *Blastomonas* were added to the *Alphaproteobacteria* lineage, all containing GSLs as cell envelope components (Hiraishi et al, 2000; Takeuchi et al, 2001).

As outer membrane components, LPS and GSL are located at the interface of the cell and its environment and are critical to processes involved in surface adhesion (Abu-Lail & Camesano, 2003; Walker et al, 2004). In the C-Amended reactor, bacteria with GSL (*Sphingobium*, *Blastomonas*, and *Novosphingobium*) show an affinity for the quartz surface where they represent 18.1% of the total community, are completely absent on all

other surfaces except Madison Limestone (2.4%) and Madison Dolostone (1.8%) (Table 3.8). Results of a recent study show that GSL had significantly larger and more uniform coverage on surfaces, especially a quartz crystal surface, when compared to LPS (Gutman et al, 2014). This strong surface adhesion, along with other physiochemical properties of GSL (namely high hydrophobicity), has been implicated in the ubiquity of GSL organisms in oligotrophic and extreme environments (Eguchi et al, 1996; Gutman et al, 2014; Laskin & White, 1999; Sun et al, 2013). Furthermore, high membrane elasticity of GSL containing cells is a property that might contribute to bacterial cell integrity, resistance, and overall survival (Gutman et al, 2014). Additionally, there is evidence that GSLs aid microorganisms in modulation of cellular pH (Sillence, 2013; Varela et al, 2014; Yamaguchi & Kasamo, 2002).

All of these properties combine to ensure stability on a quartz surface over other surfaces within the C-Amended reactor. These members of the *Alphaproteobacteria* lineage have the unique ability to tolerate a low pH environment without having to compete with the overwhelmingly dominant heterotrophic SRB on other surfaces within this reactor (Table 3.8).

3.5.4 Biofilm Accumulation and Mineralogy

ANOVA analysis of biofilm accumulated (in triplicate) on each surface revealed that revealed that P-Amended reactors had significantly lower biofilm biomass ($P<0.002$), but high-phosphate surfaces (limestone, dolostone, basalt) had significantly higher biomass (2-60X; Figure 3.5). Previously, I found that the primary control on total biomass accumulation was the concentration of mineral bound nutrients, particularly in the form of phosphate (Figure 3.5) (Jones & Bennett, 2014). These results agree with

several studies have reported that microorganisms exhibit active adhesion/detachment processes that may be a response to local nutrient availability (Araújo et al, 2010; Dawson et al, 1981; Kjelleberg & Hermansson, 1984; Marshall, 1996; Van Loosdrecht et al, 1990; Wrangstadh et al, 1990). In particular, these investigators have noted that starvation or nutrient availability can stimulate a change in the partitioning of a microbial community between the solid and aqueous phases (Ginn et al, 2002). During starvation bacteria show increased levels of adhesion by increasing production of EPS, allowing them to take advantage of organic and inorganic compounds that accumulate at solid-liquid interfaces (Dawson et al, 1981).

These previous investigations speculated that such tactics may be particularly important in oligotrophic waters where bacteria are exposed to conditions of extreme nutrient limitation. I observed that bacteria exploit these tactics in a multitude of nutrient and environmental conditions. In P-Amended reactors the magnitude of actual variation (standard deviation) in total biomass between high-P and low-P surfaces was much lower (Figure 3.5, Table 3.10). It is easy to intuit that the availability of media phosphate reduces the reliance on surface-bound phosphate for survival, but these surfaces are still favored by non-motile bacteria.

Significantly higher biofilm was also significantly correlated with the addition of a carbon source ($P<0.04$) in the form of acetate, lactate, and/or formate, regardless of both media phosphate, mineral phosphate, and media pH (Figure 3.5, Table 3.10). Both of the C-Amended reactors accumulated ~2X the total biomass of their respective P-Amended counterparts (CP-Limited 50.5 $mg \cdot cm^{-2}$ vs. C-Amended 110.1 $mg \cdot cm^{-2}$, and P-Amended 12.8 $mg \cdot cm^{-2}$ vs. CP-Amended 25.4 $mg \cdot cm^{-2}$). Carbon limitations in the C-Limited reactors resulted in reduced biofilm accumulation by decreasing the metabolic efficacy of heterotrophic populations (Matin et al, 1989). Additionally, in response to

nutrient limitations (phosphate in the C-Amended reactor), non-spore forming heterotrophic bacteria form significantly more EPS than in nutrient abundant (CP-Amended) conditions (Matin et al, 1989; Wrangstadh et al, 1990). This appears to be the case here, as the C-Amended reactors allowed for growth of heterotrophs (Tables 3.7 & 3.9). It should be noted that this dramatic increase in biofilm concentration is complex as it is likely tied to dynamic biochemical and biophysical interactions of specific heterotrophic taxa with the local environment.

Furthermore, the microbial communities on all surfaces were nearly identical (Figure 3.3c). The relatively high pHs of both P-Amended medias reduces the dependence of neutrophilic, but acid-producing SOB for highly-buffering carbonates as media buffering facilitated acid consumption. Consequently, neutrophilic SOB colonized all surfaces at high proportional abundances (Table 3.9). SOB on all surfaces were represented by the genera *Thiobacillus (Kelly & Harrison, 1989), Thiomonas (Kelly & Wood, 2000b), Thiothrix (Larkin, 1989), Thioalkalivibrio (Sorokin et al, 2006)* , *Sulfurovum (Inagaki et al, 2004),* and *Sulfurospirillum (Schumacher et al, 1992)* (Table 3.9).

Additionally, the relatively basic pH of the P-Amended reactor provided an environmental advantage for potentially alkaliphilic microorganisms, constituting a proportional abundance of 13.3-28.1% on all surfaces (Table 3.9). The most abundant of these organisms were members of the class *β-proteobacteria*. Of this lineage, *Hydrogenophaga* was the most abundant on all surfaces. Hydrogenophaga is a well-known aerobic, hydrogen-oxidizing microorganism commonly associated with subsurface serpentinization processes. Although many members of this genus were thought to be obligately neutrophilic, recently many members of this lineage have been isolated from and shown to thrive in high-alkalinity environments (Roadcap et al, 2005;

Suzuki et al, 2013; Willems et al, 1989). Finally, obligately alkaliphilic SOB of the genus *Thioalkalivibrio* are found exclusively within this reactor (Tables 3.6-3.9). Members of the genus *Thioalkalivibrio* live optimally at pHs from 7.5-10 (Sorokin et al, 2006).

3.5.5 Planktonic vs. Attached Communities

The planktonic communities and inoculants were phylogenetically distant from those in biofilms in every reactor (Figure 3.3; Tables 3.6-3.9). A majority of the microbes in the inoculants came from two dominant classes (*Epsilonproteobacteria* and *Gammaproteobacteria*) representing ~97.1% of the total sequences (Table 3.6; Jones and Bennett 2014). Despite the dominance of *Epsilonproteobacteria* in the inoculant, *Epsilonproteobacteria* were all but absent in surface samples from every reactor (Figure 3.3; Tables 3.6-3.9). *Epsilonproteobacteria* were only present in appreciable amounts in the planktonic samples obtained from the P-Amended (39.5% as *Sulfuricurvum*) and CP-Amended (23.9% as *Sulfurospirillum*) reactors.

The high degree of phylogenetic similarity (67.5%) between the two P-Amended reactors is due, at least in part, to the high proportion of *Epsilonproteobacteria* found exclusively in these samples (Figure 3.3; Tables 3.6-3.9). However, members of this lineage were composed entirely of members of the genus *Sulfuricurvum* and *Sulfurospirillum*, within the P-Amended and CP-Amended reactors, respectively. *Sulfuricurvum* is a motile, chemolithoautotrophic, facultatively anaerobic, SOB which grows best at near neutral pHs (Kodama & Watanabe, 2004). *Sulfurospirillum* is a motile, chemoheterotrophic, facultatively anaerobic, SRB which also grows best at near neutral pHs and is capable of using acetate as a carbon source and acetate and formate as

electron donors (Kodama et al, 2007). These common reactor media conditions of phosphate availability and neutral to high media pH combined with the motility of these organisms to provide suitable conditions for these organisms not achieved on any surfaces or within the other reactors.

Within the CP-Limited reactor, the relatively lower pH of the reactor media provided optimal conditions for acidophilic microorganisms to dominate resulting in a phylogenetically and taxonomically distinct community (Figure 3.3). The significant abundance of *Acidithiobacillus*, *Chloroacidobacterium*, *Acidisphaera*, *Thiobacillus*, and *Thermodesulfovibrio* supports the phylogenetic assessment that these organisms are most similar to those found on quartz, but still significantly different ($Ø_{sim}$<36% to quartz, P<0.05). Additionally, the planktonic sample in the CP-Limited reactor is the only sample to contain *Acidobacteria*, which have been shown to prefer low pH, oligotrophic environments (Table 3.6) (Fierer et al, 2007; Jones et al, 2009).

The key findings of this study are summarized in Table 3.11.

Reactor Variables	Alpha-Diversity		Beta Diversity	Biofilm Growth	
	S	H'	✔/×	✔/×	COR
Media Carbon	×	✔	✔	✔	✚
Media Phosphate	✔	✔	✔	✔	−
Media pHin	✔	✔	✔	×	×
Media pHout	×	×	✔	×	×
Surface Variables	Reactor Affected		Reactor Affected	✔/×	COR
Buffering Capacity	CPL	CPL	CPL, CPA	×	×
Mineral Type	×	×	CPL, CPA, PA	×	×
Mineral Phosphate	×	CA	CA	✔	✚

Table 3.11: Summary of impact of reactor and surface variables on microbial community structure in each reactor. Alpha diversity metrics are (S) species richness and (H') Shannon diversity. Beta diversity is UniFrac (phylogenetic) diversity. In the table (×) signifies no significant impact, (✔) significant impact, (COR) correlation type, (+) positive correlation, (−) negative correlation, (CPL) CP-Limited reactor, (CA) C-Amended reactor, (PA) P-Amended reactor, (CPA) CP-Amended reactor.

3.6 CONCLUSIONS

This study is particularly interesting due to the insights into the importance of the, as of yet, unculturable members of a microbial consortium. Different types of data analysis (taxonomy and phylogenetic) reveal important results independently, but taxonomic analysis alone fails to expose the link between mineralogy (surface type) and microbial lineage contained in the 16S rRNA of unknown organisms. It is these types of investigations that shed light upon the true extent of biogeographical influence on the natural history of life.

Additionally, I reported a statistically significant link between phylogenetic diversity of microbial communities and specific natural surface types under a variety of geochemical conditions. This suggests that phylogenetically similar microorganisms are significantly more likely to have similar surface niche requirements. In resource stressed and harsh environments, minerals could act as environmental filters providing specific microniches for metabolically similar microorganisms. Successful growth and succession would then be a function of the capacity of a microorganism, or community, to facilitate, tolerate, or adapt to microenvironmental cultivation and modification of the geochemical conditions at the microbe-mineral interface. Environmental pressures such as pH and carbon and phosphate variability will determine the extent of taxonomic disparity between mineral microniches, but surface type ultimately controls the phylogenetic diversity between these microenvironments. Due to their unique and variable chemical compositions, rocks and minerals should be considered as ecosystems that are primarily colonized by uniquely adapted microbes. Further investigation is required to determine if these phylogenetic similarities are the result of ecological shifts caused by environmental stresses imposed by localized surface geochemistry or latent adaptations by specific keystone organisms.

Finally, this study validated the use of continuous flow bioreactors to assess the dynamic microbial diversity as a function of interactions between microorganisms, growth medium composition, and surface type availability. This allowed me to assess the major biogeochemical reactions in a controlled setting and further constrain the key parameters affecting microbial diversity, not by replicating the complexity of the natural system, but by fine tuning parameters in order to evaluate their influence on microbial communities.

Chapter 4: Biogeochemical dynamics of sulfuric-acid speleogenesis: A proof of concept environment for inferring microbial community structure and function using $\delta^{13}C_{CO2}$

4.1 ABSTRACT

Our previous investigations revealed significant variation in microbial community structure as a result of changing surface chemistry and metabolites. Carbonate mineral solubility is particularly sensitive to the metabolic byproducts of sulfur metabolizing communities. Bacterial carbon cycling, through the reduction of CO_2 or oxidation of reduced carbon substrates like acetate, are associated with a kinetic isotope effect (KIE) which discriminates against ^{13}C. This could lead to significant, but unique carbon isotope signatures, dependent on the function of an active microbial community. Here I inoculated separate flow through bioreactors with 1) a pure culture of mixotrophic sulfur-oxidizing *Thiothrix unzii* and 2) a mixed culture (composed of SOB and SRB) from LKC to see if these shifts could be detected by monitoring select geochemical indicators ($\delta^{13}C_{CO2}$, $[CO_2]$, Ca^{2+}, and pH). I found that the mixed community reactor was geochemically dynamic and prediction of dominant metabolisms and guild composition (e.g. sulfide-oxidizers, sulfate-reducers, autotrophs, heterotrophs) was indeed possible. During heterotrophic sulfur reduction, the preferred consumption of $[^{12}C]$ acetate caused $\delta^{13}C_{CO2}$ to become depleted in ^{13}C. Conversely, during autotrophic sulfur oxidation to sulfate, the preferred consumption of $^{12}C_{CO2}$ caused $\delta^{13}C_{CO2}$ to become enriched in ^{13}C. Additionally, I was able to assess the effects of these rapid community functional shifts on carbonate dissolution rate. I found that dissolution was fastest (13.2X abiotic rates) in pure cultures of SOB and (8.8X abiotic rates) in mixed cultures when no external sulfur or acetate was provided. Furthermore, 16S rRNA sequencing during selected intervals reveal rapid adaptation of community structure and membership to changes in

geochemistry. Community composition shifted from an SOB dominated inoculant (~81% SOB; 12% SRB), to SRB dominated when supplied acetate (~72% SRB; ~8% SOB), back to SOB dominated when acetate was withheld (~60% SOB; ~4% SRB). The function of these communities was confirmed geochemically. This investigation provides insight into the dynamic processes taking place in microbial communities involved in mineral dissolution/precipitation within natural environments. These results also function as a proof of concept for using active sulfuric acid cave ecosystems to explore the effects of competing microbial metabolisms on carbon cycling and stable carbon isotope fractionation.

4.2 INTRODUCTION

Studies utilizing changes in stable isotope ratios as indicators of autotrophy vs. heterotrophy must take place in controlled systems (Ruby et al, 1987). It stands to reason that this system must contain metabolically sensitive peripheral geochemical indicators of metabolic shifts to buttress trends in stable isotope ratios. I propose that a carbonate system meets these criteria. Specifically, the sensitivity and responsiveness of reaction kinetics of the carbonate system when exposed to the metabolic products of active sulfuric acid cave ecosystems make LKC an ideal model ecosystem. Due to the inherently large diversity of microbial communities within these environments, there are a variety of metabolic pathways that can impact limestone dissolution and carbon cycling to varying degrees.

Microbially-mediated carbon isotope fractionation by autotrophic microbes is primarily a result of the assimilation of carbon dioxide and bicarbonate ions (Konhauser, 2007). All common pathways of autotrophic carbon fixation discriminate against heavy

^{13}C, leaving the remaining carbon pool isotopically enriched in ^{13}C (Schidlowski, 2000). This discrimination is due to kinetic isotope effects inherent in both the diffusional transport of carbon dioxide or bicarbonate ion across the cell wall and the enzymatic reaction of the assimilatory pathway that fixes carbon dioxide (Schidlowski, 2000). The magnitude of this non-equilibrium discrimination is dependent on many variables including pCO_2, pH, temperature, microbial metabolism, and other variables mentioned in (Roeske & O'Leary, 1984).

Acetate was shown in previous experiments to promote heterotrophic growth, is a key intermediate during the degradation of organic matter, and acetate consumption is linked to ~50% of all sulfate reduction (Sørensen et al, 1981). Little is known about carbon isotope fractionation during acetate utilization by microorganisms, but the consequences of these reactions should be obvious. For example, most sulfur reducers (SRB) that are capable of utilizing acetate with S^o use the tricarboxylic acid (TCA) cycle (Galushko & Schink, 2000) for the following reaction:

$$CH_3COO^- + 4S^o + H^+ + 2H_2O \rightarrow 4H_2S + 2CO_2 \qquad \Delta G^o = -39 kJ \bullet mol^{-1} \quad (1)$$

This reaction would leave the acetate pool enriched in ^{13}C, and the remaining $CO_{2(g)}/HCO_{3\,(aq)}^-/CO_{3\,(aq)}^{2-}$ system will be isotopically depleted in ^{13}C. Other SRB may be capable of utilizing acetate for sulfate reduction:

$$CH_3COO^- + SO_4^{2-} + 3H^+ \rightarrow H_2S + 2CO_2 + 2H_2O \qquad \Delta G^o = -63 kJ \bullet mol^{-1} \quad (2)$$

At first glance, it appears that reaction (2) would have an identical effect on the isotope pool as reaction (1). There are several reasons why this would not be true. First,

reaction (1) yields much less free energy than reaction (2) for each mol of acetate oxidized. Therefore, to do the same amount of work, a sulfur reducer would have to use much more acetate, resulting in a larger isotope fractionation and thus a lighter $\delta^{13}C_{CO2}$ (Goevert & Conrad, 2009).

Additionally, when these reactions take place in a carbonate system, the relative impact on pH will have consequences on carbonate solubility. While the response in carbonate dissolution rate will not reveal all utilized reaction pathways, it should be an indicator of the dominant reaction pathway. For example, a primary reaction pathway using reaction (2), would consume 3mol of H^+ for every 1mol of acetate. This would cause a greater pH increase and drop in $\Delta[Ca^{2+}]$ than reaction (1). In a calcite undersaturated system, this would also decrease carbonate dissolution rate, resulting in lower $[CO_{2(g)}]$ and lighter $\delta^{13}C_{CO2}$ than when reaction (1) is the primary pathway.

Herein, I intend to exploit the aforementioned geochemical intricacies, along with a few others, to predict changes in microbial community structure by monitoring simple geochemical parameters (i.e. pH, pCO_2, $^{13}CO_2$, $^{12}CO_2$, Ca^{2+}). This is an investigation into the fundamental nature of the microbe mineral relationship. Therefore, the goal is not to absolutely quantify an effect, but to gain further insight into the nature of these interactions. In order to monitor these variations, I outfitted a continuous flow bioreactor with a Picarro Wavelength-Scanned Cavity Ring Down Spectrometer (WS-CRDS) which continuously monitored and logged $[CO_2]$, $[^{12}CO_2]$, and $[^{13}CO_2]$. I simultaneously monitored $[Ca^{2+}]$ and pH in order to quantify the impact of microbial metabolism on limestone dissolution rate. Additionally, I utilize high-throughput 454-pyrosequencing (Margulies et al, 2005) of bacterial 16S rRNA sequences to confirm that changes in the microbial community structure support the inferred functional reaction pathways indicated by geochemical trends. I hypothesize that prediction of dominant metabolisms

(community function) and guild composition (e.g. sulfide-oxidizers, sulfate-reducers, autotrophs, heterotrophs) is possible.

4.3 MATERIALS AND METHODS

4.3.1 Solid Surface Preparation and Characterization

Previously characterized, unaltered Upper Madison Limestone from LKC was used as the reactive surface. The Madison limestone was prepared to the exact specifications laid out in Steinhauer et al, (2010). Briefly, the limestone was crushed and sieved, 1-2mm fraction collected, rinsed in DI-H_2O, dipped in 0.01N H_2SO_4 to remove surface impurities, rinsed in DI-H_2O again. Following this preparation method produces samples of Madison limestone with a geometric specific surface area of 0.0019 m^2/g and a BET surface area of 0.133 m^2/g (Kr) and 0.18 m^2/g (Ar). For consistency with previous investigations, I used the geometric surface area for calculating dissolution rates within each reactor (Steinhauer et al, 2010). The limestone chips were weighed to ± 0.1mg, with ~10.0000g of limestone for each reactor, encased in 850μm pore size mesh bags, autoclaved at 121ºC for 45 minutes, and aseptically placed into the reactors. Before and after each of the experiments, the limestone surface was imaged on a FEI-Philips XL-30 TMP SEM following previously published methods for chemical critical point drying (Bennett et al, 2006).

Laboratory chemostat experiments were used to measure reaction variables in a controlled setting while manipulating electron donor/acceptor availability. These laboratory experiments were conducted within parallel 1L Teflon chemostat chambers (one as an abiotic control, the other biotic) with multiport lids. Media was pumped through the reactor via peristaltic pump at an average rate of 1.41 ml/min while

maintaining a constant reactor headspace of 400ml. Additionally, I outfitted the continuous flow bioreactors with a Picarro Wavelength-Scanned Cavity Ring Down Spectrometer (WS-CRDS) that continuously monitored and logged $^{12}CO_2$ and $^{13}CO_2$ of the air in the reactor headspace at ppmv sensitivity and isotope ratios at <0.3‰ precision. The pump on the Picarro draws air at ~25 ml/min. The pH within each reactor was logged at regular intervals using an Omega pH probe and OM-CP-Bridge-110-10 data logger. Water samples were collected periodically from the outflow of both chambers and analyzed for [DIC] and alkalinity. $[Ca^{2+}]$ was monitored and logged using an $[Ca^{2+}]$ ion specific electrode (ISE). $[Ca^{2+}]$ was verified periodically by measuring total hardness by EDTA titration (Eaton et al, 2005), and by ICP-MS analysis. The change in hardness over time was the result of changing $[Ca^{2+}]$ due to dissolution of the Madison Limestone. Periodic thiosulfate concentrations were measured by the Sulfite Iodometric method (Eaton et al, 2005). Dissolved sulfide and sulfate were measured against standards by methylene blue complex and turbidimetric method, respectively (Chemetrics). The laboratory reactor is illustrated in Figure 4.1.

CO_2 isotope compositions are reported in the usual δ-notation (e.g., $\delta^{13}C$) expressed here in permil (‰) and defined as follows:

$$\delta_x = \left[\frac{(R_a)_{sample}}{(R_a)_{standard}} - 1\right] 10^3 \text{ (‰)}$$

where R_a is the $^{13}C/^{12}C$ ratios relative to the PDB standards.

Furthermore, the carbon isotope fractionation between two end members (A and B) will be expressed as $\Delta^{13}C_{A-B}$. which is defined as $\Delta^{13}C_{A-B} = \delta^{13}C_A - \delta 13C_B$. In the

carbonate system, it is possible to use $\Delta^{13}C_{A-B}$ as an approximation of the ^{13}C enrichment factor $\varepsilon_{A-B} = 10^3(\alpha_{A-B}-1)$.

4.3.2 Liquid Media Preparation for Chamber Experiments

DI-H_2O was equilibrated with powdered Madison Limestone with a known $\delta^{13}C_{CaCO3} = +2.5‰$. The limestone equilibrated media was then filtered through a .22μm filter and amended with 0.1 g $MgSO_4$ and 0.25 g NH_4Cl was added per liter before autoclaving at 121°C for 45 minutes. After autoclaving, 2 ml/L and 5 ml/L of filter-sterilized trace metal solution and Wolfe's Vitamin solution, respectively (Burlage, 1998). The final sterile solution was adjusted with sterile 1N HCl to a final pH of ~7.3 and contain 0.1 mM HCO_3^-, 1.0 mM Ca^{2+}, with a Ω with respect to calcite ($\Omega_{calcite}$) of ~0.01.

4.3.3 Microbial Inoculants

The mixed community inoculant was obtained from Lower Kane Cave at 196 meters from the back of the cave near the upper spring location. Samples were collected in the field in sterile falcon tubes with a small amount of stream water, and transported back to the laboratory for use in the experiments. Approximately 15ml of biomat was added to the sterilized chamber for each experiment.

Additionally, experiments were conducted using a pure culture of *Thiothrix unzii* (ATCC 49747) using an identical suite of electron donors at variable concentrations. This served as a baseline for a purely sulfur-oxidizing community versus the mixed metabolism community from LKC. *Thiothrix unzii* is a colorless, filamentous, neutrophilic, mixotrophic, sulfur-oxidizing member of the *Gammaproteobacteria* class

that is known to use both sulfide and thiosulfate as sulfur sources and have the ability to store sulfur intracellularly (Howarth et al, 1999). *T. unzii* is closely related to *Thiothrix* spp. that are known to dominate the community within Lower Kane Cave (Engel, 2004). After the reactor had stabilized with media flowing through it, 15ml of cultured *Thiothrix unzii* was added for each experimental run.

4.3.4 Experimental Variations

This experimental design is intended to investigate the effects of electron donor/acceptor type and concentration on microbial corrosion of limestone. To this end, the apparatus was constructed in order to enable complete removal of CO_2 from airflow into the chamber through the use of a CO_2 scrubber containing NaOH pellets. In some experiments the media was amended with sterile acetate in order to support heterotrophic conditions for growth. *T. unzii* is thought to be facultatively mixotrophic, but grows best as an autotroph. For this reason I ran the pure culture experiments with 0.2μm filtered ambient air as the input with ambient CO_2 concentration input matching that of laboratory air. Without this source of ambient CO_2, growth and metabolic activity was insignificant. All mixed culture experiments were run with CO_2 scrubbed air as the metabolic activity of heterotrophs provided enough CO_2 to support autotrophic growth without an outside source. Acetate was prepared from a stock of Na-acetate at varying concentrations (ranging from 0 to 9.5mM), filter sterilized, and injected via syringe pump through a 0.22μm sterile filter (Figure 4.1).

Thiosulfate was used as the reduced sulfur source as it provided multiple valences of sulfur to support oxidation or reduction. The $S_2O_3^{2-}$ was prepared from a stock 1M solution of $Na_2S_2O_3$. This solution was filter sterilized and pumped via syringe pump at

varying concentrations (ranging from 0 to 0.89mM) into the input media solution through T-fittings directly after the peristaltic pump. The final liquid media was pumped through the reactors while a magnetic stir bar, rotated by a magnetic stir plate at 115 RPM, generated mixing and shear.

4.3.5 PCR Amplification and 454 Sequencing of 16S rRNA

Changes to the microbial community structure within the bioreactors were evaluated in order to support interpretations of the biogeochemical processes occurring within the reactor. Samples were aseptically removed from reactors during select periods of geochemical fluctuations. Bacterial tag-encoded FLX-titanium amplicon pyrosequencing (bTEFAP) was used to evaluate the bacterial populations removed from the reactors at MR DNA Lab (www.mrdnalab.com, Shallowater, TX, USA). The bTEFAP procedures are based on Research and Testing Laboratory protocols http://www.researchandtesting.com and are previously described (Dowd et al, 2008). Briefly, the 16S universal Eubacterial primers 27F (5'-AGRGTTTGATCMTGGCTCAG-3') and 519R (5'-GTNTTACNGCGGCKGCTG-3') were used for amplifying the v1-v3 region of 16S rRNA genes using 30 cycles of PCR. HotStarTaq Plus Master Mix Kit (Qiagen) was used for PCR under the following conditions: 94°C for 3 min, followed by 28 cycles of 94°C for 30 s; 53°C for 40 s and 72°C for 1 min after which a final elongation step at 72°C for 5 min was performed. After PCR, all amplicon products from the different samples were mixed in equal volumes and purified using Agencourt Ampure Beads (Agencourt Bioscience Corporation, Beverly, Ma). Adaptors and barcodes for 454 pyrosequencing were ligated,

and sequencing on a Roche 454 GS-FLX Titanium™ (454 Life Sciences, Branford, CT, USA).

Sequences were preprocessed using the open source software package QIIME version 1.9 (http://qiime.sourceforge.net), which allows analysis of high-throughput community sequence data (Caporaso et al, 2010). QIIME was also used for identification of operational taxonomic units (OTUs), taxonomic assignment, and community structure statistical analyses and comparisons. In preprocessing, sequences were culled if they were <200bp long, >550bp long, if they contained ambiguous base calls >6bp, or contained homopolymer runs >6bp, if they had low quality scores <25, contained any primer mismatches, or barcode errors >1bp. Additionally, noisy sequences were discarded using the "denoise_wrapper" script (Reeder & Knight, 2010). Chimeric sequences were removed using ChimeraSlayer with the QIIME default settings after OTU-picking and taxonomic assignment.

QIIME was also used for OTU clustering and taxonomic-based analysis. The uclust method was used to pick de novo OTUs at 3% (genus level) divergences. Representative sequences for each OTU were then aligned with PyNAST and taxonomy was assigned with the uclust consensus taxonomy assigner using the greengenes_13_8 reference database. Potential contaminants and OTUs with less than 4 members were then filtered from the resulting the resulting OTU table.

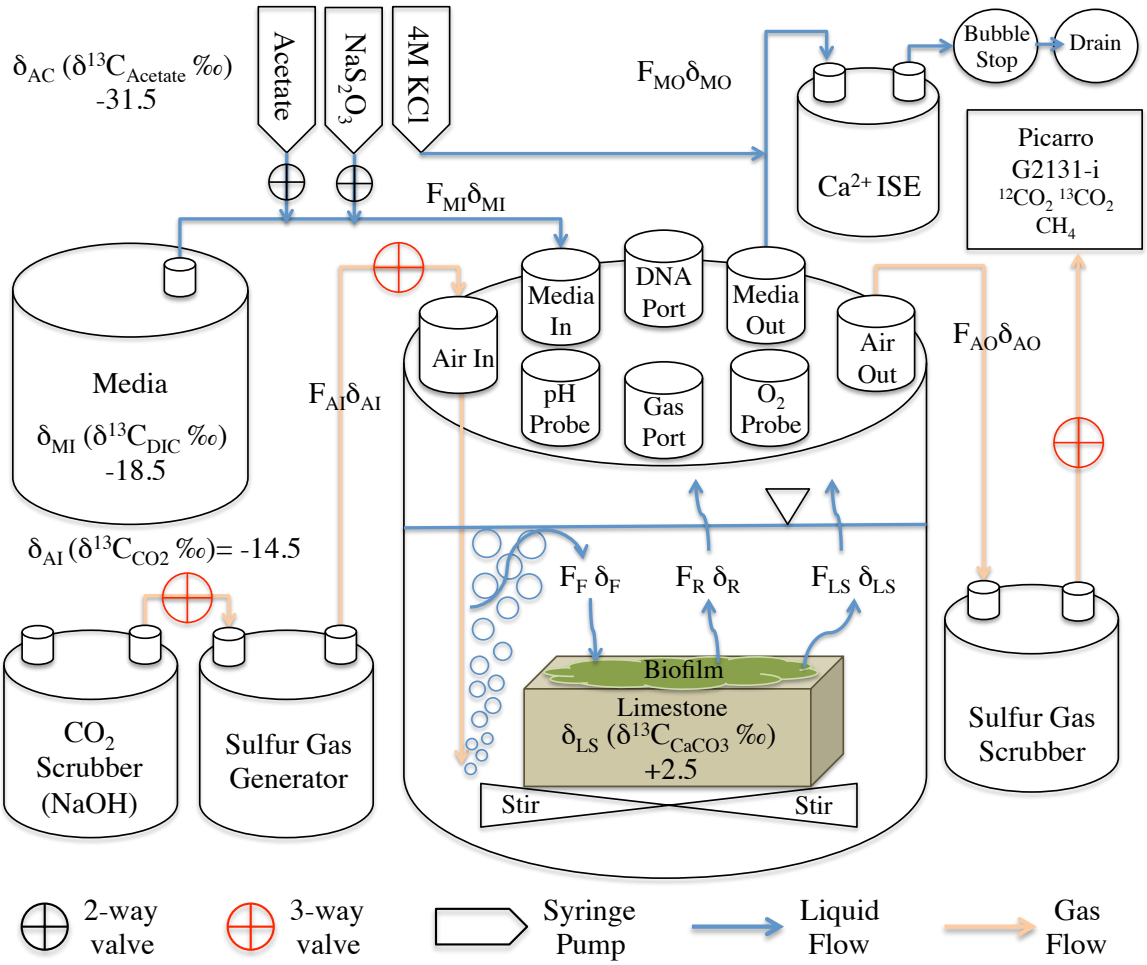

Figure 4.1: Flow-through bioreactor diagram with multi-port lid for pure and mixed culture limestone dissolution experiments. F denotes sources of carbon flux in moles. Subscripts are: F-microbial fixation, R-microbial respiration, LS-Limestone, AI-Air In, AO-Air Out, MI-Media In, MO-Media Out. Liquid media flow was set to 1.4ml/min. Air flow was 25ml/min. CO_2 Scrubber was not used during *T. unzii* experiments. Gas and liquid are filtered through 0.2µm filters before entering the reactor.

4.4 RESULTS

4.4.1 Abiotic Experiments

The average dissolution rate for abiotic reactor experiments varied slightly due to geochemical parameters (addition of acetate, $S_2O_3^{2-}$, both, or neither) of the media (Table 4.1). However, once each experiment reached steady state, abiotic limestone dissolution rate, pH, and [Ca^{2+}] remained constant. For each of the abiotic experiments steady state was reached within 24 hours of initiation. During initial equilibration with limestone the pH rose to ~8.3 which is consistent with a water in equilibrium with calcite and atmospheric CO_2. Overall, the mean dissolution rate over the entirety of the abiotic experiment was 2.97×10^{-11} mol•cm^{-2}•s^{-1}. SEM images of the limestone retrieved from an abiotic reactor run under identical conditions showed no obvious evidence of dissolution (See Chapter 2: Figure 2.3).

To mimic the conditions of the bioreactor experiments, abiotic reactors were run with CO_2 scrubbed air and with ambient CO_2 from the lab. When compared to the biotic reactors, there was relatively little variability in the $\delta^{13}C_{CO2}$ of the headspace gas within the abiotic reactor regardless if the air input was CO_2 scrubbed or not. By definition, when ambient CO_2 was not supplied CO_2 flux was due to exchange of DIC with headspace gas and carbonate dissolution. In the non-CO_2 scrubbed abiotic reactor, the mean value of $\delta^{13}C_{CO2}$ was lowest (-12.6‰) when the media was amended with 9.7 mM acetate. However, $\delta^{13}CO_2$ of the headspace was nearly identical when $S_2O_3^{2-}$ was added (-12.1‰). In the abiotic reactor with ambient CO_2, there was minor variability in $\delta^{13}C_{CO2}$ values (Table 4.2). Only when neither acetate nor $S_2O_3^{2-}$ was added to the CO2 scrubbed reactor did the abiotic mean $\delta^{13}C_{CO2}$ reached -8.1‰ (Table 4.3). However, $\delta^{13}C_{CO2}$ of the ambient CO_2 reactor was significantly lower (-19.2‰ to -18.6‰) when compared to the CO_2 scrubbed reactor (-12.6‰ to -8.1‰).

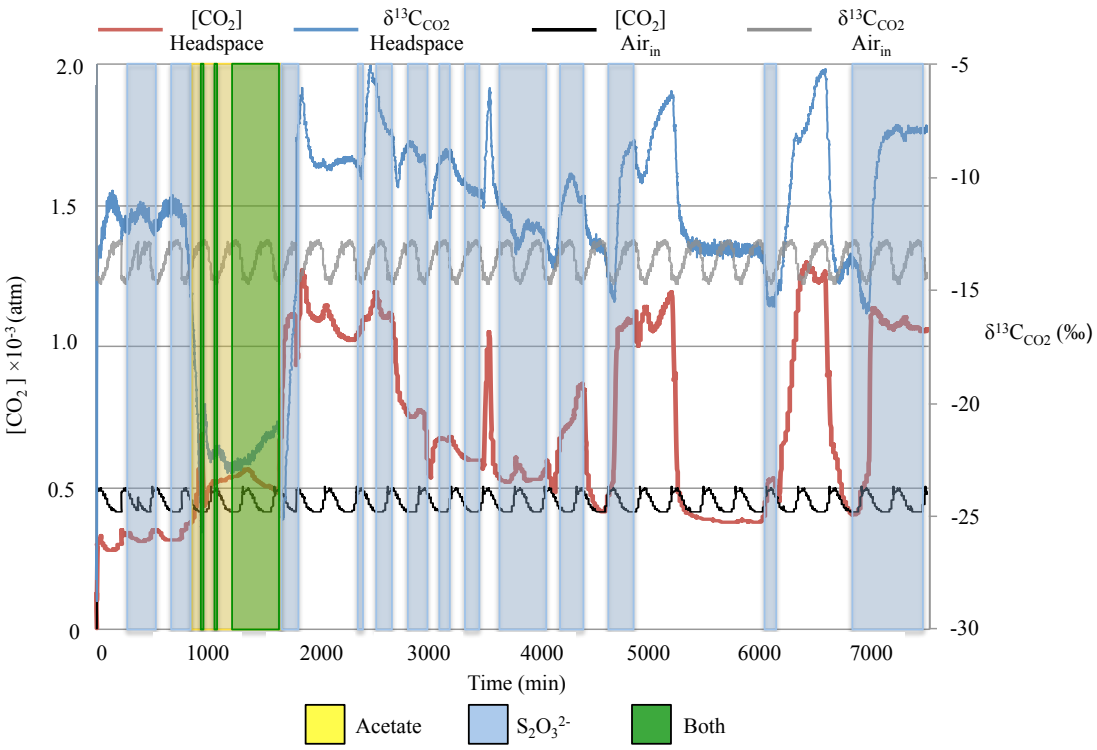

Figure 4.2: Log of CO_2 gas concentration (atm) in the headspace and $\delta^{13}C_{CO2}$ (‰) within the *Thiothrix unzii* pure culture reactor. Also shown are the flux from air in CO_2 gas concentration (atm) and the air in $\delta^{13}C_{CO2}$ (‰) since the air in for this reactor was not CO_2 scrubbed. Periods when acetate (Yellow), thiosulfate (Blue), or both acetate and thiosulfate (Green) are shaded accordingly. Note that this figure shows a representative period taken from the much longer experiment.

Interval	Mean Biotic $\delta^{13}C_{CO2}$	Mean Abiotic $\delta^{13}C_{CO2}$	High Biotic $\delta^{13}C_{CO2}$	Low Biotic $\delta^{13}C_{CO2}$	Dominant Metabolism
Acetate	-22.5	-19.2	-20.0	-25.7	Heterotrophy
$S_2O_3^{2-}$	-12.5	-18.8	-7.6	-16.1	Autotrophy
Both	-21.9	-19.0	-20.0	-22.1	Heterotrophy
None	-10.0	-18.6	-5.1	-14.7	Autotrophy
Mean	-16.8	-18.9	-13.2	-19.6	Autotrophy

Table 4.1: Table showing the mean, high, and low $\delta^{13}C_{CO2}$ (‰) within the *Thiothrix unzii* reactor for intervals when the reactor was amended with acetate, thiosulfate, both, or neither. Table also shows the likely dominant metabolism during each of these intervals. Note: this reactor had ambient CO_2 in the air into the reactor with a $\delta^{13}C_{CO2}$ = -12 to -14.5‰.

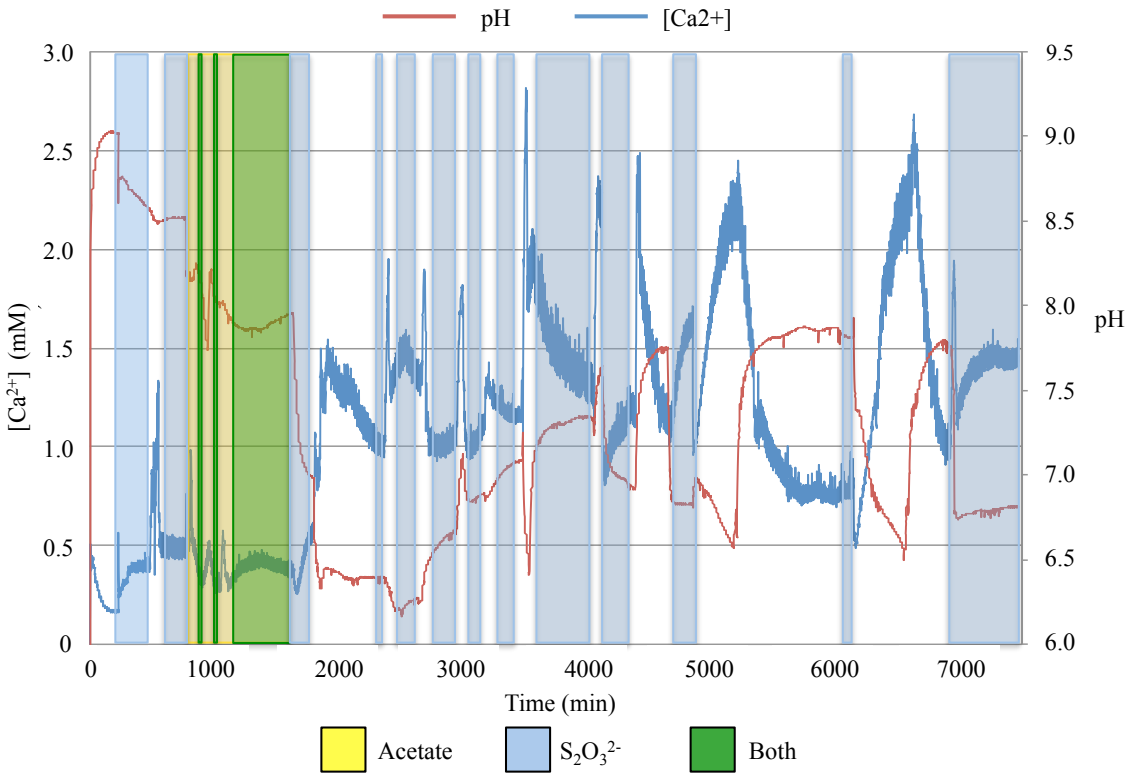

Figure 4.3: Log of calcium concentration (mM) and pH within the *Thiothrix unzii* pure culture reactor. Periods when acetate (Yellow), thiosulfate (Blue), or both acetate and thiosulfate (Green) are shaded accordingly. Note that this figure shows a representative period taken from the much longer experiment.

Interval	Mean Biotic Rate ($mol/cm^2\ s^{-1}$)	Mean Abiotic Rate ($mol/cm^2\ s^{-1}$)	High Biotic Rate ($mol/cm^2\ s^{-1}$)	Mean Rate Increase (Biotic/ Abiotic)	High Increase (Biotic/ Abiotic)
Acetate	5.1E-11	2.9E-11	8.3E-11	1.7X	2.8X
$S_2O_3^{2-}$	2.0E-10	2.6E-11	2.6E-10	7.7X	9.8X
Both	5.2E-11	3.2E-11	6.9E-11	1.6X	2.1X
None	2.5E-10	2.9E-11	4.0E-10	8.3X	13.2X
Mean	1.4E-10	2.9E-11	2.0E-10	4.8X	7.0X

Table 4.2: Table showing the mean, high, and biotic/abiotic limestone dissolution rates ($mol \bullet cm^2 \bullet s^{-1}$) within the *Thiothrix unzii* reactor for intervals when the reactor was amended with acetate, thiosulfate, both, or neither.

4.4.2 *Thiothrix unzii* Experiments

As stated in Methods, the *Thiothrix unzii* experiments failed to produce viable cultures without an outside source of CO_2. Therefore, the pure culture experiments were run with an ambient source of filtered laboratory air with an ambient [CO_2] averaging ~450ppm and $\delta^{13}C_{CO2}$ of air in (δ_{AI}) of -14.6‰. It should be noted that both [CO_2] and $\delta^{13}C_{CO2}$ of the ambient air were sensitive to laboratory conditions (e.g. human presence and diurnal fluctuations). The flux of carbon in from the air (F_{AI}) was $5.0 \times 10^{-7} \pm 3.4 \times 10^{-8}$ mol•min^{-1} as C. The flux of carbon in from the media (F_{MI}) was negligible at $4.0 \times 10^{-10} \pm 2.1 \times 10^{-11}$ mol•min^{-1} as C. Additional reactor constraints are shown on Figure 1.

Overall, the mean $\delta^{13}C_{CO2}$ was -16.8‰. When amended with acetate the headspace $\delta^{13}C_{CO2}$ was lighter with a mean value of -22.5‰. The mean $\delta^{13}C_{CO2}$ was heaviest, most ^{13}C enriched, when neither acetate nor $S_2O_3^{2-}$ were supplied (Table 4.1). The headspace $\delta^{13}C_{CO2}$ increased sharply, by as much as ~20‰ in about 65 minutes, when acetate supply is shut off (Figure 4.2). The highest $\delta^{13}C_{CO2}$ recorded in this experiment was -5.1‰ and the lowest was -25.7‰ (Table 4.1). It should be noted that these highs and lows in $\delta^{13}C_{CO2}$ coincided with highs and lows in [CO_2] (Figure 4.2).

The pH and dissolution rates achieved within the reactor inoculated with pure cultures of *T. unzii* were dynamic and quickly responded to environmental stimuli (Figure 4.3). The mean rate of dissolution achieved in this reactor (1.40×10^{-10} mol·cm^{-2}·s^{-1}) is ~4.8X faster than the mean abiotic rate (Table 4.2). The addition of acetate only resulted in a mean increase in dissolution rate ~1.80X faster than the abiotic rate and ~1.57X faster when added with $S_2O_3^{2-}$. The mean increase in dissolution rate when only $S_2O_3^{2-}$ was supplied to the media was ~7.7X faster than the mean abiotic rate with a high of ~9.8X faster (Table 4.2).

Immediately after supply of external electron donors was removed the system geochemistry had the most dramatic response. Within minutes, the pH of the entire reactor shifted as much as 2 log units (Figure 4.3). Both the highest (pH~8.0) and lowest (pH~6.2) pH values and dissolution rates were recorded during these periods. Overall, the mean dissolution rate during these periods (2.54×10^{-10} mol•cm^{-2}•s^{-1}) was ~8.3X faster than abiotic rates and ~1.8X faster than the mean *T. unzii* rate. Additionally, the highest dissolution rate of 4.04×10^{-10} mol•cm^{-2}•s^{-1} (~13.2X faster than abiotic mean) was recorded during one of these periods (Table 4.2).

4.4.3 LKC Mixed Culture Experiments

As stated in Methods, the mixed culture experiments were run with an ambient source of filtered laboratory air with the CO_2 scrubbed by NaOH. Therefore the flux of carbon in from the air (F_{AI}) was 0.0 mol•min^{-1} as C. As with the *T. unzii* experiments, there was minor flux of carbon from the media (F_{MI}) of $4.0 \times 10^{-10} \pm 2.1 \times 10^{-11}$ mol•min^{-1} as C.

Overall, the mean $\delta^{13}C_{CO2}$ was slightly lower than that of the *T. unzii* reactor with a value of 18.4‰. During intervals when acetate was delivered to the media the headspace $\delta^{13}C_{CO2}$ was substantially lower, with a mean value of -33.6‰, but reached values as low as -36.1‰, and only as high as -30.1‰ (Table 4.3). Again, the heaviest mean $\delta^{13}C_{CO2}$ was when neither acetate nor $S_2O_3^{2-}$ were supplied; reaching values as high as +3.8‰ (Table 4.3). The headspace $\delta^{13}C_{CO2}$ range (~43.0‰) was much larger than that of the *T. unzii* reactor (Figure 4.4). Although the range was greater, the mixed culture geochemical response was slower to respond to stimuli, often requiring several hundred minutes to plateau (Figure 4.4). For a summary of the variance in $\delta^{13}C_{CO2}$ see Table 4.3.

At times, these $\delta^{13}C_{CO2}$ values were heavier than the $\delta^{13}C_{CO2}$ of the Madison limestone and lower than that of the acetate substrate (Figure 4.4). Additionally, it should be noted that the highs and lows in $\delta^{13}C_{CO2}$ generally opposed the highs and lows in $[CO_{2\ (g)}]$, showing an opposite trend to that seen in *T. unzii* experiments (Figure 4.4).

The pH and dissolution rates achieved within the mixed culture reactor were dynamic, but responded less quickly to environmental stimuli (Figure 4.5). The mean rate of dissolution achieved in this reactor (8.9×10^{-11} mol•cm^{-2}•s^{-1}) is ~4.3X faster than the mean abiotic rate (Table 4.4). The addition of acetate resulted in a mean increase in dissolution rate ~1.1X faster than the abiotic rate, and at times even resulted in negative ΔCa^{2+} (Table 4.4; Figure 4.5). When $S_2O_3^{2-}$ alone was added to the media the mean dissolution rate was ~3.8X faster than the mean abiotic rate with a high of ~4.2X faster (Table 4.4). When $S_2O_3^{2-}$ and acetate were added the mean dissolution rate was cut in half (Table 4.4).

Similar to the *T. unzii* reactor, immediately after supply of acetate and thiosulfate are removed the system geochemistry has the most dramatic response (Figure 4.5). However, where these changes in the *T. unzii* occur over the course of minutes, in the mixed culture reactor these changes occurred over the course of thousands of minutes (up to 2500 minutes; ~42 hours) whereby the pH of the entire reactor would shift as much as 2 log units (Figure 4.5). The highest pH values (pH~8.6) and dissolution rate (2.7×10^{-10} mol•cm^{-2}•s^{-1}; ~8.8X faster than abiotic) were recorded during one of these intervals (Table 4.5). Overall, the mean dissolution rate during these periods (1.5×10^{-10} mol•cm^{-2}•s^{-1}) was ~4.9X faster than mean abiotic rates and ~1.7X faster than the mean mixed culture rate (Table 4.4).

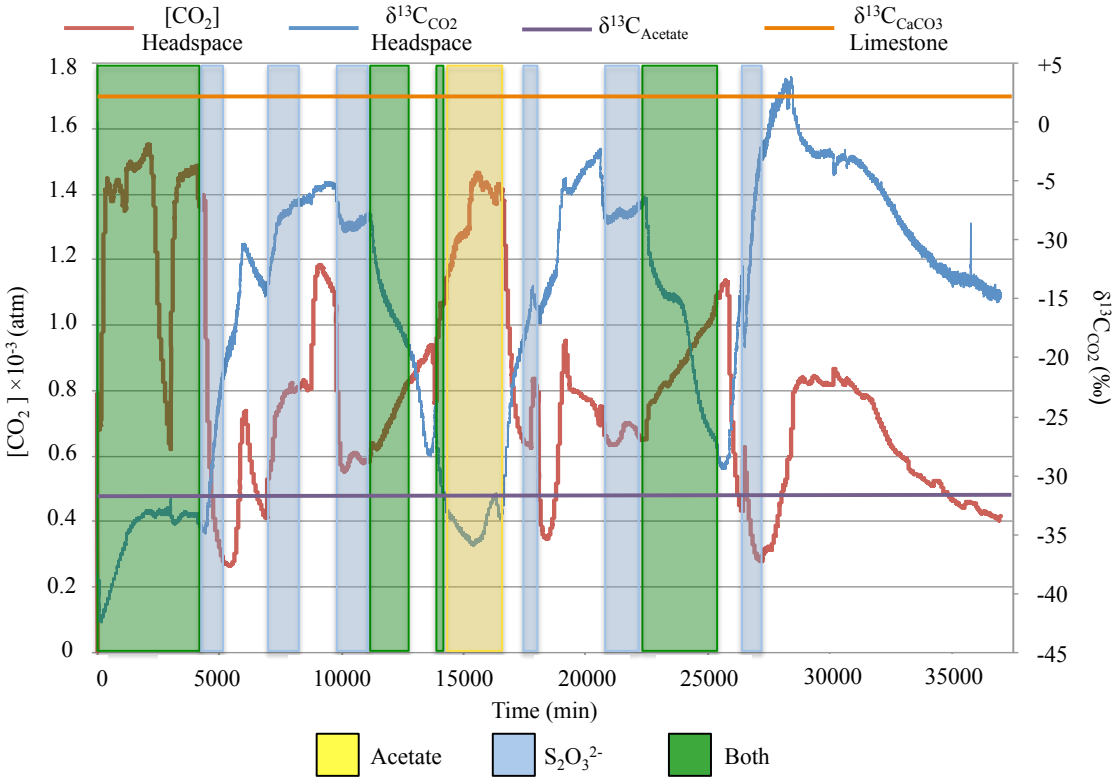

Figure 4.4: Log of CO_2 gas concentration (atm) in the headspace and $\delta^{13}C_{CO2}$ (‰) within the *LKC Mixed Culture* reactor. Also shown are the $\delta^{13}C_{Acetate}$ (‰) and $\delta^{13}C_{CaCO3}$ (‰) from limestone. The CO_2 was scrubbed from the air into this reactor. Periods when acetate (Yellow), thiosulfate (Blue), or both acetate and thiosulfate (Green) are shaded accordingly. Note that this figure shows a representative period taken from the much longer experiment.

Interval	Mean Biotic $\delta^{13}C_{CO2}$	Mean Abiotic $\delta^{13}C_{CO2}$	High Biotic $\delta^{13}C_{CO2}$	Low Biotic $\delta^{13}C_{CO2}$	Dominant Metabolism
Acetate	-33.6	-12.6	-30.1	-36.1	Heterotrophy
$S_2O_3^{2-}$	-10.5	-12.1	-1.3	-18.0	Autotrophy
Both	-22.5	-11.3	-6.8	-33.2	Heterotrophy
None	-7.1	-8.1	+3.8	-28.6	Autotrophy
Mean	-18.4	-11.0	-8.6	-29.0	Autotrophy

Table 4.3: Table showing the mean, high, and low $\delta^{13}C_{CO2}$ (‰) within the *LKC Mixed Culture* reactor for intervals when the reactor was amended with acetate, thiosulfate, both, or neither. Table also shows the likely dominant metabolism during each of these intervals.

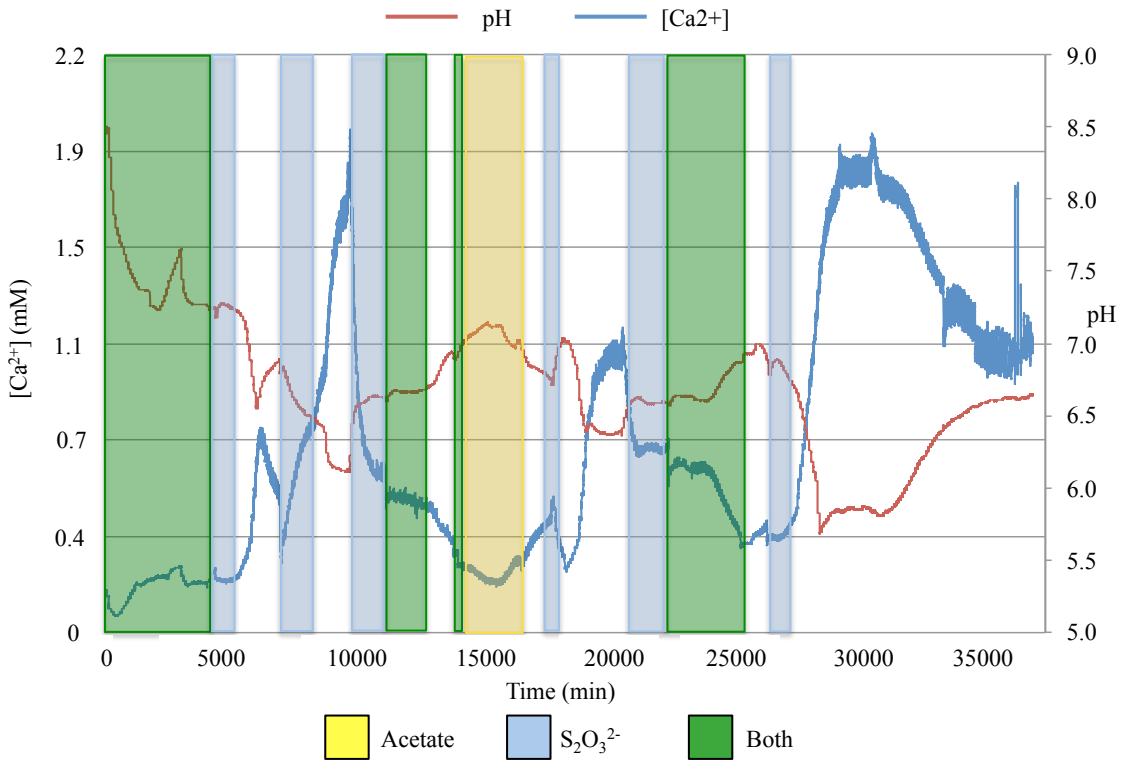

Figure 4.5: Log of calcium concentration (mM) and pH within the *LKC Mixed Culture* reactor. Periods when acetate (Yellow), thiosulfate (Blue), or both acetate and thiosulfate (Green) are shaded accordingly. Note that this figure shows a representative period taken from the much longer experiment.

Interval	Mean Biotic Rate (mol/cm^2 s^{-1})	Mean Abiotic Rate (mol/cm^2 s^{-1})	High Biotic Rate (mol/cm^2 s^{-1})	Mean Rate Increase (Biotic/ Abiotic)	High Increase (Biotic/ Abiotic)
Acetate	3.4E-11	2.9E-11	3.7E-11	0.8X	1.1X
$S_2O_3^{2-}$	1.0E-10	2.6E-11	1.1E-10	3.8X	4.2X
Both	7.2E-11	3.2E-11	9.2E-11	2.2X	2.8X
None	1.5E-10	2.9E-11	2.7E-10	4.9X	8.8X
Mean	8.9E-11	2.9E-11	1.3E-10	3.0X	4.3X

Table 4.4: Table showing the mean, high, and biotic/abiotic limestone dissolution rates (mol•cm^2•s^{-1}) within the *LKC Mixed Culture* reactor for intervals when the reactor was amended with acetate, thiosulfate, both, or neither.

4.4.4 Changes in Mixed Culture Community

Three microbial samples were collected during these experiments for community characterization by 16S rRNA sequencing. I used the resulting data, in conjunction with geochemical data, to infer the putative ecological role during periods of substantial geochemical variation within the bioreactor ecosystem. Once I classified the sequences at the genus level, I was able to examine individual responses of these OTUs and identify guilds that respond similarly to geochemical variables. There were ~30,216 total raw sequences obtained from the three samples for which sequencing was performed. Of those, a total of 21,488 (LKC-Inoculant – 6318, C-Limited – 7845, and C-Amended – 7325) bacterial 16S high-quality sequences with an average read length of 420 bp were obtained.

The taxonomic compositions of communities composing each sample are visualized in Figure 4.6 and a complete list the detected bacterial taxa (>1% proportional abundance) summarized at the class and genus level, is provided in Table 4.5. 19 genera had a relative abundance of more than 1%. At this level, the composition of microbial communities included 8 bacterial classes: *Alphaproteobacteria, Betaproteobacteria, Deltaproteobacteria, Gammaproteobacteria, Epsilonproteobacteria, Actinobacteria, Bacilli,* and *Clostridia*. Significant variation was obvious at this taxonomic level. For example, *Alphaproteobacteria* and *Betaproteobacteria* were abundant within the C-Limited sample, but not the inoculant or the C-Amended sample (Figure 4.6). Although, *Epsilonproteobacteria* are abundant in the inoculant (51.0%) they are nearly absent in both the C-Limited and C-Amended samples (Figure 4.6). Additionally, Deltaproteobacteria are significantly more abundant within the C-Amended sample (Figure 4.6).

At the genus level, community compositions vary significantly between samples. Primarily, the inoculant was composed of the greatest proportion of putative SOB (81.0%) composed primarily of members of the lineage *Thiothrix* and *Sulfurovum* (Table 4.5). The inoculant also hosted a small, but not insignificant, contingent of putative SRB (12.0%) composed exclusively of members of the genus *Desulfovibrio*. Similarly, a large proportion of C-Limited community was composed of putative SOB (59.8%), but these were mostly members of the lineages *Thioclava, Halothiobacillus, Thiomonas, and Thiobacillus*. Additionally, putative SRB were nearly absent (3.8%) from the C-Limited community (Table 4.5). In stark contrast, the C-Amended community had a substantial proportion of the putative SRB *Desulfovibrio* (72.3%), but a relatively insignificant proportional abundance of putative SOB (8.1%) (Table 4.5). Another notable difference is the relatively large proportion of gram-positive microorganisms in the C-Amended sample when compared to the other two samples.

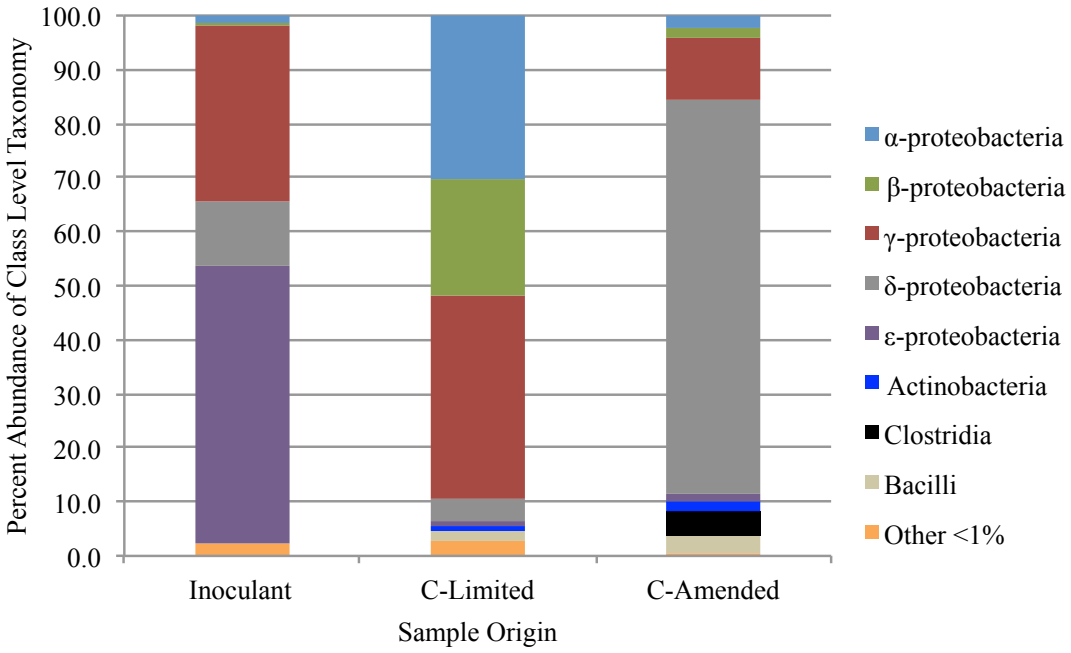

Figure 4.6: The bacterial communities composing the inoculant and reactor samples as proportional abundance (%) of taxa of representative class from 16S rRNA gene sequences.

Representative *Class*	Representative *Genus*	Inoculant	C-Limited	C-Amended
α-proteobacteria		**1.6**	**30.1**	**2.6**
	Rhodobacter	0.0	1.8	0.9
	Ensifer	0.0	5.6	0.0
	Azospirillum	0.0	2.2	0.0
	Thioclava	0.2	14.6	1.6
	Sphingopyxis	1.1	5.6	0.0
γ-proteobacteria		**32.7**	**37.3**	**11.4**
	Acinetobacter	0.1	3.6	4.3
	Halothiobacillus	1.6	16.2	3.4
	Pseudomonas	0.0	2.8	1.7
	Thiothrix	30.6	6.2	0.1
	Thermomonas	0.2	7.9	0.0
	Stenotrophomonas	0.0	0.0	1.8
β-proteobacteria		**0.2**	**21.9**	**1.8**
	Thiobacillus	0.0	8.1	0.6
	Thiomonas	0.0	13.6	1.1
ε-proteobacteria		**51.0**	**1.1**	**1.6**
	Sulfurovum	48.6	1.1	1.3
	Sulfurospirillum	2.2	0.0	0.2
δ-proteobacteria		**12.0**	**4.2**	**72.9**
	Desulfovibrio	12.0	3.8	72.1
Actinobacteria		**0.0**	**0.8**	**1.7**
	Propionibacterium	0.0	0.7	1.2
Bacilli		**0.0**	**1.6**	**3.5**
	Bacillus	0.0	1.5	3.5
Clostridia		**0.0**	**0.0**	**4.3**
	Anaerococcus	0.0	0.0	4.1
***Class* <1% Abundance/Unclassified**		**2.5**	**3.0**	**0.4**
Total Proportion SOB		**81.0**	**59.8**	**8.1**
Total Proportion SRB		**12.0**	**3.8**	**72.3**
Total Proportion Gram Positive		**0.0**	**2.4**	**9.5**

Table 4.5: Inoculant and reactor samples as proportional abundance (%) of taxa of representative class (bold) and genera from 16S rRNA gene sequences. Putative sulfur-oxidizing genera (SOB), sulfur reducing genera (SRB), and gram-positive genera are highlighted.

4.4.5 SEM Observations of Surface Features

SEM images of the carbonate coupons retrieved after 3-weeks within an acetate-amended reactor revealed stark differences in morphology of biofilm communities (Figure 4.7). Primarily single celled organisms with sparse biofilm coverage colonized the surface of calcite (Figure 4.7A-D). Calcite was covered in at least 3-different morphologies of secondary calcite precipitated within the reactor: 1) needle-like calcium-carbonate fibers (Figure 4.7B), 2) blade-like calcium carbonate (Figure 4.7D), and 3) spear-like calcium carbonate spikes (Figure 4.7A & C). The needle-like fibers tapered from a wide base to a point and were up to 20 μm long and ranged in width from ~100 nm to ~5 μm. The blade-like precipitates were up to 20 μm in both length and width. The spear-like spikes also tapered from a wide base to a point and ranged in size from a few nm in both length and width to ~15 μm wide and ~25 μm long.

The biofilm accumulated on the surfaces of both Madison Limestone and Madison Dolostone appeared more similar to each other than to that on calcite (Figure 4.7E&F; 4.7G&H, respectively). Both biofilms had spherical structures ranging in size from ~100μm to ~250μm in diameter randomly dispersed across the biofilm surface (Figure 4.7F&H). These spherical structures were composed of microorganisms, EPS, and secondarily precipitated calcite. Overall the surface of Madison Dolostone appeared to be covered in less EPS than that of Madison Limestone as the microorganisms on Madison Limestone are more easily differentiated (Figure 4.7E-H). Secondary calcite appeared to be precipitated on the biofilm on both surfaces (Figure 4.7E&G).

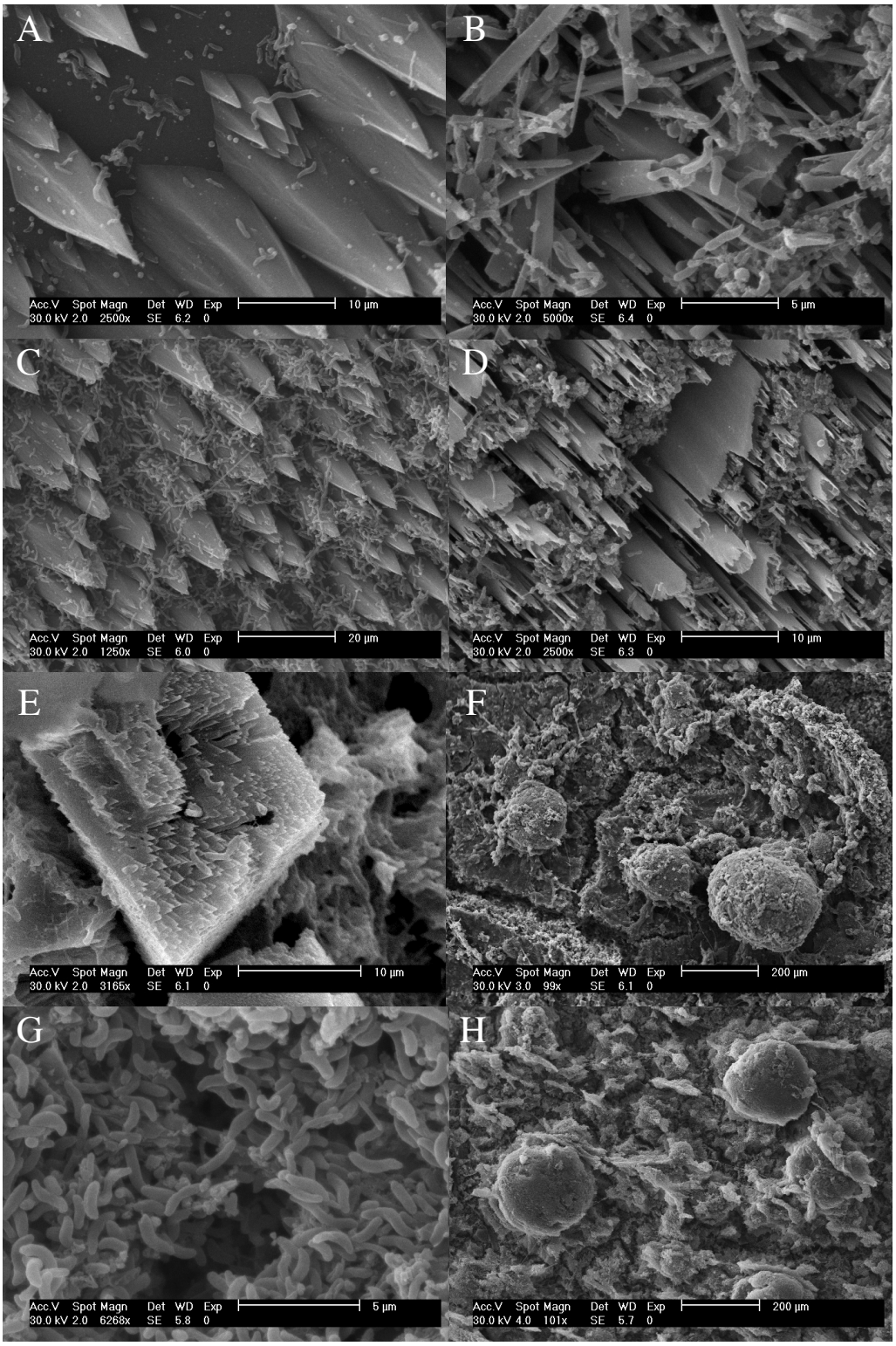

Figure 4.7 Caption on next page.

Figure 4.7: SEM images of carbonate surfaces colonized by LKC mixed cultures after 3-weeks within a CDC reactor amended with acetate. Microbial community is primarily composed of the SRB *Desulfovibrio*. A, B, C, & D are calcite surfaces with microorganisms attached; note the scale bars are 10μm, 5μm, 20μm, and 10μm, respectively. E & F are Limestone covered in biofilm; note the scale bars are 10μm and 200μm, respectively. G & H are Dolostone covered in biofilm; note the scale bars are 10μm and 200μm, respectively.

4.4.6 RESULTS OF SULFUR CHEMISTRY

Concentrations of sulfur species ($S_2O_3^{2-}$, SO_4^{2-}, and H_2S) were measured at discrete intervals to confirm inferred reaction pathways for bioreactor communities. These values are summarized as mean values in Table 4.6. In the *T. unzii* reactor, when $S_2O_3^{2-}$ was supplied at concentrations of 0.89mM with acetate, 0.77mM of $S_2O_3^{2-}$ was consumed. Under all other condition intervals, $S_2O_3^{2-}$ was completely consumed. Sulfate production was detected in every reactor except *T. unzii* reactor supplied with acetate and $S_2O_3^{2-}$. H_2S was only detected in every interval within the mixed culture reactor except intervals supplied with $S_2O_3^{2-}$ and acetate (Table 4.6).

4.5 DISCUSSION

4.5.1 Limestone Dissolution by *Thiothrix unzii*

When first described by Winogradsky in 1888, bacteria of the genus *Thiothrix* were hypothesized to be autotrophic. Since then, it has been shown that many *Thiothrix spp*. strains are capable of switching between heterotrophy, mixotrophy, and autotrophy, depending on environmental conditions (Odintsova et al, 1993; Rossetti et al, 2003). The effects and geochemical consequences of the dynamic mixotrophic behavior of *Thiothrix unzii* (on SAS) were directly observable throughout these experiments. Figure 4.8 serves to summarize the impact of *T. unzii* on limestone dissolution under heterotrophic (acetate + thiosulfate, acetate only) and autotrophic (thiosulfate only, thiosulfate and acetate withheld) conditions and the inferred dominant metabolic pathways during these intervals.

The limestone mean dissolution rate in the *T. unzii* reactor was ~4.8X the abiotic rate over the course of the entire experiment (Table 4.2). Time intervals with the lowest

dissolution rates (2.1-2.8X mean abiotic rates) coincided with intervals where acetate was supplied (Table 4.2). During periods when acetate was supplied *T unzii* was using heterotrophy by the following reaction (Nielsen et al, 2000):

$$2CH_3COO^- + S_2O_3^{2-} + O_2 + 2H^+ \rightarrow S^o + SO_3^{2-} + 4CO_2 + 4H_2O \quad (3)$$

$$\Delta G^o = +26.8kJ \bullet (\text{mol S-substrate})^{-1}$$

Acetate supplied with $S_2O_3^{2-}$ has been shown to increase the efficacy of $S_2O_3^{2-}$ conversion to S^o and SO_3^{2-} as well as expedite $S_2O_3^{2-}$ oxidation to SO_4^{2-} in the presence of O_2 (Nielsen et al, 2000). Herein, this causes small increases in the pH of the reactor during these periods, a decrease in ΔCa^{2+}, and a significantly lighter mean value of $\delta^{13}C_{CO2}$ (Figure 4.8A). Despite the decrease in limestone dissolution rate, the increased metabolic production of CO_2 by heterotrophy shown in reaction (3) increases headspace $[CO_2]$ (Figure 4.2). The headspace $[CO_2]$ rises to a slightly higher $[CO_2]$, but much lighter $\delta^{13}C_{CO2}$ than the $\delta^{13}C_{CO2}$ of the Air_{in} (Figure 4.8A). This is most likely due to selective oxidation of $^{12}C_{Acetate}$ and results in a $\Delta^{13}C_{HS-Air} \cong 8\text{-}12‰$ (Figure 4.8A).

When acetate was supplied without $S_2O_3^{2-}$, heterotrophy is again performed by *T. unzii* through the following reaction (Nielsen et al, 2000):

$$2S^o + 2CH_3COO^- + 7O_2 \rightarrow 2SO_4^{2-} + 4CO_2 + 2H^+ + 2H_2O \quad (4)$$

$$\Delta G^o = -507.4kJ \bullet (\text{mol S-substrate})^{-1}$$

Whereby, mixotrophic strains of Thiothrix have been shown to pair acetate with sulfur oxidation against oxygen, resulting in increased growth yield (Nielsen et al, 2000; Odintsova et al, 1993). This causes a slightly higher mean dissolution rate than the

acetate and $S_2O_3^{2-}$ intervals as there is some light acid production from oxidation of internal S^o (Figure 4.8B). This was confirmed by measuring production of SO_4^{2-} (0.08mM) during these intervals (Table 4.6). Additional confirmation comes from the increase in $[CO_2]$ and lighter $\delta^{13}C_{CO2}$ than when acetate and $S_2O_3^{2-}$ are supplied (Table 4.1; Figure 4.2; Figure 4.8).

Major geochemical changes occurred when $S_2O_3^{2-}$ was provided in the absence of acetate. The significant increase in $[CO_2]$ and enrichment of $\delta^{13}C_{CO2}$ in $^{13}CO_2$ are accompanied by a large drop in pH and increase in $[Ca^{2+}]$. This trend is indicative of a switch towards autotrophy by the *T. unzii* that likely follows this reaction (Kelly, 1999):

$$6CO_2 + 3S_2O_3^{2-} + 9H_2O \rightarrow C_6H_{12}O_6 + 6SO_4^{2-} + 6H^+ \quad (5)$$

$$\Delta G^o = -738.4 kJ \bullet (\text{mol S-substrate})^{-1}$$

This reaction also selects for the relatively light $^{12}CO_2$ over $^{13}CO_2$ leaving the headspace reservoir heavier (Figure 4.2, Figure 4.8C). Although CO_2 is being consumed through autotrophy the $[CO_2]$ increases dramatically due to the significant increase in limestone dissolution and drop in pH of the media, which release CO_2 back into the headspace (Figure 4.8C). As further confirmation of this reaction pathway, sulfur species measurements during these periods showed a complete removal of $S_2O_3^{2-}$ from the media across the reactor (Table 4.6). This was accompanied by SO_4^{2-} production to a ~1.25X higher concentration than $S_2O_3^{2-}$ consumed (Table 4.6).

The highest rates of limestone dissolution were recorded when no acetate or $S_2O_3^{2-}$ were provided (Table 4.2, Figure 4.8D). During these intervals the heaviest $\delta^{13}C_{CO2}$, highest CO_2, and lowest pHs were also recorded. This trend is again indicative of autotrophy that likely follows this reaction:

$$6CO_2 + 4S° + 10H_2O \rightarrow C_6H_{12}O_6 + 4SO_4^{2-} + 8H^+ \quad (6)$$

$$\Delta G^o = -507.4 kJ \bullet (\text{mol S-substrate})^{-1}$$

Thiothrix unzii has been shown to oxidize internally stored sulfur during these periods when $S_2O_3^{2-}$ is withheld (Steinhauer et al, 2010). Production of SO_4^{2-} was confirmed photometrically at mean concentrations of ~1.90mM during these periods (Table 4.6). Again the increased $[CO_2]$ despite autotrophy is due to the significant increase in limestone dissolution (~13X abiotic rates) and drop in pH (up to 2 log units) of the media, which release relatively heavy CO_2 ($\Delta^{13}C_{LS-Air} \cong 16‰$) back into the headspace (Figure 4.3; Figure 4.8D).

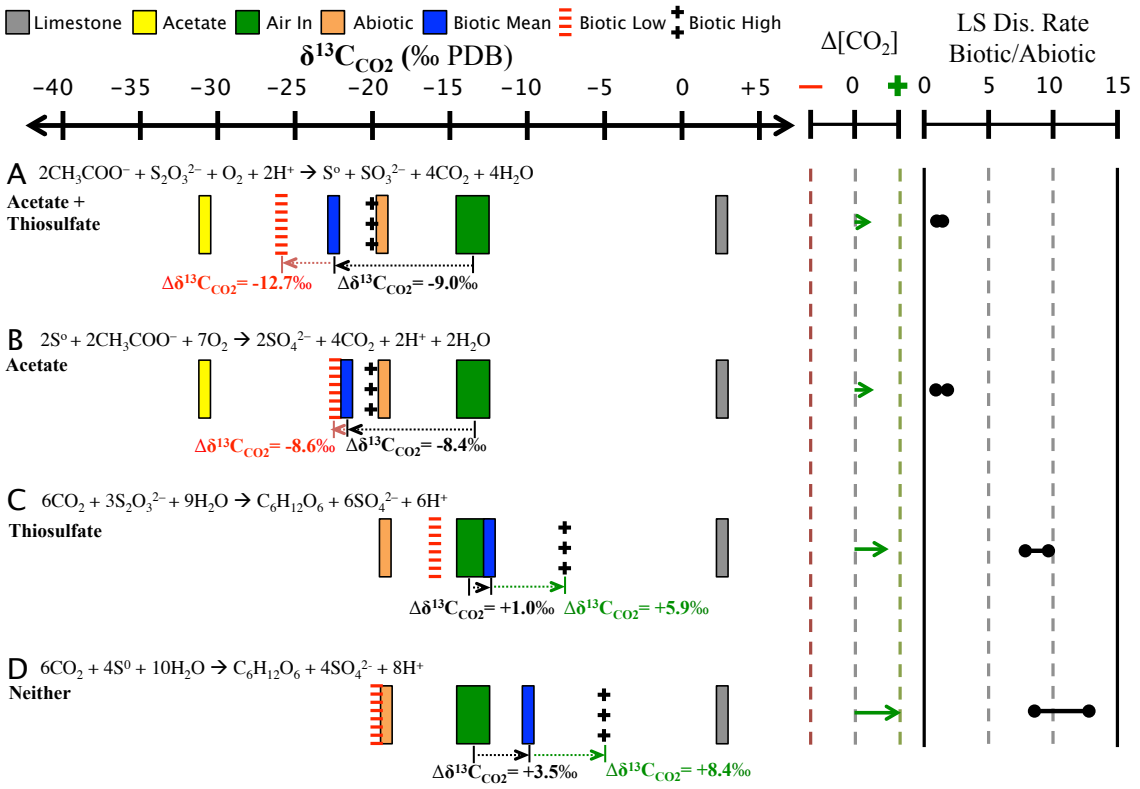

Figure 4.8: Limestone dissolution is the result of both autotrophy and heterotrophy in *Thiothrix unzii* pure cultures. For each of the specified intervals: Gray is the $\delta^{13}C_{CaCO3}$, yellow is $\delta^{13}C_{Acetate}$, green is $\delta^{13}C_{CO2}$ of the ambient air entering the reactor, orange is the $\delta^{13}C_{CO2}$ of the headspace under abiotic conditions, blue is the mean $\delta^{13}C_{CO2}$ of the biotic reactor, red (-) are the lowest biotic $\delta^{13}C_{CO2}$, black (+) are the highest biotic $\delta^{13}C_{CO2}$. A. Heterotrophy when acetate and thiosulfate are supplied. B. Heterotrophy when acetate is supplied and thiosulfate withheld. C. Autotrophy when thiosulfate is supplied and acetate is withheld. D. Autotrophy when both acetate and thiosulfate are withheld.

4.5.2 Limestone Dissolution by LKC Mixed Communities

Our previous investigations revealed significant variation in microbial community structure, composition, and growth (See Chapter 3). Here I inoculated a reactor with a mixed culture from LKC to see if I could detect these shifts by monitoring select geochemical indicators ($\delta^{13}C_{CO2}$, [CO_2], Ca^{2+}, and pH). I found that the mixed community reactor was geochemically dynamic and prediction of dominant metabolisms and guild makeup was indeed possible. Figure 4.9 serves to summarize the impact of *LKC mixed* communities on limestone dissolution under heterotrophic (acetate + thiosulfate, acetate only) and autototrophic (thiosulfate only, thiosulfate and acetate withheld) conditions and the inferred dominant metabolic pathways during these intervals.

The inoculant was primarily composed of putative SOB (81.0%) most closely related to members of the genera *Thiothrix* and *Sulfurovum* (Table 4.5). The inoculant also contained putative SRB (12.0%) composed exclusively of members of the genus *Desulfovibrio*. The presence of a diverse consortium, composed of autotrophs, mixotrophs, and heterotrophs is confirmation that the inoculant was ideal to test our hypotheses. Additionally, this inoculant is very similar to the inoculant used in bioreactors from Chapters 2 and 3 (Jones & Bennett, 2014).

Shortly after inoculation, the media was amended with $S_2O_3^{2-}$ and acetate. Although there were periods of both high and low reactor pH, after equilibration, pH was relatively high and ΔCa^{2+} was relatively low during these intervals (Figure 4.5). Additionally, the lightest mean and overall $\delta^{13}C_{CO2}$ were achieved during these intervals (Figure 4.4). This indicates heterotrophy and when combined with geochemical trends suggests dominance of the reaction pathway (Cypionka, 2000):

$$CH_3COO^- + S_2O_3^{2-} + O_2 + 2H^+ \rightarrow S^o + SO_3^{2-} + 4CO_2 + 4H_2O \quad (7)$$

$$\Delta G^o = +26.8\text{kJ}\bullet(\text{mol S-substrate})^{-1}$$

This ability to pair sulfur-reduction with O_2 reduction to H_2O has been shown in *Desulfovibrio* in previous experiments and has been implicated in carbonate precipitation (Cypionka, 2000; Dupraz et al, 2009). During these intervals, as $\delta^{13}C_{CO2}$ decreases there is a proportional increase in headspace [CO_2] consistent with the increased metabolic production of CO_2 by heterotrophy shown in this reaction (Figure 4.4; Figure 4.9A).

Interestingly, this reaction generally consumes acidity, but there is still a net increase in limestone dissolution rate of ~2.8X abiotic rates (Table 4.4; Figure 4.9A). Additionally, for these time periods SO_4^{2-} was measured at 0.28mM and all 0.89mM $S_2O_3^{2-}$ was consumed. The increase in dissolution rate was nearly identical to that achieved in pure culture experiments using heterotrophy, but ~4X as much SO_4^{2-} was generated in the mixed culture reactor (Table 4.6). This suggests the following reaction pathway is also taking place driven by autotrophic SOB (Kelly, 1999):

$$2S^o + 3O_2 + 2H_2O \rightarrow 4SO_4^{2-} + 4H^+ \quad (8)$$

$$\Delta G^o = -507.4\text{kJ}\bullet(\text{mol S-substrate})^{-1}$$

Examination by light microscopy revealed visible sulfur globules in filaments before and absence of these globules after these intervals. The ability to oxidize internally stored sulfur by *Thiothrix spp*. has been shown previously (Howarth et al, 1999; Steinhauer et al, 2010).

During intervals when acetate was supplied without $S_2O_3^{2-}$, the mean dissolution rate is nearly identical to the abiotic rate (Table 4.4; Figure 4.9B). However, the mean

$\delta^{13}C_{CO2}$ during these intervals is up to ~21.9‰ lighter than the mean abiotic $\delta^{13}C_{CO2}$; indicating heterotrophy (Figure 4.9B). This trend combined with the increased [CO_2] and high pHs during these intervals suggests the dominant reaction pathway (Goevert & Conrad, 2009):

$$CH_3COO^- + SO_4^{2-} \rightarrow HS^- + 2CO_2 + 2OH^- \quad (9)$$

$$\Delta G^o = -24.2 kJ \bullet (\text{mol S-substrate})^{-1}$$

This was validated by detection of sulfide during this interval (Table 4.6). It should be noted that both olfactory and photometric methods detected sulfide.

During a period of sulfide production, I aseptically removed biomass from the bioreactor for 16S rRNA sequencing. Results of this analysis revealed significant taxonomic changes to the community compared to the inoculant (Table 4.5). The overwhelming dominance of *Desulfovibrio* is consistent with previous bioreactor experiments amended with acetate whereby the addition of acetate to reactors promoted chemoheterotrophic growth (See Chapter 3).

Indeed, *Desulfovibrio* is a motile, heterotrophic, sulfur-reducing microorganism capable of growth on a variety of sulfur substrates, including $S_2O_3^{2-}$ and SO_4^{2-} (Cypionka, 2000; Liu & Peck, 1981). If the metabolism of members of this genus went unchecked, the resulting pH increase might lead calcite precipitation. However, sequencing also revealed the minor presence of SOB (8.1%) in this community. The presence of SOB here, but not in the community attached to limestone in the acetate-amended reactor from Chapter 3 is likely due to frequent changes in geochemical conditions within these reactors from autotrophic to heterotrophic.

The metabolic activity of SRB in biofilms has been previously linked to calcite precipitation (Baumgartner et al, 2006; Dupraz et al, 2009; Lyons et al, 1984; Van Lith et al, 2003; Visscher et al, 2000; Walter et al, 1993). Visual evidence that carbonate precipitation occurs when *Desulfovibrio* metabolism occurs becomes apparent by examining SEM images of carbonates from the acetate-amended reactor from Chapter 3 (Figure 4.7A-E). The communities attached to carbonates had up to ~82% proportional abundance (Chapter 3; Table 3.8)

The exopolymers that make up the EPS of SRB, including species of *Desulfovibrio,* tend to bind copious amounts of calcium ions. This is due to the high proportion of low pKa exopolymers; specifically carboxylic acids (pKa=3), sulfinic acids (pKa=7.0-7.1), and amino groups (pKa=8.4-9.2) (Braissant et al, 2007; Dupraz et al, 2009). Any increase in pH due to metabolism of *Desulfovibrio* would cause more of these exopolymers to deprotonate, binding additional calcium ions, increasing the saturation with respect to calcite. Even the cell walls of metabolically inactive SRB have been shown to seed calcite precipitation (Bosak & Newman, 2003; Bosak & Newman, 2005; Ferris, 2000). Furthermore, Bosak and Newman (2005) extracted EPS from *Desulfovibrio desulfuricans* and showed that the presence of EPS alone resulted in more numerous calcite nucleations, compared to control experiments. Also, Aloisi et al. (2006) showed that metabolizing cells of *Desulfovibrio* produce cell-bound nanoglobules, composed of EPS, that seed calcium precipitation prior to release from the cell (Aloisi et al, 2006). As a consequence of some, if not all, of these mechanisms calcite precipitates on carbonate surfaces and on microbial biofilms in acetate-amended reactors (Figure 4.7).

The variety of morphologies of secondary calcite precipitation is likely the result of these processes, as well. The needle-like, spear-like, and blade-like calcium carbonate morphologies (Figure 4.7A-D) have been shown to be caused by environmentally driven,

passive mineralization where the mineral surface serves as the template for crystal nucleation (Dupraz et al, 2009; Perry et al, 2007). The spherical microbialite structures that are present on Madison Limestone and Madison Dolostone (Figure 4.7F&H) are consistent with calcium carbonate structures resulting directly from concentrated microbial metabolism due to high biomass concentration; whereby the significant EPS and organic matrix serves as the template for crystal morphologies (Dupraz et al, 2009).

Limestone dissolution rates were highest during intervals when acetate was not supplied (Table 4.4; Figure 4.9C&D). Geochemical trends during these intervals suggested autotrophy to be dominant (Figure 4.9C&D). In both of these intervals $\delta^{13}C_{CO2}$ became heavier, $[CO_2]$ increased, pH dropped, and $[Ca^{2+}]$ increased (Figure 4.4 & Figure 4.5). These trends suggest the following reactions to be dominant:

$$6CO_2 + 3S_2O_3^{2-} + 9H_2O \rightarrow C_6H_{12}O_6 + 6SO_4^{2-} + 6H^+ \quad (10)$$

$$\Delta G^o = -738.7 kJ \bullet (\text{mol S-substrate})^{-1}$$

when $S_2O_3^{2-}$ was supplied and:

$$6CO_2 + 4S^\circ + 10H_2O \rightarrow C_6H_{12}O_6 + 4SO_4^{2-} + 8H^+ \quad (11)$$

$$\Delta G^o = -507.4 kJ \bullet (\text{mol S-substrate})^{-1}$$

if neither $S_2O_3^{2-}$ nor acetate were supplied (Kelly, 1999).

Stoichiometrically, reaction (11) produces more acidity and lead to greater dissolution rates. Indeed, when $S_2O_3^{2-}$ is supplied, limestone dissolution takes place at nearly half the rate as when none is supplied (Table 4.4, Figure 4.9C&D). Additionally, sulfide and sulfate were both produced, indicating minor heterotrophy taking place within

the reactor during both intervals. Autotrophic activity in $S_2O_3^{2-}$ amended intervals produced less sulfate (producing acidity) while heterotrophic activity produced more sulfide (consuming acidity) when compared to the $S_2O_3^{2-}$ and acetate limited interval (Table 4.6). It should also be noted that dissolution rates are relatively lower in the mixed culture reactor than pure culture reactor; likely due to the presence and metabolism of SRB..

16S rRNA sequencing of samples taken during intervals without acetate confirms our intuition that autotrophic SOB dominate during these intervals. This community structure was significantly different than that of both the inoculant and samples taken during acetate amended intervals (Figure 4.6). The overwhelming dominance of SOB (~60%) is consistent with previous CP-Limited (carbon and phosphate-limited) bioreactor experiments whereby autotrophic SOB dominated on carbonate surfaces (See Chapter 3).

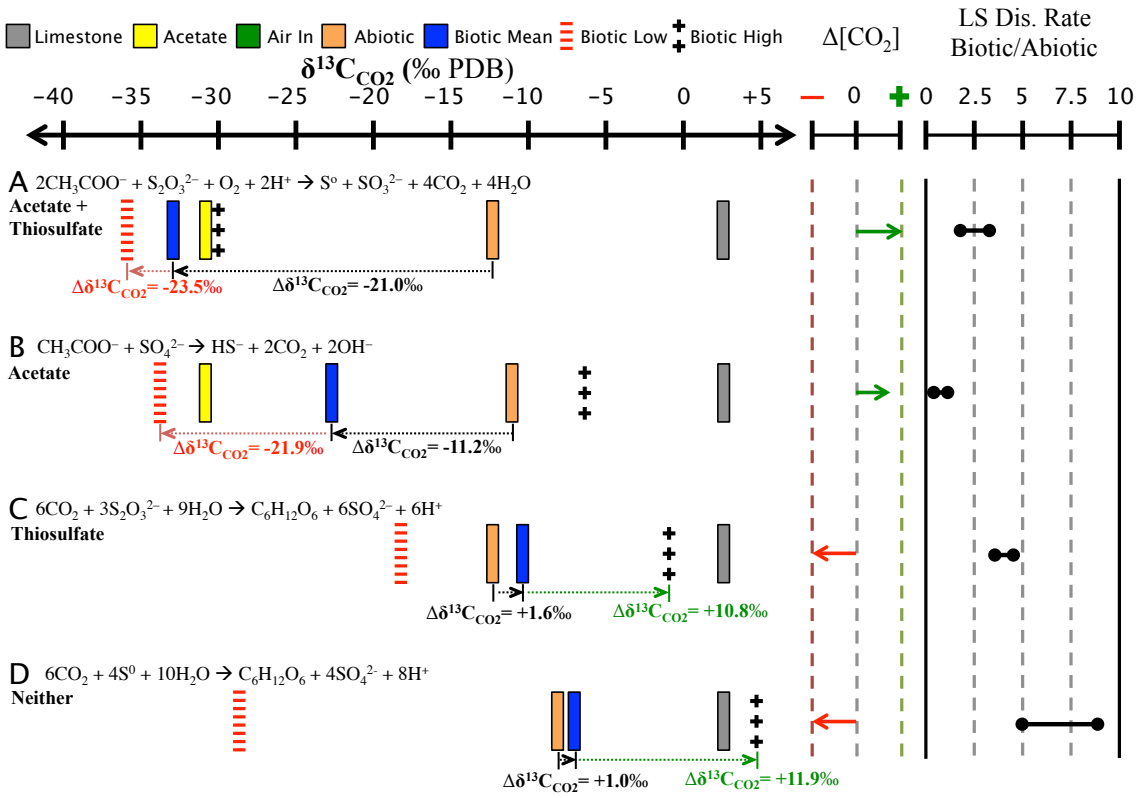

Figure 4.9: Limestone dissolution is the result of both autotrophy and heterotrophy in the *LKC Mixed* culture reactor. For each of the specified intervals: Gray is the $\delta^{13}C_{CaCO3}$, yellow is $\delta^{13}C_{Acetate}$, green is $\delta^{13}C_{CO2}$ of the ambient air entering the reactor, orange is the $\delta^{13}C_{CO2}$ of the headspace under abiotic conditions, blue is the mean $\delta^{13}C_{CO2}$ of the biotic reactor, red (-) are the lowest biotic $\delta^{13}C_{CO2}$, black (+) are the highest biotic $\delta^{13}C_{CO2}$. Note that there is no $\delta^{13}C_{CO2}$ for the ambient air entering this reactor. A. Heterotrophy when acetate and thiosulfate are supplied. B. Heterotrophy when acetate is supplied and thiosulfate withheld. C. Autotrophy when thiosulfate is supplied and acetate is withheld. D. Autotrophy when both acetate and thiosulfate are withheld.

	$S_2O_3^{2-}$ (Yes/No)	Acetate (Yes/No)	$\Delta^{13}C_{HS}$ Mean	$\Delta[CO_2]$	Dominant Reaction Pathway Dominant Metabolism	$\Delta S_2O_3^{2-}$ (mM)	ΔSO_4^{2-} (mM)	ΔH_2S (mM)	LS Dis. Rate Mean: High (Biotic/Abiotic)
T. Unzii	Yes	Yes	~0	~0	$2CH_3COO^- + S_2O_3^{2-} + O_2 + 2H^+ \rightarrow S^o + SO_3^{2-} + 4CO_2 + 4H_2O$ Heterotrophic	-0.77	~0	0	1.6X : 2.1X
	No	Yes	Lighter	~0	$2S^o + 2CH_3COO^- + 7O_2 \rightarrow 2SO_4^{2-} + 4CO_2 + 2H^+ + 2H_2O$ Heterotrophic	N/A	0.08	0	1.7X : 2.8X
	Yes	No	Heavier	Increase	$6CO_2 + 3S_2O_3^{2-} + 9H_2O \rightarrow C_6H_{12}O_6 + 6SO_4^{2-} + 6H^+$ Autotrophic	-0.89	+1.10	0	7.7X : 9.8X
	No	No	Heavier	Increase	$6CO_2 + 4S^0 + 10H_2O \rightarrow C_6H_{12}O_6 + 4SO_4^{2-} + 8H^+$ Autotrophic	N/A	+1.90	0	8.3 : 13.2X
LKC Mixed Culture	Yes	Yes	Lighter	Increase	$2CH_3COO^- + S_2O_3^{2-} + O_2 + 2H^+ \rightarrow S^o + SO_3^{2-} + 4CO_2 + 4H_2O$ Heterotrophic	-0.89	+0.28	0	2.2X : 2.8X
	No	Yes	Lighter	Increase	$CH_3COO^- + SO_4^{2-} \rightarrow HS^- + 2CO_2 + 2OH^-$ Heterotrophic	N/A	+0.01	+0.22	0.8X : 1.1X
	Yes	No	Heavier	Decrease	$6CO_2 + 3S_2O_3^{2-} + 9H_2O \rightarrow C_6H_{12}O_6 + 6SO_4^{2-} + 6H^+$ Autotrophic	-0.89	+0.52	+0.17	3.8X : 4.2X
	No	No	Heavier	Decrease	$6CO_2 + 4S^0 + 10H_2O \rightarrow C_6H_{12}O_6 + 4SO_4^{2-} + 8H^+$ Autotrophic	N/A	+1.63	+0.04	4.9X : 8.8X

Table 4.6: Summary of mean Δ [Sulfur] (mM) of various sulfur species during specific periods and overall summary of findings from this study. When $S_2O_3^{2-}$ in is 0.89mM, Acetate in is 2mM, SO_4^{2-} in from $MgSO_4$ is 0.94mM.

4.6 CONCLUSIONS

Through these experiments, unique patterns emerged allowing me to link geochemical trends to community structure and function. $\delta^{13}C_{CO2}$ of headspace gas can be used in a bioreactor to distinguish between heterotrophic and autotrophic contribution to CO_2 efflux. However, this method may be limited to an experimental system composed of metabolically sensitive peripheral geochemical indicators of metabolic shifts. An ideal system would contain minerals near equilibrium conditions with the liquid media and diverse functional communities able to metabolize under a wide range of geochemical conditions. Herein, a laboratory reactor synthetic sulfuric acid carbonate karst system met these criteria. Furthermore, the sensitivity and responsiveness of the reaction kinetics of the carbonate system when exposed metabolic byproducts provided insight into the constraints on biogenesis of sulfuric acid caves. By simultaneously measuring and logging ($\delta^{13}C_{CO2}$, $[CO_2]$, Ca^{2+}, and pH), I showed increased calcite dissolution rates up to ~13X abiotic rates under autotrophic conditions and limited dissolution under heterotrophic conditions. Additionally, I observed complete shift of metabolic function of the microbial communities and taxonomic composition within a matter of hours. Community composition shifted from a SOB dominated inoculant, to SRB dominated when supplied acetate, and finally back to SOB dominated when acetate was withheld. These changes initiated within minutes of changing geochemical input. Additionally, the methodology for monitoring changes laid out here is minimally invasive to the community function, resulting in low experimental bias.

It is important to note that the goal was not to absolutely quantify an effect, but to gain further insight into the nature of these interactions. Additional trends may be observed through a more critical analysis of this substantial data set. Although it was outside of the scope of this investigation, a mass balance of carbon concentrations and

isotopic compositions was not achievable without simultaneous monitoring of DIC in the media outflow from the reactor. Future laboratory bioreactor experiments should be conducted with this in mind. If this is done, this method has the potential to resolve the microbial community function, composition, and carbon balance to an exceptional level of detail.

Chapter 5: Synthesis and Concluding Remarks

5.1 Synthesis of Doctoral Research

The ubiquity and scale of microorganisms existing in biofilms attached to mineral surfaces likely makes it one of the most important and impactful geochemical processes on earth. The vast majority of previous research into mechanisms behind, or consequences of mineral colonization have been narrowly focused on isolated factors such as nutrients, energy, protection, attractive forces, or pH buffering to name a few. This may be the first comprehensive study assessing the relative impacts of environmental pressures (carbon source, pH, phosphate availability) and surface chemistry pressures (buffering ability, nutrient availability) on community structure, phylogenetic diversity, taxonomic diversity, membership, and biofilm accumulation.

We conclude that the development, evolution, and diversification of microbial life was influenced by the biogeochemical interactions with mineral surfaces. Throughout geologic time, microorganisms have enhanced survival by colonizing mineral surfaces and developing complex biofilm communities, the structure and function of which is best suited to that specific mineral habitat. The insights that led to this conclusion were serendipitous and resulted in an early departure from the original course of this research.

In the early stages of this investigation, I tested a hypothesis that, when given a variety of mineral surfaces, neutrophilic SOB would preferentially colonize highly buffering carbonate surfaces in order to buffer the acidity generated by their metabolism. I conceived flow through-bioreactor experiments optimized to entice SOB to demonstrate this behavior. The media had to be at a sufficiently low pH to not buffer the metabolically generated acidity. Nutrients had to be kept to a minimum to limit planktonic growth, but critical vitamins would need to be supplied or nothing would grow. The mineral suite had to offer unique incentives to the community and disprove

the null-hypothesis. Under these conditions, I showed that neutrophilic, but acid producing microorganisms preferentially colonize highly buffering carbonates in both pure and mixed cultures (Chapter 2).

Fortuitously, these CP-Limited conditions also provided the required environmental impetus for preferential surface selection by other metabolic guilds. Acidophiles preferentially colonized non-buffering silicates, silicates selected for gram-positives, and aluminosilicates selected for aluminotolerant microorganisms. Additionally, biofilm accumulation was highest on minerals with abundant phosphate content. In summary, similar taxa, with presumably similar metabolic functions and environmental tolerances were found on similar minerals. I concluded that microorganisms colonize mineral surfaces according to these functions and tolerances; for nutrient limited subsurface environments. More importantly, I asked if this relationship would hold up under other geochemical conditions.

We hypothesized that under heterotrophic conditions SRB would dominate on all surfaces, eliminating the selective bias. If I increased the pH, to 8.3, and added phosphate, media buffering might also eliminate the observed selective bias. Additionally, if provided phosphate in the media, biofilm accumulation should be similar on all surfaces. So, I designed medias to test these hypotheses.

In short, our intuitions were validated in Chapter 3. Briefly, media phosphate was correlated with decreased biofilm accumulation on P-bearing minerals. Adding acetate to the CP-Limited media encouraged heterotrophic growth of SRB on nearly every surface (exceptions, acidophiles on quartz, G+ on basalt) and nearly eliminated taxonomic bias. Increasing the pH to 8.3 and adding phosphate eliminated all of the taxonomic biases observed in the CP-limited media from Chapter 2 and SOB thrived on all surfaces. Adding both acetate and phosphate to the media also eliminated taxonomic biases, but

SOB and SRB both thrived on all surfaces. The planktonic samples were exceptional in all reactors except the C-Amended reactor.

Trends in diversity and guild abundance (e.g. sulfur-oxidizers/reducers, G+, acidophiles, heterotrophs, autotrophs) were observed and statistically validated for whole reactor conditions. At the genus level, there were no taxa shared between all 4-reacotors. This suggested that the community structure was more sensitive to environmental stimuli than previously expected. The addition of acetate was correlated with shifts from autotrophy to heterotrophy, SRB occurrence, increased alpha-diversity, and decreased beta-diversity. The addition of phosphate was most strongly correlated with decreased alpha-diversity and beta-diversity.

Despite the high taxonomic variation between reactors, there was surprisingly little taxonomic variation between surfaces within each reactor. It was only after I calculated phylogenetic distances (UniFrac) for the 16S rRNA sequences from each surface and subjected the distance matrixes to permutational multivariate analysis of variance (PERMANOVA) that I was able to correlate community composition with surface type. Once this was accomplished I found that surface type (carbonate, silicate, aluminosilicate, or planktonic) controlled up to 90% of the variance in phylogenetic diversity within each reactor. Succinctly, microbes on similar surfaces were more genetically similar. This is strong evidence in favor of our hypothesis that mineral selection is genetically engrained. However, further investigations are needed to determine if this is the case or if the communities diverge genetically after colonization. However, due to the short duration of the experiments, the former is significantly more likely.

Finally, I explored the biogeochemical consequences of these community shifts on mineral dissolution (Chapter 4). So, I exploited the knowledge gained in these

experiments to investigate the effect of dynamic shifts in community structure on sulfuric-acid speleogenesis. Autotrophic conditions favored autotrophic acid-producing SOB and heterotrophic conditions favored growth of acidity-consuming-heterotrophic SRB. I hypothesized opposing effects on geochemical participants of the carbonate system precipitation/dissolution. I also hypothesized that I could detect shifts in community function, and possibly structure, by monitoring changes in $\delta^{13}C_{CO2}$ of the headspace of a bioreactor.

All of these hypotheses were confirmed. Autotrophic conditions favored the growth of SOB leading to increased dissolution rates up to ~13X abiotic rates, heterotrophic conditions led to much slower dissolution rates and even intervals of calcite precipitation. Through 16S rRNA sequencing I confirmed that $^{13}C_{CO2}$-enriched $\delta^{13}C_{CO2}$ was an indicator of autotrophic SOB and $^{13}C_{CO2}$-depleted $\delta^{13}C_{CO2}$ was an indicator of heterotrophic SRB. These effects were substantial with heterotrophic intervals as low as $\delta^{13}C_{CO2}$=-36.1 and autotrophic intervals as high as $\delta^{13}C_{CO2}$=+3.8.

These geochemical changes indicating shifting metabolic function in microbial communities (ultimately taxonomic composition) were incredibly fast. Within minutes, geochemical changes initiated and complete community overturn occurred within a matter of hours. I concluded that the responsiveness and geochemical consequences of these shifts demonstrate a proof of concept for using active sulfuric acid cave ecosystems to explore the effects of competing microbial metabolisms on carbon cycling and stable carbon isotope fractionation.

References

Abdollahi H, Wimpenny JWT. (1990). Effects of oxygen on the growth of *Desulfovibrio desulfuricans*. *J Gen Microbiol* **136:** 1025.

Abu-Lail NI, Camesano TA. (2003). Role of Ionic Strength on the Relationship of Biopolymer Conformation, DLVO Contributions, and Steric Interactions to Bioadhesion of *Pseudomonas putida* KT2442. *Biomacromolecules* **4:** 1000-1012.

Albertsen M, Hugenholtz P, Skarshewski A, Nielsen KL, Tyson GW, Nielsen PH. (2013). Genome sequences of rare, uncultured bacteria obtained by differential coverage binning of multiple metagenomes. *Nat Biotech* **31:** 533-538.

Aloisi G, Gloter A, Krüger M, Wallmann K, Guyot F, Zuddas P. (2006). Nucleation of calcium carbonate on bacterial nanoglobules. *Geology* **34:** 1017-1020.

Anderson MJ. (2001). A new method for non-parametric multivariate analysis of variance. *Austral Ecology* **26:** 32-46.

Anderson MJ, Crist TO, Chase JM, Vellend M, Inouye BD, Freestone AL, Sanders NJ, Cornell HV, Comita LS, Davies KF, Harrison SP, Kraft NJB, Stegen JC, Swenson NG. (2011). Navigating the multiple meanings of β diversity: a roadmap for the practicing ecologist. *Ecology Letters* **14:** 19-28.

Anderson RT, Chapelle FH, Lovley DR. (2001). Comment on "Abiotic Controls on H2 Production from Basalt–Water Reactions and Implications for Aquifer Biogeochemistry". *Environmental Science & Technology* **35:** 1556-1557.

Appanna VD, Finn H, Pierre MS. (1995). Exocellular phosphatidylethanolamine production and multiple-metal tolerance in *Pseudomonas fluorescens*. *FEMS Microbiol Lett* **131:** 53-56.

Araújo E, de Andrade N, da Silva L, de Carvalho A, de Sá Silva C, Ramos A. (2010). Control of Microbial Adhesion as a Strategy for Food and Bioprocess Technology. *Food Bioprocess Technol* **3:** 321-332.

Balkwill D. (2005). Ensifer Casida 1982, 343 VP. In *Bergey's Manual® of Systematic Bacteriology*, Brenner D, Krieg N, Garrity G, Staley J, Boone D, Vos P, Goodfellow M, Rainey F, Schleifer K-H (eds), 87, pp 354-358. Springer US.

Banfield JF, Barker WW, Welch SA, Taunton A. (1999). Biological impact on mineral dissolution: Application of the lichen model to understanding mineral weathering in the rhizosphere *Proceedings of the National Academy of Sciences* **96** 3404-3411.

Banfield JF, Hamers RJ. (1997). Processes at minerals and surfaces with relevance to microorganisms and prebiotic synthesis. In *Geomicrobiology: Interactions Between Microbes and Minerals, Reviews in Mineralogy Volume 35*, Banfield JF, Nealson KH (eds), pp 81-122. Washington, D.C.: Mineralogical Society of America.

Banik S, Dey B. (1982). Available phosphate content of an alluvial soil as influenced by inoculation of some isolated phosphate-solubilizing micro-organisms. *Plant and Soil* **69:** 353-364.

Barriuso J, Valverde J, Mellado R. (2011). Estimation of bacterial diversity using next generation sequencing of 16S rDNA: a comparison of different workflows. *BMC Bioinformatics* **12:** 1-12.

Barskov IS. (2008). Biomineralization and Evolution. Coevolution of Mineral and Biological Worlds. In *Biosphere Origin and Evolution*, Dobretsov N, Kolchanov N, Rozanov A, Zavarzin G (eds), 15, pp 211-218. New York, USA: Springer US.

Barton HA, Luiszer F. (2005). Microbial metabolic structure in a sulfidic cave host spring: Potential mechanisms of biospeleogenesis. *Journal of Cave and Karst Studies* **67:** 28-38.

Battistuzzi FU, Hedges SB. (2009). A Major Clade of Prokaryotes with Ancient Adaptations to Life on Land. *Mol Biol Evol* **26:** 335-343.

Baumgartner LK, Reid RP, Dupraz C, Decho AW, Buckley DH, Spear JR, Przekop KM, Visscher PT. (2006). Sulfate reducing bacteria in microbial mats: Changing paradigms, new discoveries. *Sedimentary Geology* **185:** 131-145.

Bennett PC, Engel AS, Roberts JA. (2006). Counting and imaging bacteria on mineral surfaces. *Methods of Investigating Microbial-Mineral Interactions* **14:** 37-78.

Bennett PC, Hiebert FK, Choi WJ. (1996). Microbial colonization and weathering of silicates in a petroleum-contaminated groundwater. *Chemical Geology* **132:** 45-53.

Bennett PC, Hiebert FK, Rogers JR. (2000). Microbial control of mineral–groundwater equilibria:Macroscale to microscale. *Hydrogeology Journal* **8:** 47-62.

Bennett PC, Rogers JR, Choi WJ. (2001). Silicates , Silicate Weathering , and Microbial Ecology. *Geomicrobiology Journal* **18:** 3-19.

Beveridge TJ. (1981). Ultrastructure, Chemistry, and Function of the Bacterial Wall. In *International Review of Cytology*, G.H. Bourne JFD, Jeon KW (eds), Vol. Volume 72, pp 229-317. Academic Press.

Beveridge TJ. (1988). The bacterial surface: general considerations towards design and function. *Can J Microbiol* **34:** 363-372.

Bohannan BJ, Hughes J. (2003). New approaches to analyzing microbial biodiversity data. *Curr Opin Microbiol* **6:** 282-287.

Borg I, Groenen PJ. (2005). *Modern multidimensional scaling: Theory and applications*: Springer Science & Business Media.

Bosak T, Newman DK. (2003). Microbial nucleation of calcium carbonate in the Precambrian. *Geology* **31:** 577-580.

Bosak T, Newman DK. (2005). Microbial kinetic controls on calcite morphology in supersaturated solutions. *Journal of Sedimentary Research* **75:** 190-199.

Bousserrhine N, Gasser U, Jeanroy E, Berthelin J. (1998). Effect of aluminium substitution on ferri-reducing bacterial activity and dissolution of goethites. *Comptes Rendus de l' Academie des Sciences, Serie II Sciences de la Terre et des Planetes* **326:** 617-624.

Bowen De León K, Ramsay B, Fields M. (2012). Quality-Score Refinement of SSU rRNA Gene Pyrosequencing Differs Across Gene Region for Environmental Samples. *Microb Ecol* **64:** 499-508.

Braissant O, Decho AW, Dupraz C, Glunk C, Przekop KM, Visscher PT. (2007). Exopolymeric substances of sulfate-reducing bacteria: Interactions with calcium at alkaline pH and implication for formation of carbonate minerals. *Geobiology* **5:** 401--411.

Brazelton WJ, Ludwig KA, Sogin ML, Andreishcheva EN, Kelley DS, Shen C-C, Edwards RL, Baross JA. (2010). Archaea and bacteria with surprising microdiversity show shifts in dominance over 1,000-year time scales in hydrothermal chimneys. *Proceedings of the National Academy of Sciences* **107:** 1612-1617.

Burlage RS. (1998). *Techniques in microbial ecology*, New York, NY, USA: Oxford University Press, USA.

Campbell BJ, Jeanthon C, Kostka JE, Luther III GW, Cary SC. (2001). Growth and phylogenetic properties of novel bacteria belonging to the Epsilon subdivision of the *Proteobacteria* enriched from *Alvinella pompejana* and deep-sea hydrothermal vents. *AEM* **67:** 4566-4572.

Caporaso JG, Kuczynski J, Stombaugh J, Bittinger K, Bushman FD, Costello EK, Fierer N, Pena AG, Goodrich JK, Gordon JI, Huttley GA, Kelley ST, Knights D, Koenig JE, Ley RE, Lozupone CA, McDonald D, Muegge BD, Pirrung M, Reeder J, Sevinsky JR, Turnbaugh PJ, Walters WA, Widmann J, Yatsunenko T, Zaneveld J, Knight R. (2010). QIIME allows analysis of high-throughput community sequencing data. *Nature Methods* **7:** 335-336.

Carson JK, Campbell L, Rooney D, Clipson N, Gleeson DB. (2009). Minerals in soil select distinct bacterial communities in their microhabitats. *FEMS Microbiology Ecology* **67:** 381–388.

Casida LE. (1982). Ensifer adhaerens gen. nov., sp. nov.: A Bacterial Predator of Bacteria in Soil. *International Journal of Systematic Bacteriology* **32:** 339-345.

Chao A, Chazdon RL, Colwell RK, Shen T-J. (2005). A new statistical approach for assessing similarity of species composition with incidence and abundance data. *Ecology Letters* **8:** 148-159.

Chapelle FH, O'Neil KO, Bradley PM, Methe BA, Ciufo SA, Knobel LL, Lovley DR. (2002). A hydrogen-based subsurface microbial community dominated by methanogens. *Nature* **415:** 312-315.

Chen Y, Wu L, Boden R, Hillebrand A, Kumaresan D, Moussard H, Baciu M, Lu Y, Colin Murrell J. (2009). Life without light: microbial diversity and evidence of sulfur- and ammonium-based chemolithotrophy in Movile Cave. *The ISME journal* **3:** 1093-1104.

Chou L, Wollast R. (1985). Steady-state kinetics and dissolution mechanisms of albite. *American Journal of Science* **285:** 963-993.

Chu H, Fierer N, Lauber CL, Caporaso J, Knight R, Grogan P. (2010). Soil bacterial diversity in the Arctic is not fundamentally different from that found in other biomes. *Environmental Microbiology* **12:** 2998-3006.

Cockell CS, Kelly LC, Marteinsson V. (2013). *Actinobacteria*—An Ancient Phylum Active in Volcanic Rock Weathering. *Geomicrobiology Journal* **30:** 706-720.

Corre E, Reysenbach A-L, Prieur D. (2001). e-*Proteobacterial* diversity from a deep-sea hydrothermal vent on the Mid-Altantic Ridge. *FEMS Microbiol Lett* **205:** 329-335.

Craven PA, Hayasaka SS. (1982). Inorganic phosphate solubilization by rhizosphere bacteria in a Zostera marina community. *Can J Microbiol* **28:** 605-610.

Cypionka H. (2000). Oxygen respiration by *Desulfovibrio* species. *Annu Rev Microbiol* **54:** 827-848.

Dalton HM, Poulsen Lk Fau - Halasz P, Halasz P Fau - Angles ML, Angles Ml Fau - Goodman AE, Goodman Ae Fau - Marshall KC, Marshall KC. (1994). Substratum-induced morphological changes in a marine bacterium and their relevance to biofilm structure. *J Bacteriol* **176:** 6900-6906.

Davis KJ, Nealson KH, Luttge A. (2007). Calcite and dolomite dissolution rates in the context of microbe-mineral surface interactions. *Geobiology* **5:** 191-205.

Dawson MP, Humphrey B, Marshall K. (1981). Adhesion: A tactic in the survival strategy of a marine vibrio during starvation. *Curr Microbiol* **6:** 195-199.

DeSantis TZ, Hugenholtz P, Larsen N, Rojas M, Brodie EL, Keller K, Huber T, Dalevi D, Hu P, Andersen GL. (2006). Greengenes, a Chimera-Checked 16S rRNA Gene Database and Workbench Compatible with ARB. *Appl Environ Microbiol* **72:** 5069-5072.

Dilworth MJ, Rynne FG, Castelli JM, Vivas-Marfisi AI, Glenn AR. (1999). Survival and exopolysaccharide production in *Sinorhizobium meliloti* WSM419 are affected by calcium and low pH. *Microbiology* **145:** 1585-1593.

Döbereiner J, Pedrosa F. (1987). The genus *Azospirillum*. Nitrogen-fixing bacteria in non-leguminous crop plants. Madison: Science Tech. Publishers.

Dowd SE, Wolcott RD, Sun Y, McKeehan T, Smith E, Rhoads D. (2008). Polymicrobial nature of chronic diabetic foot ulcer biofilm infections determined using bacterial tag encoded FLX amplicon pyrosequencing (bTEFAP). *PLoS one* **3:** e3326.

Draghi WO, Del Papa MF, Pistorio M, Lozano M, De LosÁngeles Giusti M, Torres Tejerizo GA, Jofré E, Boiardi JL, Lagares A. (2010). Cultural conditions required for the induction of an adaptive acid-tolerance response (ATR) in *Sinorhizobium meliloti* and the question as to whether or not the ATR helps rhizobia improve their symbiosis with alfalfa at low pH. *FEMS Microbiol Lett* **302:** 123-130.

Dulov LE, Lein AY, Dubinina GA, Pimenov NV. (1991). Microbial Processes at the Lost City vent field, mide-atlantic ridge. *Microbiology* **74:** 97-103.

Dupraz C, Reid RP, Braissant O, Decho AW, Norman RS, Visscher PT. (2009). Processes of carbonate precipitation in modern microbial mats. *Earth-Science Reviews* **96:** 141-162.

Eaton AD, Clesceri LS, Rice EW, Greenberg AE. (2005). *Standard Methods for the Examination of Water and Wastewater*, 21 edn. Washington, DC: American Public Health Association, American Water Works Association, Water Environment Federation.

Eboigbodin KE, Ojeda JJ, Biggs CA. (2007). Investigating the Surface Properties of *Escherichia coli* under Glucose Controlled Conditions and Its Effect on Aggregation. *Langmuir* **23:** 6691-6697.

Edwards KJ, Bach W, McCollom TM. (2005). Geomicrobiology in oceanography: microbe–mineral interactions at and below the seafloor. *Trends Microbiol* **13:** 449-456.

Edwards KJ, Becker K, Colwell F. (2012). The Deep, Dark Energy Biosphere: Intraterrestrial Life on Earth. *Annual Review of Earth and Planetary Sciences* **40:** 551-568.

Egemeier SJ. (1981). Cavern development by thermal waters. *National Speleological Society Bulletin* **43:** 31-51.

Eguchi M, Nishikawa T, MacDonald K, Cavicchioli R, Gottschal JC, Kjelleberg S. (1996). Responses to Stress and Nutrient Availability by the Marine Ultramicrobacterium *Sphingomonas* sp. Strain RB2256. *Appl Environ Microbiol* **62:** 1287-1294.

Ehrlich HL. (1996). How microbes influence mineral growth and dissolution. *Chemical Geology* **132:** 5-9.

Ellwood DC, Keevil CW, Marsh PD, Brown CM, Wardell JN, Roux NL. (1982). Surface-Associated Growth [and Discussion]. *Philosophical Transactions of the Royal Society of London B, Biological Sciences* **297:** 517-532.

Engel AS. (2004). Geomicrobiology of sulfuric acid speleogenesis; microbial diversity, nutrient cycling, and controls on cave formation. University of Texas, Austin, Austin, TX.

Engel AS, Lee N, Porter ML, Stern LA, Bennett PC, Wagner M. (2003). Filamentous "*Epsilonproteobacteria*" Dominate Microbial Mats from Sulfidic Cave Springs *Appl Environ Microbiol* **69** 5503-5511.

Engel AS, Porter ML, Stern La, Quinlan S, Bennett PC. (2004a). Bacterial diversity and ecosystem function of filamentous microbial mats from aphotic (cave) sulfidic springs dominated by chemolithoautotrophic "*Epsilonproteobacteria*". *FEMS Microbiology Ecology* **51:** 31-53.

Engel AS, Stern LA, Bennett PC. (2004b). Microbial contributions to cave formation: New insights into sulfuric acid speleogenesis. *Geology* **32:** 369-372.

Eschemann A, Kühl M, Cypionka H. (1999). Aerotaxis in *Desulfovibrio*. *Environmental Microbiology* **1:** 489.

Felsenstein J. (2004). Inferring phylogenies. *Sinauer Associates Incorporated* **Sunderland, Massachusetts**

Ferris FG. (2000). Microbe-Metal Interactions in Sediments. In *Microbial Sediments*, Riding R, Awramik S (eds), 14, pp 121-126. Springer Berlin Heidelberg.

Fierer N, Bradford MA, Jackson RB. (2007). Toward an Ecological Classification of Soil Bacteria. *Ecology* **88:** 1354-1364.

Fierer N, Jackson RB. (2006). The diversity and biogeography of soil bacterial communities. *Proc Natl Acad Sci U S A* **103:** 626-631.

Flis SE, Glen AR, Dilworth MJ. (1993). The interaction between aluminium and root-nodule bacteria. *Soil Biol Biochem* **25:** 403-441.

Galushko AS, Schink B. (2000). Oxidation of acetate through reactions of the citric acid cycle by Geobacter sulfurreducens in pure culture and in syntrophic coculture. *Arch Microbiol* **174:** 314-321.

Garrity G, Holt J. (2001). Phylum BVIII. Nitrospirae phy. nov. In *Bergey's Manual® of Systematic Bacteriology*, Boone D, Castenholz R (eds), 25, pp 451-464. Springer New York.

Ginn TR, Wood BD, Nelson KE, Scheibe TD, Murphy EM, Clement TP. (2002). Processes in microbial transport in the natural subsurface. *Advances in Water Resources* **25:** 1017-1042.

Gleeson D, Clipson N, Melville K, Gadd G, McDermott F. (2005). Characterization of Fungal Community Structure on a Weathered Pegmatitic Granite. *Microb Ecol* **50:** 360-368.

Gleeson D, Kennedy N, Clipson N, Melville K, Gadd G, McDermott F. (2006). Characterization of Bacterial Community Structure on a Weathered Pegmatitic Granite. *Microb Ecol* **51:** 526-534.

Goevert D, Conrad R. (2009). Stable carbon isotope fractionation by acetotrophic sulfur-reducing bacteria. *FEMS Microbiology Ecology* **71:** 218-225.

Goldstein A, Lester T, Brown J. (2003). Research on the metabolic engineering of the direct oxidation pathway for extraction of phosphate from ore has generated preliminary evidence for PQQ biosynthesis in *Escherichia coli* as well as a possible role for the highly conserved region of quinoprote. *Biochimica et Biophysica Acta (BBA) - Proteins & Proteomics* **1647:** 266-271.

Goldstein AH. (1986). Bacterial solubilization of mineral phosphates: Historical perspective and future prospects. *American Journal of Alternative Agriculture* **1:** 51-57.

Gomez-Alvarez V, King GM, Nüsslein K. (2007). Comparative bacterial diversity in recent Hawaiian volcanic deposits of different ages. *FEMS Microbiology Ecology* **60:** 60--73.

Good IJ. (1953). The population frequencies of species and the estimation of population parameters. *Biometrika* **40:** 237-264.

Gordienko AS, Kurdish IK. (2007). Electrical properties and interaction with silicon dioxide particles of *Bacillus subtilis* cells. *Biofizika* **52:** 314-317.

Gutman J, Kaufman Y, Kawahara K, Walker SL, Freger V, Herzberg M. (2014). Interactions of Glycosphingolipids and Lipopolysaccharides with Silica and Polyamide Surfaces: Adsorption and Viscoelastic Properties. *Biomacromolecules* **15:** 2128-2137.

Haas BJ, Gevers D, Earl AM, Feldgarden M, Ward DV, Giannoukos G, Ciulla D, Tabbaa D, Highlander SK, Sodergren E, Methé B, DeSantis TZ, Consortium THM, Petrosino JF, Knight R, Birren BW. (2011). Chimeric 16S rRNA sequence formation and detection in Sanger and 454-pyrosequenced PCR amplicons. *Genome Res* **21:** 494-504.

Hamel R, Appanna VD. (2003). Aluminum detoxification in *Pseudomonas fluorescens* is mediated by oxalate and phosphatidylethanolamine. *Biochimica et Biophysica Acta (BBA) - General Subjects* **1619:** 70-76.

Hao C-b, Zhang H-x, Bai Z-h, Hu Q, Zhang B-g. (2007). A novel acidophile community populating waste ore deposits at an acid mine drainage site. *Journal of Environmental Sciences* **19:** 444-450.

Hartmann M, Frey B, Mayer J, Mader P, Widmer F. (2015). Distinct soil microbial diversity under long-term organic and conventional farming. *ISME J* **9:** 1177-1194.

Hathaway JJM, Garcia MG, Balasch MM, Spilde MN, Stone FD, Dapkevicius MDLNE, Amorim IR, Gabriel R, Borges PAV, Northup DE. (2014). Comparison of Bacterial Diversity in Azorean and Hawai'ian Lava Cave Microbial Mats. *Geomicrobiology Journal* **31:** 205-220.

Hazen RM. (2006). Mineral surfaces and the prebiotic selection and organization of biomolecules. *American Mineralogist* **91:** 1715-1729.

Hazen RM, Papineau D, Bleeker W, Downs RT, Ferry JM, McCoy TJ, Sverjensdy DA, Yang H. (2008). Mineral evolution. *American Mineralogist* **93:** 1693-1720.

Hazen TC, Jimenez L, de Victoria GL. (1991). Comparison of bacteria from deep subsurface sediment and adjacent ground water. *Microb Ecol* **22:** 293-304.

Hiebert FK, Bennett PC. (1992). Microbial control of silicate weathering in organic-rich ground water. *Science* **258:** 278-281.

Hill TCJ, Walsh KA, Harris JA, Moffett BF. (2003). Using ecological diversity measures with bacterial communities. *FEMS Microbiology Ecology* **43:** 1-11.

Hiraishi A, Kuraishi H, Kawahara K. (2000). Emendation of the description of *Blastomonas natatoria* (Sly 1985) Sly and Cahill 1997 as an aerobic photosynthetic bacterium and reclassification of *Erythromonas ursincola* Yurkov et al. 1997 as *Blastomonas ursincola* comb. nov. *International journal of systematic and evolutionary microbiology* **50:** 1113-1118.

Howarth F. (1981). Community structure and niche differentiation in Hawaiian lava tubes. *US/IBP synthesis series*

Howarth R, Unz RF, Seviour EM, Seviour RJ, Blackall LL, Pickup RW, Jones JG, Yaguchi J, Head IM. (1999). Phylogenetic relationships of filamentous sulfur bacteria (*Thiothrix spp*. and Eikelboom type 021N bacteria) isolated from wastewatertreatment plants and description of *Thiothrix eikelboomii sp. nov*., *Thiothrix unzii sp. nov*., *Thiothrix fructosivorans sp. . International Journal of Systematic and Evolutionary Microbiology* **49** 1817-1827.

Huang C-T, Xu KD, McFeters GA, Stewart PS. (1998). Spatial Patterns of Alkaline Phosphatase Expression within Bacterial Colonies and Biofilms in Response to Phosphate Starvation. *Appl Environ Microbiol* **64:** 1526-1531.

Huber JA, Welch DBM, Morrison HG, Huse SM, Neal PR, Butterfield DA, Sogin ML. (2007). Microbial Population Structures in the Deep Marine Biosphere. *Science* **318:** 97-100.

Hugenholtz P, Tyson GW, Webb RI, Wagner AM, Blackall LL. (2001). Investigation of Candidate Division *TM7*, a Recently Recognized Major Lineage of the Domain Bacteria with No Known Pure-Culture Representatives. *Appl Environ Microbiol* **67:** 411-419.

Inagaki F, Takai K, Nealson KH, Horikoshi K. (2004). *Sulfurovum lithotrophicum* gen. nov., sp. nov., a novel sulfur-oxidizing chemolithoautotroph within the *ε-Proteobacteria* isolated from Okinawa Trough hydrothermal sediments. *International Journal of Systematic and Evolutionary Microbiology* **54:** 1477-1482.

Indrasumunar A, Menzies NW, Dart PJ. (2012). Calcium affects the competitiveness of acid-sensitive and acid-tolerant strains of *Bradyrhizobium japonicum* in nodulating and fixing nitrogen with two soybean cultivars in acid soil. *Soil Biology and Biochemistry* **46:** 115-122.

Jannasch HW, Mottl MJ. (1985). Geomicrobiology of Deep-Sea Hydrothermal Vents. *Science* **229:** 717-725.

Jansson M. (1987). Anaerobic dissolution of iron-phosphorus complexes in sediment due to the activity of nitrate-reducing bacteria. *Microb Ecol* **14:** 81-89.

Jones AA, Bennett PC. (2014). Mineral Microniches Control the Diversity of Subsurface Microbial Populations. *Geomicrobiology Journal* **31:** 246-261.

Jones B. (2010). Microbes in caves: agents of calcite corrosion and precipitation. *Geological Society, London, Special Publications* **336:** 7-30.

Jones RT, Robeson MS, Lauber CL, Hamady M, Knight R, Fierer N. (2009). A comprehensive survey of soil acidobacterial diversity using pyrosequencing and clone library analyses. *ISME J* **3:** 442-453.

Kalanetra KM, Huston SL, Nelson DC. (2004). Novel, Attached, Sulfur-Oxidizing Bacteria at Shallow Hydrothermal Vents Possess Vacuoles Not Involved in Respiratory Nitrate Accumulation. *Appl Environ Microbiol* **70:** 7487-7496.

Kalyuzhnaya MG, De Marco P, Bowerman S, Pacheco CC, Lara JC, Lidstrom ME, Chistoserdova L. (2006). *Methyloversatilis universalis* gen. nov., sp. nov., a novel taxon within the *Betaproteobacteria* represented by three methylotrophic isolates. *International Journal of Systematic and Evolutionary Microbiology* **56:** 2517-2522.

Kelly DP. (1999). Thermodynamic aspects of energy conservation by chemolithotrophic sulfur bacteria in relation to the sulfur oxidation pathways. *Arch Microbiol* **171:** 219-229.

Kelly DP, Harrison AP. (1989). The genus *Thiobacillus*. In *Bergey's Manual of Determinative Bacteriology*, Staley JT, Pfenning N, Bryant MP, Holdt JG (eds), Vol. 3, pp 1842-1858. Baltimore: Williams and Wilkins.

Kelly DP, Shergill JK, Lu W-P, Wood AP. (1997). Oxidative metabolism of inorganic sulfur compounds by bacteria. *Antonie Van Leeuwenhoek* **71:** 95-107.

Kelly DP, Wood AP. (2000a). Reclassification of some species of *Thiobacillus Acidithiobacillus* gen . nov ., *Halothiobacillus*. *International Journal of Systematic and Evolutionary Microbiology* **50:** 511-516.

Kelly DP, Wood AP. (2000b). Reclassification of some species of Thiobacillus to the newly designated genera Acidithiobacillus gen. nov., Halothiobacillus gen. nov. and Thermithiobacillus gen. nov. *International Journal of Systematic and Evolutionary Microbiology* **50:** 511-516.

Kelly DP, Wood AP, Jordan SL, Padden AN, Gorlenko VM, Dubinina GA. (1994). Biological production and consumption of gaseous sulphur compounds. *Biochemical Society Transactions, Atmospheric Gas Production and Consumption* **22:** 1011-1014.

Kelly LC, Cockell Cs Fau - Herrera-Belaroussi A, Herrera-Belaroussi A Fau - Piceno Y, Piceno Y Fau - Andersen G, Andersen G Fau - DeSantis T, DeSantis T Fau - Brodie E, Brodie E Fau - Thorsteinsson T, Thorsteinsson T Fau - Marteinsson V, Marteinsson V Fau - Poly F, Poly F Fau - LeRoux X, LeRoux X. (2010). Bacterial diversity of terrestrial crystalline volcanic rocks, Iceland. *Environmental Microbiology*

Kjelleberg S, Hermansson M. (1984). Starvation-induced effects on bacterial surface characteristics. *Appl Environ Microbiol* **48:** 497-503.

Knapp CW, Fowle DA, Kulczycki E, Roberts JA, Graham DW. (2007). Methane monooxygenase gene expression mediated by methanobactin in the presence of mineral copper sources. . *Proc Natl Acad Sci U S A* **104:** 12040-12045.

Kodama Y, Ha LT, Watanabe K. (2007). *Sulfurospirillum cavolei* sp. nov., a facultatively anaerobic sulfur-reducing bacterium isolated from an underground crude oil storage cavity. *International Journal of Systematic and Evolutionary Microbiology* **57:** 827-831.

Kodama Y, Watanabe K. (2004). *Sulfuricurvum kujiense* gen. nov., sp. nov., a facultatively anaerobic, chemolithoautotrophic, sulfur-oxidizing bacterium isolated from

an underground crude-oil storage cavity. *International Journal of Systematic and Evolutionary Microbiology* **54:** 2297-2300.

Kolari M, Nuutinen J, Rainey FA, Salkinoja-Salonen MS. (2003). Colored moderately thermophilic bacteria in paper-machine biofilms. *J Ind Microbiol Biotechnol* **30:** 225-238.

Konhauser KO. (2007). *Introduction to Geomicrobiology*, Malden, MA: Blackwell.

Korber DR, Lawrence JR, Lappin-Scott HM, Costerton JW. (1995). Growth of microorganisms on surfaces, . In *Microbial Biofilms*, Lappin-Scott HM, Costerton JW (eds), pp 15-45. Cambridge, UK: University Press.

Kugaprasatham S, Nagaoka H, Ohgaki S. (1992). Effect of turbulence on nitrifying biofilms at non-limiting substrate conditions. *Water Research* **26:** 1629-1638.

Lane DJ. (1991). 16S/23S rRNA sequencing. In *Nucleic Acid Techniques in Bacterial Systematics*, Stackebrandt E, Goodfellow M (eds), pp 115-175. New York: Wiley.

Larkin LM. (1989). Genus II. *Thiothrix* Winogradsky 1888. In *Bergey's Manual of Systematic Bacteriology*, Staley JP, Bryant MP, Pfenning N, Holt JG (eds), Vol. 3, pp 2098-2101. Baltimore: Williams and Wilkins.

Larson CA, Passy SI. (2013). Rates of species accumulation and taxonomic diversification during phototrophic biofilm development are controlled by both nutrient supply and current velocity. *Appl Environ Microbiol* **79:** 2054-2060.

Laskin AI, White DC. (1999). Preface to special issue on *Sphingomonas*. *J Ind Microbiol Biotechnol* **23:** 231-231.

Lauber CL, Hamady M, Knight R, Fierer N. (2009). Pyrosequencing-based assessment of soil pH as a predictor of soil bacterial community structure at the continental scale. *Appl Environ Microbiol* **75:** 5111-5120.

Lawrence JR, Korber DF, Hoyle BD, Costerton JW, Caldwell DE. (1991). Optical sectioning of microbial biofilms. *J Bacteriol* **173:** 6558-6567.

Leon-Barrios M, Gutierrez-Navarro AM, Perez-Galdona R, Corzo J. (1991). Characterization of canary island isolates of *Bradyrhizobium* sp. (*Chamaecytisus proliferus*). *Soil Biology and Biochemistry* **23:** 487-489.

Leyval C, Berthelin J. (1989). Interactions between *Laccaria laccata*, *Agrobacterium radiobacter* and beech roots: Influence on P, K, Mg, and Fe mobilization from minerals and plant growth. *Plant and Soil* **117:** 103-110.

Liu CL, Peck HD. (1981). Comparative bioenergetics of sulfate reduction in *Desulfovibrio* and *Desulfotomaculum* spp. *Journal of Bacteriology* **145:** 966.

Lovley DR, Phillips EJP. (1986). Organic matter mineralization with reduction of ferric iron in anaeorbic sediments. *Appl Environ Microbiol* **51:** 683-689.

Lozupone C, Knight R. (2005). UniFrac: a New Phylogenetic Method for Comparing Microbial Communities. *Appl Environ Microbiol* **71:** 8228-8235.

Lozupone C, Lladser ME, Knights D, Stombaugh J, Knight R. (2011). UniFrac: an effective distance metric for microbial community comparison. *The ISME journal* **5:** 169-172.

Lüderitz O, Freudenberg MA, Galanos C, Lehmann V, Rietschel ET, Shaw DH. (1982). Lipopolysaccharides of gram-negative bacteria. *Current topics in membranes and transport* **17:** 79-151.

Lyons WB, Long DT, Hines ME, Gaudette HE, Armstrong PB. (1984). Calcification of cyanobacterial mats in Solar Lake, Sinai. *Geology* **12:** 623-626.

Macalady JL, Dattagupta S, Schaperdoth I, Jones DS, Druschel GK, Eastman D. (2008). Niche differentiation among sulfur-oxidizing bacterial populations in cave waters. *The ISME Journal* **2:** 590-601.

Macalady JL, Jones DS, Lyon EH. (2007). Extremely acidic, pendulous cave wall biofilms from the Frasassi cave system, Italy. *Environmental Microbiology* **9:** 1402-1414.

Macalady JL, Lyon EH, Koffman B, Albertson LK, Meyer K, Galdenzi S, Mariani S. (2006). Dominant Microbial Populations in Limestone-Corroding Stream Biofilms, Frasassi Cave System, Italy. *Appl Environ Microbiol* **72:** 5596-5609.

Madigan MT, Martinko JM, Dunlap PV, Clark DP. (2009). *Brock Biology of Microorganisms*, 12th edn. San Francisco, CA: Pearson Benjamin Cummings.

Margulies M, Egholm M, Altman WE, Attiya S, Bader JS, Bemben LA, Berka J, Braverman MS, Chen Y-J, Chen Z, Dewell SB, Du L, Fierro JM, Gomes XV, Godwin BC, He W, Helgesen S, Ho CH, Irzyk GP, Jando SC, Alenquer MLI, Jarvie TP, Jirage KB, Kim J-B, Knight JR, Lanza JR, Leamon JH, Lefkowitz SM, Lei M, Li J, Lohman KL, Lu H, Makhijani VB, McDade KE, McKenna MP, Myers EW, Nickerson E, Nobile

JR, Plant R, Puc BP, Ronan MT, Roth GT, Sarkis GJ, Simons JF, Simpson JW, Srinivasan M, Tartaro KR, Tomasz A, Vogt KA, Volkmer GA, Wang SH, Wang Y, Weiner MP, Yu P, Begley RF, Rothberg JM. (2005). Genome sequencing in microfabricated high-density picolitre reactors. *Nature* **437:** 376-380.

Marshall KC. (1996). *Adhesion as a strategy for access to nutrients*: Wiley: New York.

Matin A, Auger EA, Blum PH, Schultz JE. (1989). Genetic Basis of Starvation Survival in Nondifferentiating Bacteria. *Annu Rev Microbiol* **43:** 293-314.

McArdle BH, Anderson MJ. (2001). Fitting Multivariate Models to Community Data: A Comment on Distance-Based Redundancy Analysis. *Ecology* **82:** 290-297.

Mera MU, Beveridge TJ. (1993). Mechanism of silicate binding to the bacterial cell wall in Bacillus subtilis. *J Bacteriol* **175:** 1936-1945.

Moyer CL, Dobbs FC, Karl DM. (1995). Phylogenetic diversity of the bacterial community from a microbial mat at an active, hydrothermal vent system, Loihi Seamount, Hawaii. *Appl Environ Microbiol* **61:** 1555-1562.

Nielsen PH, Aquino de Muro M, Nielsen JL. (2000). Studies of the in situ physiology of *Thiothrix spp*. present in activated sludge. *Environmental Microbiology* **2:** 389-398.

Northup D, Melim L, Spilde M, Hathaway J, Garcia M, Moya M, Stone F, Boston P, Dapkevicius M, Riquelme C. (2011). Lava cave microbial communities within mats and secondary mineral deposits: implications for life detection on other planets. *Astrobiology* **11:** 601-618.

Odintsova EV, Wood AP, Kelly DP. (1993). Chemolithoautotrophic Growth Of *Thiothrix-Ramosa*. *Arch Microbiol* **160:** 152-157.

Ohashi A, Viraj de Silva DG, Mobarry B, Manem JA, Stahl DA, Rittmann BE. (1995). Influence of substrate C/N ratio on the structure of multi-species biofilms consisting of nitrifiers and heterotrophs. *Water Science and Technology* **32:** 75-84.

Ozawa T, Imai Y, Sukiman HI, Karsono H, Ariani D, Saono S. (1999). Low pH and aluminum tolerance of *Bradyrhizobium* strains isolated from acid soils in Indonesia. *Soil Science and Plant Nutrition* **45:** 987-992.

Palmer AN. (1991). Origin and morphology of limestone caves. *Geological Society Of America Bulletin* **103:** 1-21.

Perry RS, McLoughlin N, Lynne BY, Sephton MA, Oliver JD, Perry CC, Campbell K, Engel MH, Farmer JD, Brasier MD, Staley JT. (2007). Defining biominerals and organominerals: Direct and indirect indicators of life. *Sedimentary Geology* **201:** 157-179.

Peterson JA. (1984). *Stratigraphy and Sedimentary Facies of the Madison Limestone and Associated Rocks in Parts of Montana, Nebraska, North Dakota, South Dakota, and Wyoming*, Alexandria, VA: Deptartment of the Interior, U.S. Geological Survey.

Plummer LN, Busby F, Lee RW, Hanshaw BB. (1990). Geochemical modeling of the Madison Aquifer in parts of Montana, Wyoming, and South Dakota. *Water Resources Res* **26:** 1981-2014.

Quince C, Lanzen A, Davenport R, Turnbaugh P. (2011). Removing Noise From Pyrosequenced Amplicons. *BMC Bioinformatics* **12:** 38.

Reeder J, Knight R. (2010). Rapidly denoising pyrosequencing amplicon reads by exploiting rank-abundance distributions. *Nature methods* **7:** 668-669.

Roadcap GS, Kelly WR, Bethke CM. (2005). Geochemistry of Extremely Alkaline (pH> 12) Ground Water in Slag–Fill Aquifers. *Groundwater* **43:** 806-816.

Roberts JA, Bennett PC, Gonzalez LA, Macpherson GL, Milliken KL. (2004). Microbial precipitatoin of dolomite in methanogenic groundwater. *Geology* **32:** 277-280.

Roeske CA, O'Leary MH. (1984). Carbon isotope effects on enzyme-catalyzed carboxylation of ribulose bisphosphate. *Biochemistry (Mosc)* **23:** 6275-6284.

Rogers JR, Bennett PC. (2004). Mineral stimulation of subsurface microorganisms: release of limiting nutrients from silicates. *Chemical Geology* **203:** 91-108.

Rogers JR, Bennett PC, Choi WJ. (1998). Feldspars as a source of nutrients for microorganisms *American Mineralogist* **83** 1532-1540.

Rogers JR, Bennett PC, Choi WJ. (2001). Enhanced weathering of silicates by subsurface microorganisms: a strategy to release liminity inorganic nutrients? *10th International Symposium on Water-Rock Interaction*

Rossetti S, Blackall LL, Levantesi C, Uccelletti D, Tandoi V. (2003). Phylogenetic and physiological characterization of a heterotrophic, chemolithoautotrophic Thiothrix strain isolated from activated sludge. *International Journal of Systematic and Evolutionary Microbiology* **53:** 1271-1276.

Ruby EG, Jannasch HW, Dueser WG. (1987). Fractionation of stable carbon isotopes during chemoautotrophic growth of sulfur-oxidizing bacteria. *Appl Environ Microbiol* **53:** 1940-1943.

Sarbu SM, Galdenzi S, Menichetti M, Gentile G. (2000). Geology and biology of Grotte di Frasassi (Frasassi Caves) in Central Italy, an ecological multi-disciplinary study of a hypogenic underground karst system. In *Ecosystems of the World: Subterranean Ecosystems*, Wilkens H, Culver, D., Humphreys, S. (ed), Vol. 30, pp 361-381. Oxford: Elsevier Science.

Sarbu SM, Kane TC, Kinkle BK. (1996). Chemoautotrophically based cave ecosystem. *Science* **272:** 1953-1955.

Schauer R, Røy H, Augustin N, Gennerich H-H, Peters M, Wenzhoefer F, Amann R, Meyerdierks A. (2011). Bacterial sulfur cycling shapes microbial communities in surface sediments of an ultramafic hydrothermal vent field. *Environmental microbiology* **13:** 2633-2648.

Schidlowski M. (2000). Carbon isotopes and microbial sediments. In *Microbial Sediments*, Riding RE, Awaramik, S.M. (ed), pp 84-95. Berlin: Springer-Verlag.

Schloss PD, Westcott SL, Ryabin T, Hall JR, Hartmann M, Hollister EB, Lesniewski RA, Oakley BB, Parks DH, Robinson CJ, Sahl JW, Stres B, Thallinger GG, Van Horn DJ, Weber CF. (2009). Introducing mothur: Open-Source, Platform-Independent, Community-Supported Software for Describing and Comparing Microbial Communities. *Appl Environ Microbiol* **75:** 7537-7541.

Schultze-Lam S, Fortin D, Davis B, Beveridge T. (1996). Mineralization of bacterial surfaces. *Chemical Geology* **132:** 171-181.

Schumacher W, Kroneck PMH, Pfenning N. (1992). Comparative systematic study on "Spirillum" 5175, *Campylobacter*, and *Wolinella* species - description of "Spirillum" 5175 as *Sulfurospirillum deleyianum* gen., nov. spec. nov. *Arch Microbiol* **158:** 287-293.

Semrau JD, DiSpirito AA, Yoon S. (2010). Methanotrophs and copper. *FEMS Microbiol Rev* **34:** 496-531.

Siciliano SD, Palmer AS, Winsley T, Lamb E, Bissett A, Brown MV, van Dorst J, Ji M, Ferrari BC, Grogan P. (2014). Soil fertility is associated with fungal and bacterial richness, whereas pH is associated with community composition in polar soil microbial communities. *Soil Biology and Biochemistry* **78:** 10-20.

Sillence DJ. (2013). Glucosylceramide modulates endolysosomal pH in Gaucher disease. *Mol Genet Metab* **109:** 194-200.

Singh R, Beriault R, Middaugh J, Hamel R, Chenier D, Appanna V, Kalyuzhnyi S. (2005). Aluminum-tolerant *Pseudomonas fluorescens*: ROS toxicity and enhanced NADPH production. *Extremophiles* **9:** 367-373.

Singh R, Lemire J, Mailloux RJ, Chénier D, Hamel R, Appanna VD. (2009). An ATP and Oxalate Generating Variant Tricarboxylic Acid Cycle Counters Aluminum Toxicity in *Pseudomonas fluorescens*. *PLoS ONE* **4:** e7344.

Smith D, Strohl W. (1991). Sulfur-oxidizing bacteria. In *Variations in Autotrophic Life*, Shively J, Barton L (eds), p 356. London: Academic Press.

Smith JV. (1998). Biochemical evolution. I. Polymerization on internal, organophilic silica surfaces of dealuminated zeolites and feldspars. *Proceedings of the National Academy of Sciences* **95:** 3370–3375.

Sogin ML, Morrison HG, Huber JA, Welch DM, Huse SM, Neal PR, Arrieta JM, Herndl GJ. (2006). Microbial diversity in the deep sea and the underexplored "rare biosphere". *Proceedings of the National Academy of Sciences* **103:** 12115-12120.

Sørensen J, Christensen D, Jørgensen BB. (1981). Volatile Fatty Acids and Hydrogen as Substrates for Sulfate-Reducing Bacteria in Anaerobic Marine Sediment. *Appl Environ Microbiol* **42:** 5-11.

Sorokin DY, Banciu H, Robertson LA, Kuenen JG. (2006). Haloalkaliphilic sulfur-oxidizing bacteria. In *The prokaryotes*, pp 969-984. Springer.

Stackebrandt E, Schumann P. (2006). Introduction to the Taxonomy of Actinobacteria. In *The Prokaryotes*, Dworkin M, Falkow S, Rosenberg E, Schleifer K-H, Stackebrandt E (eds), 16, pp 297-321. Springer New York.

Staley J, Crawford R. (1975). The biologist's chamber: lava tube slime. *Cascade Caver* **14:** 20-21.

Steinhauer ES, Omelon CR, Bennett PC. (2010). Limestone Corrosion by Neutrophilic Sulfur-Oxidizing Bacteria: A Coupled Microbe-Mineral System. *Geomicrobiology Journal* **27:** 723-738.

Stevens T. (1997). Lithoautotrophy in the subsurface. *FEMS Microbiol Rev* **20:** 327-337.

Stevens TO, McKinley JP. (1995). Lithoautotrophic microbial ecosystems in deep basalt aquifers. *Science* **270:** 450-454.

Stock GM, Riihimaki CA, Anderson RS. (2006). Age constraints on cave development and landscape evolution in the Bighorn Basin of Wyoming, USA. *Journal of Cave and Karst Studies* **68:** 76-84.

Sun W, Liu W, Cui L, Zhang M, Wang B. (2013). Characterization and identification of a chlorine-resistant bacterium, *Sphingomonas* TS001, from a model drinking water distribution system. *Sci Total Environ* **458–460:** 169-175.

Suzuki S, Ishii Si, Wu A, Cheung A, Tenney A, Wanger G, Kuenen JG, Nealson KH. (2013). Microbial diversity in The Cedars, an ultrabasic, ultrareducing, and low salinity serpentinizing ecosystem. *Proceedings of the National Academy of Sciences* **110:** 15336-15341.

Sylvan JB, Toner BM, Edwards KJ. (2012). Life and Death of Deep-Sea Vents: Bacterial Diversity and Ecosystem Succession on Inactive Hydrothermal Sulfides. *mBio* **3:** e00279-00211.

Takeuchi M, Hamana K, Hiraishi A. (2001). Proposal of the genus *Sphingomonas* sensu stricto and three new genera, *Sphingobium*, *Novosphingobium* and *Sphingopyxis*, on the basis of phylogenetic and chemotaxonomic analyses. *International Journal of Systematic and Evolutionary Microbiology* **51:** 1405-1417.

Uroz S, Turpault MP, Delaruelle C, Mareschal L, Pierrat JC, Frey-Klett P. (2011). Minerals Affect the Specific Diversity of Forest Soil Bacterial Communities. *Geomicrobiology Journal* **29:** 88-98.

Van Lith Y, Warthmann R, Vasconcelos C, McKenzie JA. (2003). Sulphate-reducing bacteria induce low-temperature Ca-dolomite and high Mg-calcite formation. *Geobiology* **1:** 71--79.

Van Loosdrecht M, Lyklema J, Norde W, Zehnder A. (1990). Influence of interfaces on microbial activity. *Microbiol Rev* **54:** 75-87.

Varela ARP, Gonçalves da Silva AMPS, Fedorov A, Futerman AH, Prieto M, Silva LC. (2014). Influence of Intracellular Membrane pH on Sphingolipid Organization and Membrane Biophysical Properties. *Langmuir* **30:** 4094-4104.

Vinuesa P, León-Barrios M, Silva C, Willems A, Jarabo-Lorenzo A, Pérez-Galdona R, Werner D, Martínez-Romero E. (2005). *Bradyrhizobium canariense* sp. nov., an acid-tolerant endosymbiont that nodulates endemic genistoid legumes (Papilionoideae:

Genisteae) from the Canary Islands, along with *Bradyrhizobium japonicum* bv. *genistearum, Bradyrhizobium* genospecies alpha and *Bradyrhizobium* genospecies beta. *International Journal of Systematic and Evolutionary Microbiology* **55:** 569-575.

Visscher PT, Reid RP, Bebout BM. (2000). Microscale observations of sulfate reduction: Correlation of microbial activity with lithified micritic laminae in modern marine stromatolites. *Geology* **28:** 919-922.

Walker SL, Redman JA, Elimelech M. (2004). Role of Cell Surface Lipopolysaccharides in *Escherichia coli* K12 Adhesion and Transport. *Langmuir* **20:** 7736-7746.

Walter LM, Bischof SA, Patterson WP, Lyons TW, O'Nions RK, Gruszczynski M, Sellwood BW, Coleman ML. (1993). Dissolution and Recrystallization in Modern Shelf Carbonates: Evidence from Pore Water and Solid Phase Chemistry. *Philosophical Transactions: Physical Sciences and Engineering* **344:** 27-36.

Weber CF, King GM. (2010). Distribution and diversity of carbon monoxide-oxidizing bacteria and bulk bacterial communities across a succession gradient on a Hawaiian volcanic deposit. *Environmental Microbiology* **12:** 1855--1867.

White WB. (1988). *Geomorphology and hydrology of karst terrains*, Vol. 464: Oxford University Press New York.

Willems A, Busse J, Goor M, Pot B, Falsen E, Jantzen E, Hoste B, Gillis M, Kersters K, Auling G. (1989). *Hydrogenophaga*, a new genus of hydrogen-oxidizing bacteria that includes *Hydrogenophaga flava* comb. nov.(formerly *Pseudomonas flava*), *Hydrogenophaga* palleronii (formerly *Pseudomonas* palleronii), *Hydrogenophaga pseudoflava* (formerly *Pseudomonas pseudoflava* and "*Pseudomonas carboxydoflava*"), and *Hydrogenophaga taeniospiralis* (formerly *Pseudomonas taeniospiralis*). *International journal of systematic bacteriology* **39:** 319-333.

Winsley TJ, Snape I, McKinlay J, Stark J, van Dorst JM, Ji M, Ferrari BC, Siciliano SD. (2014). The ecological controls on the prevalence of candidate division *TM7* in polar regions. *Frontiers in microbiology* **5**

Wood M. (1995). Mechanism of aluminium toxicity to soil bacteria and possible ecological implications. *Plant and Soil* **171:** 63-69.

Wrangstadh M, Szewzyk U, Ostling J, Kjelleberg S. (1990). Starvation-specific formation of a peripheral exopolysaccharide by a marine *Pseudomonas* sp., strain S9. *Appl Environ Microbiol* **56:** 2065-2072.

Yabuuchi E, Yano I, Oyaizu H, Hashimoto Y, Ezaki T, Yamamoto H. (1990). Proposals of *Sphingomonas paucimobilis* gen. nov. and comb. nov., *Sphingomonas parapaucimobilis* sp. nov., *Sphingomonas yanoikuyae* sp. nov., *Sphingomonas adhaesiva* sp. nov., *Sphingomonas capsulata* comb, nov., and Two Genospecies of the Genus *Sphingomonas*. *Microbiol Immunol* **34:** 99-119.

Yamaguchi M, Kasamo K. (2002). Modulation of proton pumping across proteoliposome membranes reconstituted with tonoplast H+-ATPase from cultured rice (Oryza sativa L. var. Boro) cells by acyl steryl glucoside and steryl glucoside. *Plant Cell Physiol* **43:** 816-822.

Zisu B, Shah NP. (2003). Effects of pH, Temperature, Supplementation with Whey Protein Concentrate, and Adjunct Cultures on the Production of Exopolysaccharides by *Streptococcus thermophilus* 1275. *J Dairy Sci* **86:** 3405-3415.